EXPERIMENTAL INVESTIGATION OF SOLAR DRIVEN MULTI-STAGE STEPPED BUBBLER HUMIDIFIER

BY

HAFIZ MUHAMMAD ABD-UR-REHMAN

A Thesis Presented to the

DEANSHIP OF GRADUATE STUDIES

KING FAHD UNIVERSITY OF PETROLEUM & MINERALS

DHAHRAN, SAUDI ARABIA

In Partial Fulfillment of the
Requirements for the Degree of

MASTER OF SCIENCE

In

MECHANICAL ENGINEERING

DECEMBER 2015

KING FAHD UNIVERSITY OF PETROLEUM & MINERALS

DHAHRAN- 31261, SAUDI ARABIA

DEANSHIP OF GRADUATE STUDIES

This thesis, written by HAFIZ NUHAMMAD ABD-UR-REHMAN under the direction of his thesis advisor and approved by his thesis committee, has been presented and accepted by the Dean of Graduate Studies, in partial fulfillment of the requirements for the degree of **MASTER OF SCIENCE IN MECHANICAL ENGINEERING**.

Dr. Fahad A. Al-Sulaiman
(Advisor)

Dr. Zuhair Mattoug Gasem
Department Chairman

Dr. Mohamed A. Antar
(Member)

Dr. Salam A. Zummo
Dean of Graduate Studies

Dr. Atia E. Khalifa
(Member)

27/1/16

Date

DEDICATION

I would like to dedicate this work to my beloved parents who sacrifice so much each and every day to see me succeed.

ACKNOWLEDGMENTS

"In the name of ALLAH, The Most Gracious and The Most Merciful"

All praise to Allah (subhana wa taala) for blessing me with health, patience, and knowledge to complete my MS research thesis. I am thankful to my parents who sacrifice so much each and every day to see me succeed. Alhamdulillah, for His limitless guidance in accomplishing the things that offer happiness to my parents.

I would like to acknowledge my advisor Dr. Fahad Al-Sulaiman for his technical and moral support throughout my MS degree. I am thankful to him for introducing me to the research world, for flourishing my research capabilities, for teaching me the art of technical writing, and assisting me to effectively present my research work. I am also thankful to Dr. Antar for suggesting the valuable ideas and providing the scientific directions to implement these ideas. I am grateful to Dr. Atia Khalifa for his immense efforts in arranging the advance data acquisition workshops and guiding me in the instrumentation phase. I also acknowledge the sincere and untiring efforts of Mr. Karam, who helped me in preparing the experimental set-up and assisted me during all stages of my experiments.

Finally, I would like to express my deepest gratitude to my mother, father, sisters, my wife, and all my friends, for their emotional and moral support throughout my academic career and also for their love, patience, encouragement, and prayers.

TABLE OF CONTENTS

LIST OF TABLES

LIST OF FIGURES

LIST OF ABBREVIATIONS

Acronyms

GOR	Gain Output Ratio
HCR	Heat Capacity Ratio
HDH	Humidification Dehumidification

Roman Symbols

a_s	specific interfacial area	$m^2\ m^{-3}$
c_p	specific heat capacity	$J\ kg^{-1}\ k^{-1}$
D_{AB}	diffusion coefficient	$m^2\ s^{-1}$
H	liquid column height	cm
$\dot{H}$	enthalpy rate	W
h_a	specific enthalpy of air–vapor mixture	$J\ kg^{-1}$
h_{fg}	specific enthalpy of vaporization	$J\ kg^{-1}$
h_t	heat-transfer coefficient	$W\ m^{-2}\ k^{-1}$
j	mass flux	$Kg\ m^2\ s^{-1}$
k	thermal conductivity	$W\ m^{-1}\ k^{-1}$
$\dot{m}$	mass flow rate	$Kg\ s^{-1}$
q	total heat flux	$W\ m^{-2}$
q_{latent}	latent heat flux	$W\ m^{-2}$
$q_{sensible}$	sensible heat flux	$W\ m^{-2}$
$R_{sensible}$	thermal resistance for sensible heat	$K\ m^2\ W^{-1}$
T_{air}	temperature of air	°C
T_{bulk}	bulk temperature of the liquid column	°C

T_{lmtd}	log mean temperature difference	°C
V_c	velocity of fluid circulation	m s^{-1}
Vsg	air superficial velocity	cm s^{-1}
V_r	velocity in radial direction	m s^{-1}
vol	volume of liquid column	m^3

Greek symbols

α	thermal diffusivity	m^2 s^{-1}
Δ	change or difference	-
ε	effectiveness	-
ρ	density	kg m^{-3}
σ	surface tension	N m^{-1}
ω	specific humidity	kg_w kg_a^{-1}

Subscripts

a	air
b	bulk
g	gas
H	humidifier
i	inlet
l	liquid
max	maximum
o	outlet
sat	saturated
w	water

ABSTRACT

Full Name : Hafiz Muhammad Abd-ur-Rehman

Thesis Title : Experimental Investigation of Solar Driven Multi-Stage Stepped Bubbler Humidifier

Type Major : Mechanical Engineering

Date of Degree : December 2015

The scarcity of fresh water is an issue of high concern as most of the world population suffers from clean water shortage. One potential solution to tackle this issue is to develop an efficient, reliable, and cost effective decentralized water desalination system to make the clean water accessible for most of the world population. Humidification-dehumidification (HDH) is a carrier gas based thermal technique that is ideal for a small scale decentralized water desalination system. An innovative design approach is to use the bubble column humidifier to enhance the performance of the HDH water desalination system. Therefore, a novel multi-stage stepped bubble column humidifier is proposed that is operated through solar thermal energy as the main source of energy input. The overall objective of this work is to experimentally investigate the main operating parameters of the humidifier. The study addresses the significance of the perforated plate geometric features, optimum balance of air superficial velocity and water column height, and the influence of inlet water temperature and inlet air relative humidity on the performance of the humidifier. The day round performance of the humidifier is investigated in single stage, two stage, and three stage configuration, in which each configuration was tested with and without the integration of Fresnel lens. Findings show that the average day round absolute humidity increased by 9 % for the two stage configuration and 23 % for the three stage configuration

as compared to the single stage configuration of the humidifier. The integration of the Fresnel lens further increased the absolute humidity up to 26 % as compared to the results obtained without the integration of the Fresnel lens under the same prevailing conditions. The day round performance of the humidifier was tested in two different months (June and August) to experience the effect of varying relative humidity of the inlet air. Findings reveal that the humidifier shows a higher humidification efficiency in the climatic conditions that have a lower inlet air relative humidity. An electric heater is installed to analyze the performance of the humidifier at a higher water inlet temperature and the results are compared with other published studies related to bubble column humidification. The comparison indicates that the proposed humidifier design operated in the three stage configuration shows a higher humidification efficiency and experiences a lower pressure drop. The performance of the humidifier is also analyzed in terms of energy based effectiveness to anticipate its true potential as an effective mean of heat and mass exchange. Findings signpost the significant increase in the effectiveness with the increase in the number of stages of the humidifier. The maximum value of the effectiveness achieved is 49 % for the single stage configuration, 60 % for the two stage configuration, and 81 % for the three stage configuration of the humidifier.

The outcomes from this study are of pivotal importance to understand the optimum operating conditions of the humidifier for its possible integration with the dehumidifier. Consequently, an improved HDH system can be obtained. One major advantage of this proposed humidifier is its ability to have direct solar thermal heating. Subsequently, it can be located in remote areas.

ملخص الرسالة

الاسم الكامل: حافظ محمد عبدالرحمن

عنوان الرسالة: دراسة معملية لمرطب متعدد المراحل بالفقاعات المكثفة ويعمل بالطاقة الشمسية

التخصص: الهندسة الميكانيكية

تاريخ الدرجة العلمية: ديسمبر 2015

تعد ندرة المياه العذبة من المسائل المثيرة للقلق على مستوى عال حيث أن معظم سكان العالم يعاني من نقص المياه المحلاة. أحد الحلول المحتملة لمعالجة هذه القضية هو تطوير نظام تحلية مياه لامركزي ذو كفاءة عالية، وفعال من حيث التكلفة لجعل المياه العذبة في متناول معظم سكان العالم. تعتبر عملية تحلية المياه بالترطيب ثم التجفيف HDH التقنية الحرارية المثلى لنظام تحلية المياه اللامركزي على نطاق صغير. أحد التصاميم المبتكرة لتحسين أداء نظام تحلية المياه بالترطيب ثم التجفيف HDH هو استخدام عمود الترطيب بالفقاعات المكثفة. إذ يقترح استخدام مرطب ذو مراحل متعددة باستخدام عمود الترطيب بالفقاعات المكثفة الذي يتم تشغيله من خلال الطاقة الحرارية الشمسية كمصدر رئيسي للطاقة. الهدف الرئيسي من هذا العمل هو إجراء تجارب معملية لمعرفة معايير التشغيل الرئيسية لتصميم المرطب المقترح. تتناول الدراسة أهمية اللوحة المثقبة ذات الخصائص الهندسية، كما تدرس التوازن الأمثل لسرعة الهواء السطحية وارتفاع عمود الماء، بالإضافة إلى دراسة تأثير درجة حرارة المياه المدخلة والرطوبة النسبية للهواء المدخل على أداء المرطب. على ضوء هذه الدراسة، تم التحقق من أداء المرطب اليومي المكون على مرحلة واحدة وعلى مرحلتين وعلى ثلاثة مراحل، مع أو بدون دمج عدسة فريسنل Fresnel. تشير النتائج إلى أن متوسط الرطوبة المطلقة في اليوم زادت بنسبة 9٪ للمرطب المكون على مرحلتين و23٪ للمرطب المكون على ثلاثة مراحل وذلك بالمقارنة مع المرطب المكون على مرحلة واحدة. بعد دمج عدسة فريسنل Fresnel زادت نسبة الرطوبة المطلقة لتصل إلى 26٪ بالمقارنة مع النتائج التي تم الحصول عليها قبل دمج عدسة فريسنل Fresnel في ظل نفس الظروف السائدة. تم اختبار الأداء الجولة من المرطب يوميا في شهرين مختلفة (يونيو و أغسطس) لتجربة تأثير متفاوتة الرطوبة النسبية للهواء مدخل . يعمل المرطب بكفاءة أعلى أثناء عملية الترطيب في الظروف المناخية التي تقل فيها الرطوبة النسبية للهواء المدخل. تم تثبيت سخان كهربائي لتحليل أداء المرطب في ارتفاع درجة الحرارة مدخل المياه و تتم مقارنة النتائج مع

الدراسات المنشورة الأخرى ذات الصلة إلى العمود فقاعة الترطيب . تشير هذه المقارنة إلى أن المرطب المقترحة تعمل في ثلاث التكوين مرحلة يظهر أعلى كفاءة الترطيب والخبرات أقل انخفاض الضغط . ويتم تحليل أداء المرطب أيضا من حيث الفعالية على الطاقة لاستباق امكانياتها الحقيقية كما سيلة فعالة للحرارة وتبادل الشامل. النتائج الصوة الزيادة الكبيرة في فعالية مع الزيادة في عدد من مراحل المرطب. الحد الأقصى لقيمة و فعالية تحقيقه هو 49 ٪ لتكوين مرحلة واحدة ، و 60٪ لمدة التكوين المرحلة، و 81 ٪ لمدة ثلاثة التكوين مرحلة من مراحل المرطب.

النتائج المستخلصة من هذه الدراسة ذات أهمية محورية لفهم الظروف المثلى لتشغيل المرطب في حال الإندماج مع المجفف. ونتيجة لذلك، يمكن الحصول على نظام محسن للتحلية بطريقة الترطيب ثم التجفيف.HDH أحد المميزات الرئيسية لهذا المرطب المقترح هو قدرته على أن يكون التسخين بشكل مباشر من الطاقة الشمسية وبالتالي يمكن استخدامه في المناطق النائية.

CHAPTER 1

INTRODUCTION

1.1 Motivation

The fresh water scarcity, energy crisis, and climate change are the most intimidating concerns for mankind as it brought many disquiets like health, pollution, and environmental issues. The problem is more severe in developing countries where the population growth projection is much higher as compared to developed countries [1]. The increase in world population growth resulted in high demand for potable water which is estimated to reach 6,900 billion m^3 by 2030. The existing supply of fresh water is 4,200 billion m^3 that is well below the projection of potable water demand [2]. The challenge is to provide sustainable solution to balance the potable water requirements by secure and affordable energy with the pressing issue of climate change.

Water is the most substantial resource available on earth and it covers more than 70 % of earth's surface. However, greater percentage of this water on earth is saline leaving behind only 2.5 % fresh water. Major part of the fresh water is hard to access as it is frozen as icecaps and glaciers. Therefore, very little quantity of fresh water is available to support our lives. Some 88 developing countries that share about 50 % of the world's population are affected by severe water shortage. The clean water unavailability is the root cause of 80 - 90 % of all diseases in these countries. These diseases are known as water born diseases

(WBD) and are responsible for 30 % of all deaths. Furthermore, these numbers are likely to escalate four times over the next 25 years [3].

The rapid population growth resulted in higher fresh water demands for domestic and agriculture sectors to produce adequate quantities of food. While the fresh water demand is rising exponentially, the industrial revolution is making the fresh water scarcity situation more alarming by polluting the lakes and rivers by industrial waste. Given the fact that the population on earth continues to increase and industrial growth shows no signs of slowing down, it is inevitable that conventional sources of freshwater are not sufficient. However, the only water resource that is inexhaustible is the oceans. Thus a solution for sustainability may exist in low cost seawater desalination.

1.2 Water Desalination

The process "water desalination'' can be defined as the production of fresh drinkable water by removal of pollutants and dissolved minerals from brackish water, treated waste water, or sea water. It is a mature technology and is being adopted by many countries to yield potable water. Middle East and North Africa (MENA) regions are quite dry regions and most of the desalination plants are located in these regions. By the end of 2010, more than 15 thousand desalinations units were installed in different parts of world with a daily unit size of 100 m^3 or more.

The process of desalination of water is an energy intensive process. Therefore, the cost of production is quite high. It was estimated that to produce 1000 m^3/day of potable water, annually ten thousand tons of oil is required [4]. Fortunately, a constant decrease in desalination cost over the years made this process competitive to other conventional water resources. However, different ways to reduce the cost have to be explored as many developing countries will have to depend on desalination of water (specially MENA region) because is the only acceptable and most suitable way to produce potable water [5].

1.3 Overview on Desalination Processes

Desalination systems are categorized in two main technologies; membrane technologies and thermal or phase change technologies. This classification is made on basis of the transport phenomena in separation process.

1.3.1 Membrane Technologies

In these technologies, saline water is passed through semi permeable membranes leading to the separation of salts and fresh water. The two most commonly used membrane based water purification techniques are electro dialysis (ED) and reverse osmosis (RO). In ED process, the driving force is the electrolytic charge difference on a pair of separation membranes. In RO process, osmotic pressure is outbalanced when high pressure difference is applied on the membranes leading to the separation. In membrane technologies, the energy consumption is less comparative to thermal processes as no phase change occurs in membrane based water purification. However, the attainable quality of water in membrane based technologies is low as compared to thermal technologies.

1.3.2 Thermal Technologies

In these technologies, separation is done based on the liquid-vapor phase change due to the addition of heat. There are different techniques of thermal desalination among which the most employed are vapor compression (VC), multiple effect distillation (MED) and multistage flash (MSF). In a general thermal desalination process, vapors are generated by heating and partially evaporating sea water. The generated vapor is then condensed back

yielding potable water and waste brine is left behind containing high concentration of salts. During condensation process, latent heat is released by the vapors. This latent heat can be used for evaporating water in next stage or preheating the feed-in sea water. Thermal desalination technology produces highly purified potable water as compared to membrane technologies.

1.3.3 Energy Requirements

Thermal distillation processes require sensible heat or low temperature steam to carry out distillation and electric power to drive mechanical components like pumps. Whereas membrane technologies rely on electrical power for distillation. The electric power requirements of majority of the desalination plants are fulfilled from co-located power plant or by the public grids.

Fossil fuels like oil and gas are conventional fuels and have been used for centuries as a major source of energy. However there are some downsides of such fuels e.g sustainability, price volatility, GHG emissions etc. Sustainability concerns of conventional energy based seawater desalination in the long run is stimulating attention of renewable energy based seawater desalination.

The conventional water desalination systems are highly energy intensive and economically suited only on large scale. However, desalination systems are more needed on small scale for decentralized supply of fresh water in remote areas for small communities. Therefore, it is highly desirable to develop an efficient, reliable, and cost effective decentralized water desalination system to make the clean water accessible for remote communities.

1.4 Proposed Design

Solar humidification-dehumidification (HDH) is an appropriate choice for decentralized small scale water desalination system, especially in remote regions where inexpensive land and abundant solar radiations are available. The challenge is to come up with an efficient, reliable, and cost effective design approach to explore the true potential of the HDH water desalination systems. Several studies are available that explore HDH as an effective means of seawater desalination. However, the main focus of these studies was to improve the dehumidification process of the HDH system and very less attention is given towards the improvement of humidification process.

Humidification is one of the fundamental processes in the solar HDH water desalination system. An innovative design approach is to use the bubble column humidifier to improve the humidification process and hence enhance the performance of the HDH water desalination system. Therefore, a novel multi-stage stepped bubble column humidifier is proposed in this work. The schematic of the proposed multi-stage steeped bubble column humidifier is shown in figure 1.

In this design, air is guided in multi-stages to pass through perforated plates to form bubbles in the pool of hot water. The bubble formation increases the time and surface of contact, which results in an improvement of humidification performance. This design takes the advantage of its stepped configuration to maintain a minimum water depth, which results in less pressure drop and lower blower power consumption.

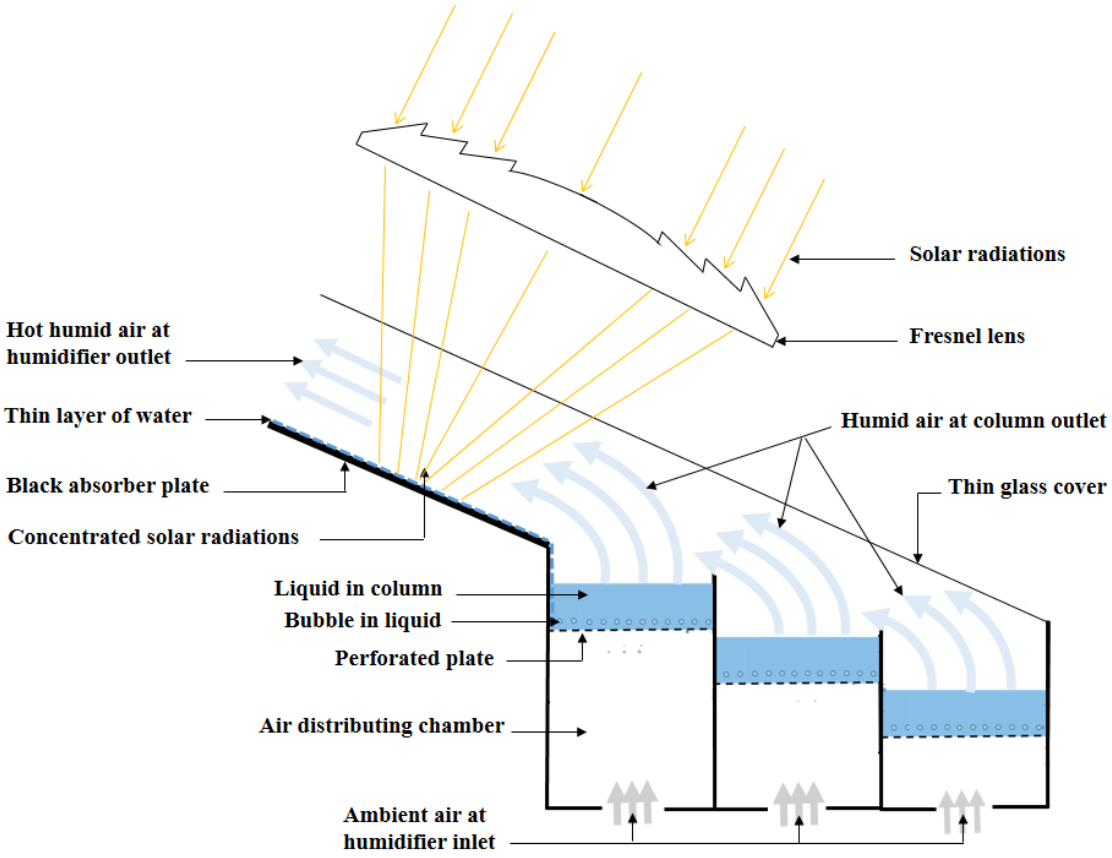

Figure 1 Schematic diagram of the proposed multi-stage stepped bubble column humidifier.[1]

[1] Patent
Al-sulaiman, Fahad A., and Mohamed A. Antar. "HUMIDIFICATION-DEHUMIDIFACTION DESALINATION SYSTEM." U.S. Patent No. 20,150,353,377. 10 Dec. 2015.

1.5 Objectives

The overall objective of this work is to develop and to test the novel humidifier to identify the optimum performance operating conditions for its possible integration with a dehumidifier. Consequently an improved HDH performance system can be obtained. The specific objectives of this work are:

- Designing, manufacturing, and testing the novel air humidifier.
- Experimental investigation of single stage humidifier operated through solar thermal energy.
- Experimental investigation of multi-stage humidifier operated through solar thermal energy and compares its performance with the single stage humidifier.
- Thermodynamic analysis of the humidifier developed considering the results obtained from the experimental work.

The objectives are designed to provide the deliverables which are mainly related to the experimental analysis of the humidifier operated through solar energy. The study addresses the significance of the perforated plate geometric features, optimum balance of air superficial velocity and water column height, and the influence of inlet water temperature and inlet air relative humidity on the performance of the humidifier. The results of the work will be a valuable reference for both researchers and engineers in the area of water desalination and air conditioning.

CHAPTER 2

LITERATURE REVIEW

Solar distillation is an appropriate choice for decentralized small scale water desalination systems, especially in remote regions where inexpensive land and abundant solar radiations are available. [6]. Conventional basin type solar stills and humidification-dehumidification (HDH) systems are two well-known solar distillation techniques for decentralized small scale water desalination.

2.1 Conventional Solar Stills

The oldest and simplest method to obtain clean water is from solar stills. The fact that water tends to evaporate when exposed to solar radiations is utilized by the solar stills. In this technique all functional processes for water desalination (solar absorption, evaporation, and condensation) occur within the single compartment as shown in Figure 2. These solar stills produce potable water by capturing that evaporated water and condensing it on a cold surface. To absorb maximum energy, solar stills possess black colored pan that is filled with water. This pan is covered by a clear thin glass that allow maximum transmittance of solar irradiance. This glass cover also act as a cold surface to condense the evaporated water. The condensed water then flow along the tilted surface and collected as fresh water distillate.

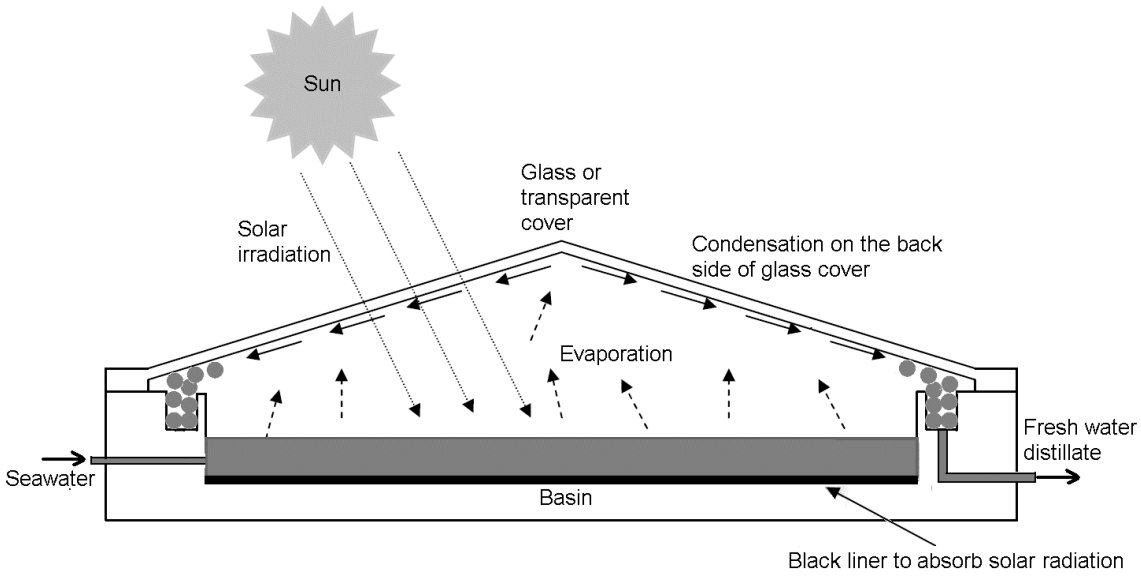

Figure 2 Conventional basin-type solar still.

The major disadvantage of solar still is its low efficiency. The main reason of low efficiency is instant loss of latent heat of condensation through thin transparent glass cover when evaporated water condensed on its inner surface. This type of solar distillation experiences very low productivity and requires relatively large area.

2.2 Humidification-Dehumidification (HDH) Technique

An improved technique is known as humidification-dehumidification (HDH) technique in which various functional processes (solar absorption, evaporation, and condensation) occur within a separate component as shown in Figure 3. These separate compartments are known as humidifier, dehumidifier, and external thermal energy source. In the humidifier, the warm saline water is sprayed in the form of tiny droplets that fall under the force of gravity. Air is injected from the bottom to come in a direct contact with the falling water droplets in a counter flow arrangement. The aim of the humidifier is to raise the humidity of the air by diffusion of water into air stream. Consequently, air comes out hot and humid at the exit of the humidifier. Then, this humid air is passed through the dehumidifier in which cold seawater is moved in counter flow direction. The cold seawater acts as a condensation source for warm humid air and extract water out of the humidified air. Meanwhile the seawater is preheated by the latent heat of condensation and reduce the amount of heat required by external thermal energy source.

Because of the better control over condensation and evaporation processes, efficiency has been improved noticeably in HDH process as compared to solar still. Other advantages of HDH process include its simple functionality, ability to utilize waste heat resources and low grade energy, usage of low- cost construction materials, and moderate investment constraint.

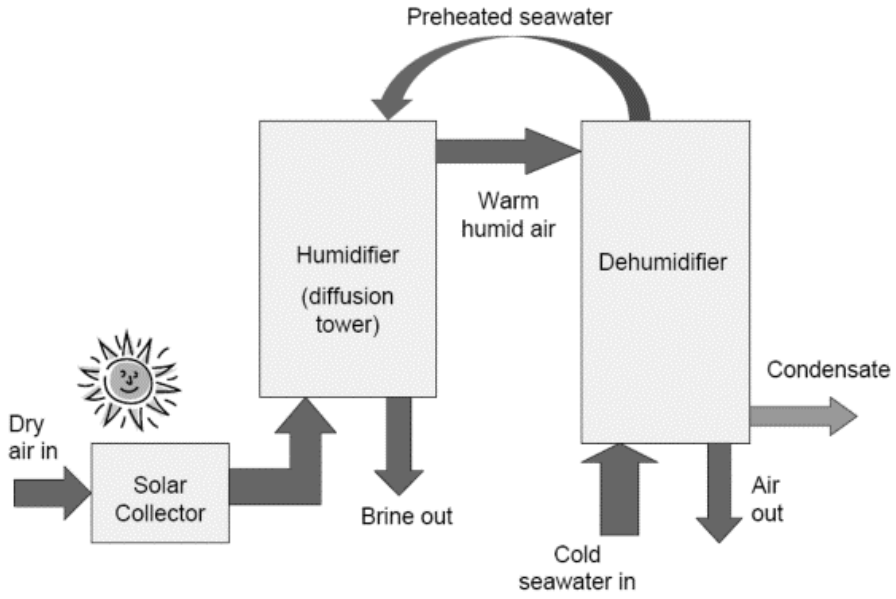

Figure 3 Schematic of humidification-dehumidification (HDH) unit [6].

2.2.1 Heat and Mass Balances

By applying the principle of mass conservation, the mass flow rate of air always remain same throughout the system. Therefore,

$$\dot{m}_{a,i} = \dot{m}_{a,o} = \dot{m}_a \quad (1)$$

In the humidifier, hot saline water transfers the mass and heat to unsaturated air. The mass and energy balance of the humidifier is defined by the following equations:

Mass balance:

$$\dot{m}_{w,i} = \dot{m}_{w,o} + \dot{m}_a(\omega_{a,o} - \omega_{a,i}) \quad (2)$$

Energy balance:

$$\dot{m}_{w,i}h_{w,i} = \dot{m}_{w,o}h_{w,o} - \dot{m}_a\left(h_{a,i} - h_{a,o}\right) \quad (3)$$

In the dehumidifier, feed water only exchanges heat with hot humid air. No mass transfer take place to or from the feed water. Therefore, mass flow rate of the feed water is constant in dehumidifier and hence,

$$\dot{m}_{w,o} = \dot{m}_{w,i} \quad (4)$$

The hot humid air condensed in the dehumidifier to form the distilled water. The mass and energy balance of the dehumidifier is described by the following equations:

Mass balance:

$$\dot{m}_{fw} = \dot{m}_a(\omega_{a,i} - \omega_{a,o}) \quad (5)$$

Energy balance:

$$\dot{m}_a\left(h_{a,i}\right) + \dot{m}_{w,i}(h_{w,i}) = \dot{m}_a(\,h_{a,o}) + \dot{m}_{w,o}(h_{w,o}) + \dot{m}_{fw}h_{fw} \quad (6)$$

2.3 Classification of HDH systems

HDH systems can be classified in three main categories. The first one is based on the form of energy used such as solar, thermal, geothermal, or hybrid systems. The second classification of HDH system is based on its cycle configuration such as closed water-open air (CWOA) cycle, open water-open air (OWOA) cycle, closed water-closed air (CWCA) cycle, and open water-closed air (OWCA) cycle. The air in these systems can be circulated by either natural convection or forced convection. It is of pivotal importance to understand the relative technical advantages of each of these cycles and choose the one that is best in terms of efficiency and cost of water production. The third classification of the HDH systems is based on the type of heating such as water heating systems or air heating systems.

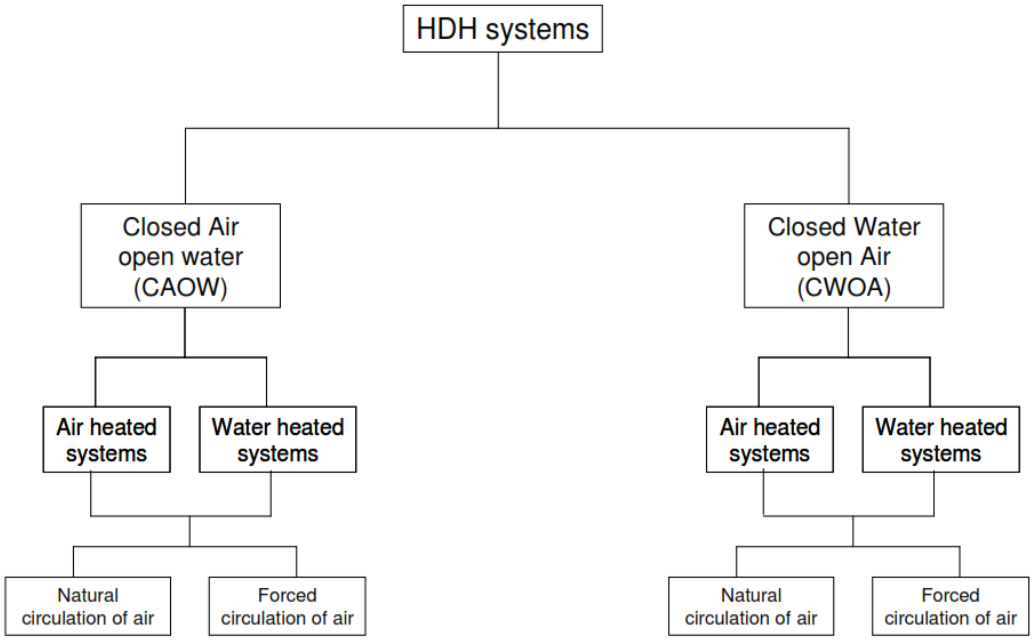

Figure 4 Classification of HDH systems [6].

2.3.1 Close-air open-water (CAOW) water heated HDH cycle

In this configuration, the saline water in introduced into the condenser, where it is preheated by the latent heat of condensation of water vapors. This preheated water is further heated at higher temperature before entering the humidifier. The water heating at higher temperature results is higher heat and mass transfer in the direct contact humidifier that improve the productivity of HDH system. The brine at the exit of the humidifier is not reused in CAOW configuration while the air at the exit of dehumidifier is again introduced into the humidifier. This type of configuration take the advantage of some heat recovery by recirculation of air. The brine rejection and introduction of cold saline water results in efficient condensation of vapors due to higher temperature gradient in the dehumidifier. The schematic diagram of the CAOW water heated HDH system along with the psychometric chart is shown in figure 5. The line A–B in the psychometric chart represents the ideal air humidification process. The ideal dehumidification process in the close-air HDH system is also represented by the same line follow in the reverse direction, i.e., from B-A. The previous work done by of researchers on close-air open-water (CAOW) water heated cycle is summarized in Table 1.

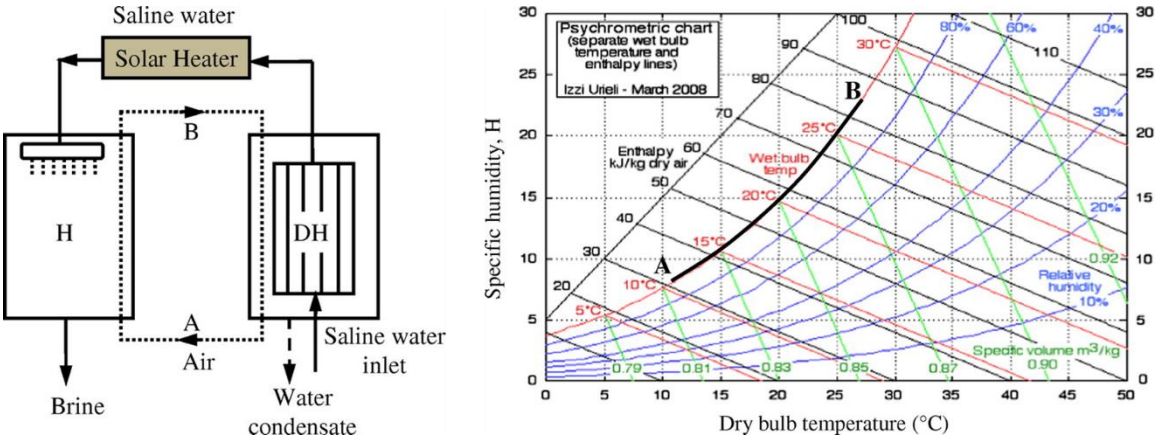

Figure 5 Schematic diagram and psychometric chart for close-air open-water (CAOW), water heated HDH system.[2]

Table 1 Literature review on close-air open-water (CAOW) water heated HDH cycle.

Al-hajaj et al. [7]	**Unit Description**	The water was heated up to 70 °C using a tubeless-flat plate solar collector of 2 m^2 area. The performance of the system is analyzed under forced and natural air circulation. The humidifier surface area of 87 m^2/m^3 and 14m^2/m^3 were used for bench unit and pilot unit. Condenser had a bench unit area of 0.6 m^2 and pilot unit area of 8 m^2.
	Specific Outcomes	Their analysis exhibited that the performance of plant is maximum at an optimum value water flow rate. They concluded that the forced air convection was suitable for low temperatures and natural air circulation was suitable for higher temperatures.

[2] Published in: Wael Abdelmoez; Mohamed S. Mahmoud; Taha E. Farrag; *Desalination and Water Treatment* **2014,** 52, 4622-4640.
DOI: 10.1080/19443994.2013.804457

H. B. Bacha et al. [8]	**Unit Description**	A solar collector of 6 m^2 area was used for water heating purpose. A thorn trees packed bed humidifier was used as a humidification device. A storage tank was integrated with the system that runs with minimum temperature constraint. The dehumidifier consisted of plates of polypropylene and brackish water was used as cooling medium in the dehumidifier.
	Specific Outcomes	The reported daily water production was 19 Liters. To produce same quantity of distillate without thermal storage attached, 16 % increase in area of the solar collector was required. The study also concluded that the performance of plant greatly depends on the temperature of water at the humidifier inlet, the water and air flow rate, and packing material of humidifier.
M.M. Farid et al. [9]	**Unit Description**	A solar collector of 1.9 m^2 area was used to heat water. Humidifier used wooden shaving as a packing material. The dehumidifier used multi-pass shell and tube heat exchanger
	Specific Outcomes	The achieved water production was 12 Liters/m^2 with an optimum value of water flow rate. The study concluded that it was complicated to relate velocity of air and its effect on production.

H. Garg et al. [10]	**Unit Description**	A system was integrated with a 5 liters capacity thermal storage for its extended operation. A solar collector area of 2 m^2 was used to heat water. The air was naturally circulated in the system. The latent heat was partially recovered in this study.
	Specific Outcomes	The study concluded that the performance of the cycle was greatly dependent on the inlet water temperature of humidifier. The study also emphasize on the careful consideration of heat loses for accurately rate the performance of the HDH system.
A. Nafey et al. [11]	**Unit Description**	The study introduced a unique dual heating system scheme by heating the both air and water stream separately. The system contained packed bed type humidifier with canvas packing. An air cooled dehumidifier was used that limits the possibility of latent heat recovery.
	Specific Outcomes	A maximum daily production of 9 Liters was reported (1.2 Liters/hour). The study concluded that an increase in air flow caused a reduction in humidifier inlet temperature, consequently, lower system productivity was experienced at higher air flow rate.

H. MÜLler-Holst [12]	**Unit Description**	A closed-air open-water water heating system with 38 m^2 collector area was studied. The system was analyzed with 2 m^3 thermal storage for 24 h operation. Water was heated up to 90 °C and latent heat recovery unit was considered to heat water up to 75 °C.
	Specific Outcomes	A 500 Liters daily production of water and a gain output ratio (GOR) of 3-4.5 was reported for a Tunisia based pilot plant. The use of thermal storage resulted in a continuous operation of system leading to 50 % cost reduction of produced water.
Y. Li et al. [13]	**Unit Description**	The study featured an HDH cycle with direct contact packed bed dehumidifier. The water was heated up to 60 °C by utilizing the waste heat. A share of water obtained from dehumidifier was utilized as coolant and the heat from this coolant was recovered in another heat exchanger.
	Specific Outcomes	This process was able to yield 8 % water production efficiency. The energy consumption for such a yield was reported as 0.56 kWh per kg of produced fresh water when the feed water was heated at 60 °C. The amount of solar used in the system was not incorporated in energy consumption calculations.

M. A. Younis et al. [14]	**Unit Description**	An HDH system coupled with 1700 m^2 solar pond was studied. The system featured a force convection of air and a latent heat recovery unit which pre-heated the feed water before entering in the humidifier by recovering latent heat in condenser.
	Specific Outcomes	The study concluded that the performance was not affected by the water flow rate. However, production of water was greatly influenced by the air flow rate.
G. P. Narayan et al. [15]	**Unit Description**	In this study, humidifier and dehumidifier were operated at different pressures. An expander and a thermal vapor compressor (TVC) were used to maintain pressure difference. RO unit desalinated the brine from humidifier by using the recovered work.
	Specific Outcomes	The research indicated that the system worked more efficiently by recovering energy in expansion process as compared to system using isenthalpic throttling process. Use of high pressure steam and an efficient TVC are most important factors to obtain minimum specific consumption of energy of an HDH-TVC-RO system.

2.3.2 Close-air open-water (CAOW) air heated HDH cycle

In this configuration, the air is heated before it is introduced into the humidifier. The air heating results is higher moisture content at the exit of the humidifier that leads to an improvement of cycle efficiency. The drawback of air heating before the humidifier is its heat loss during humidification process. The air enters at lower temperature in the dehumidifier as compared to water heated cycle. This results in lower temperature gradient in dehumidifier that leads to inefficient condensation in the dehumidifier. This drawback can be removed by placing another air heater after the humidifier that improve the efficiency but it comes at the expense of additional heaters and higher input energy. The schematic diagram of the CAOW air heated HDH system along with the psychometric chart is shown in figure 6. The constant humidity line A-B in the psychometric chart represents the air heating process before entering the humidifier. The line B-C represents the state of air in the humidifier where it is cooled and saturated. The saturated air is then dehumidified and cooled as represented by line C–A. The previous work done by of researchers on Close-air open-water (CAOW) air heated cycle is summarized in Table 2.

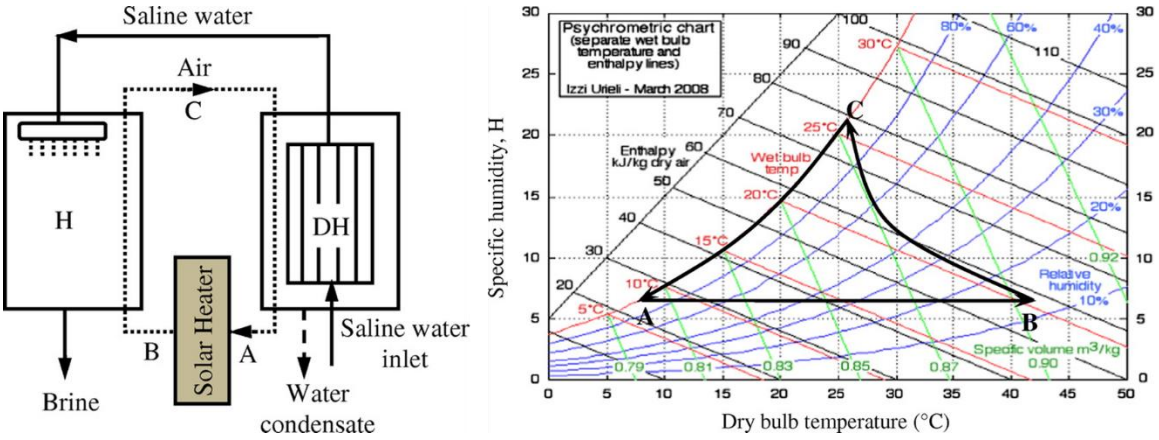

Figure 6 Schematic diagram and psychometric chart for close-air open-water (CAOW), air heated HDH system.[3]

Table 2 Literature review on close-air open-water (CAOW) air heated HDH cycle.

E. Chafik [16]	**Unit Description**	A multistage heating and humidification system having fourfold web-plate (FFWP design) solar collectors of area 2.08 m^2 was used to heat air up to 80 °C along with 3 separate recovery stages.
	Specific Outcomes	The system was costly and 40 % of the total cost was constituted by the solar air heaters. He reported that the system has a potential of further improvement which can be accomplishes by reducing the pressure drop through dehumidifier and evaporator.

[3] Published in: Wael Abdelmoez; Mohamed S. Mahmoud; Taha E. Farrag; *Desalination and Water Treatment* **2014,** 52, 4622-4640.
DOI: 10.1080/19443994.2013.804457

I. Houcine et al. [17]	**Unit Description**	A multistage system having 5 humidification and heating stages was used to heat air up to 90 °C. The first two stages were made up of nine 4.98 m^2 fourfold web-plate (FFWP) type collectors. Rest of the stages used the conventional commercially available solar collectors. The area of third, fourth, and last stage was 45 m^2, 45 m^2, and 27 m^2 respectively.
	Specific Outcomes	The reported results showed that a maximum of 516 Liters/day water was produced and the production cost for this quantity of water was quite high (~ 28.65 \$/m^3). The higher cost of water production was attributed to solar collectors that constituted 37 % of the total cost.
M. Ben Amara et al. [18]	**Unit Description**	A fourfold web-plate (FFWP) type solar collectors made up of polycarbonate covers and blackened strips of aluminum was used to heat air up to 90 °C. The system was insulated using polyurethane and aluminum foil. The investigations were made to analyze the performance of system under the variation of air humidity, inlet air temperature, wind velocity, air mass flow rate, and solar irradiation.
	Specific Outcomes	When endurance test was conducted on polycarbonate material it was revealed that the material cannot endure peak temperatures and it got melted in summers. Therefore, a blower is required. The maximum collector efficiency was obtained at minimum wind velocity.

C. Yamalı and İ. Solmus [19]	**Unit Description**	A single stage double pass flat plate solar collector was used for water heating. The system featured finned tube heat exchanger dehumidifier and a pad humidifier. It also contained a water storage tank of 0.5 m^3 capacity.
	Specific Outcomes	This plant had a maximum daily production of 4 kg. The studies showed that increasing flow rate of air did not affect the performance of the system. However, an increase in mass flow rate of water caused an increase in productivity. Turning on the solar water heater allowed operating it for longer time and water production up to 10kg/day was acheived.
J. Orfi et al. [20]	**Unit Description**	A solar heater with collector surface area of 2 m^2 was used to heat both air and water. The humidifier is incorporated with a spongy material for packing and possess unique configuration in which heated water wetted the horizontal surface and capillaries provide the wetting means to the vertical plates. The system included the heat recovery unit for preheating the sea water.
	Specific Outcomes	The evaporator was incorporated with capillaries to ensure the wetness the vertical surfaces. The results showed that the maximum humidification was obtained at an optimum water-to-air mass flow rate ratio. However, the ratio was different for different ambient conditions.

2.3.3 Close-water open-air (CWOA) water heated HDH cycle

In this configuration, ambient fresh air is withdrawn and discharged to the surroundings for each HDH cycle, while feed brine is recirculated. The disadvantage of this type of configuration is the lower temperature gradient in dehumidifier that leads to inefficient condensation in the dehumidifier. The schematic diagram of the CAOW air heated HDH system along with the psychometric chart is shown in figure 7. The air humidification process is represented by line A-B on the psychometric chart. The saturated air at the exit of the humidifier is fed to the dehumidifier where it undergoes dehumidification process along the saturation line as represented by line B–C. The previous work done by of researchers on Close-water open-air (CAOW) water heated cycle is summarized in Table 3.

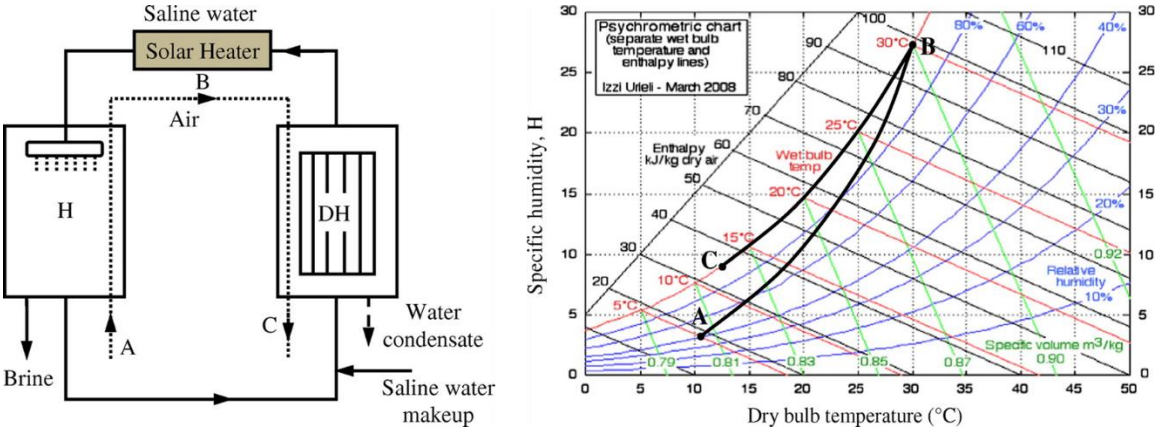

Figure 7 Schematic diagram and psychometric chart for close-water open-air (CWOA), water heated HDH system.[4]

[4] Published in: Wael Abdelmoez; Mohamed S. Mahmoud; Taha E. Farrag; *Desalination and Water Treatment* **2014,** 52, 4622-4640.
DOI: 10.1080/19443994.2013.804457

Table 3 Literature review on close-water open-air (CWOA) water heated HDH cycle.

G. Al-Enezi et al. [21]	**Unit Description**	In a study, authors focused their interest in knowing the variations in heat and mass transfer coefficient and daily water production with respect to change in water flow rate, air flow rate, hot water supply temperature, and cooling water temperature. They used solar collector for air heating up to 90 ˚C. Other features included the forced air circulation, humidifier with plastic packing material, cooling water circuit for condenser, and preheaters for water heating up to 45 ˚C.
	Specific Outcomes	The estimations concluded that minimum work was independent of the involved devices. The amount of work required for dehumidification process was increased by increasing relative humidity keeping the humid air temperature constant.
Y. J. Dai and H. F. Zhang [22]	**Unit Description**	They analyzed an HDH system having a forced air circulation, humidifier with honeycomb paper as packing material, and fin tube-type condenser. The condenser also performs the job of recovering the latent heat by preheating sea water.
	Specific Outcomes	They concluded that there were various factors which strongly influenced the system performance including process air mass flow rate, saline water mass flow rate, and saline water temperature at the inlet of the humidifier. The study reported that there is an optimum air flow rate corresponding to every inlet water temperature value that leads to better system performance.

SM. Khedr [23]	**Unit Description**	The study incorporated the pioneer direct contact condenser in HDH system. It had packed tower dehumidifier containing 50 mm ceramic rings. The study used numerical approach to calculate the performance parameters.
	Specific Outcomes	The system gain output ratio (GOR) was quite low (0.8) that indicate the limited heat recovery. Their economic analysis showed that the HDH possess a significant potential for small decentralized water desalination plants.

2.4 Improvements in HDH Systems

Humidification-dehumidification (HDH) is a carrier gas based thermal technique that is ideal for small scale water desalination systems [24]. Several literature studies are available that explore HDH as an effective mean of seawater desalination. The main focus of the researchers in developing a small scale water desalination unit is to achieve efficient evaporation and condensation in these systems. Some of the early work includes those by El-Dessouky [25], Abdel-Salam et al. [26], Al-Hallaj et al. [7], Muller-Holst et al. [27], Bourouni et al. [28], and Xiong et al. [29]. In these studies conventional shell and tube heat exchangers were used as condensers for the dehumidification process. Film condensation over tubes is extremely inefficient as the process involves condensing water vapor out of air-water vapor mixture. The presence of air in water vapors is an issue of high concerns as it adversely affects the access of water vapors to the cold tube surface and results in a lower efficiency of HDH system. To enhance the condensation in the presence of air, a direct contact condenser was used in diffusion-driven desalination technology described by Klausner and co-workers at the University of Florida [13, 30, 31]. The heat transfer coefficient is higher for the direct contact dehumidifier but the system heat recovery is low and the energy consumption is high. Narayan et al. [32] proposed an innovative design approach to use bubble column dehumidifier for efficient condensation. In their study, the moist air is mainly condensed in a pool of cold water instead of condensing on cold surface. In all the aforementioned studies, the main focus is to improve the dehumidification process of the HDH system and very less attention is given towards the improvement of humidification process.

Humidification is one of the fundamental processes in the solar HDH water desalination system. There are many devices which can be used for the humidification purpose. These devices include spray tower, wetted wall tower, packed bed tower, and bubble column [33]. The aim of all these devices is to raise the humidity of the air by diffusion of water into unsaturated air stream. This diffusion phenomena is caused by the concentration variance between the water vapor in the air and air-water interface.

Several studies considered using spray tower as a humidification device in their HDH system. In the spray tower, water is sprayed in the form of droplets that falls under the force of gravity. Air is injected from the bottom to come in a direct contact with the falling water droplets in a counter flow arrangement. These type of devices have low humidification effectiveness due to the low water holdup. Other limitations include the use of mist eliminators which are essential to avoid the water entrainment in the air at the exit of the spray tower. Furthermore, the losses in the spray nozzles caused a high pressure drop in the water stream. Younis et al. [14], Ben-Amara et al. [18], and Orfi et al. [34] used spray tower as a humidification device and studied the effect of water-to-air mass flow rate ratio on the humidification efficiency. They varied the water-to-air mass flow rate ratio while keeping the inlet air absolute humidity and inlet water temperature constant. Moreover, the sprayed water temperature (60 ˚C) was kept less than the inlet air temperature (80 ˚C). The results showed that the air outlet absolute humidity increased with increasing the amount of sprayed water to a certain level. However, further increase in the quantity of water initiated the air cooling and condensation that resulted in the decrease of absolute humidity. This implies that air heated HDH cycle provides maximum air humidity at an optimum

water-to-air mass flow rate ratio. Therefore, use of the multi stage air heated HDH system increases the production of fresh water.

Wetted wall towers could also be used in an HDH system for air humidification purpose. In this type, thin water film flows downward on the inner perimeter to form a wetted surface along a tower length. The air stream can either flow upward or downward to have a direct contact with the falling water thin film. These towers have a higher humidification efficiency and a lower air side pressure drop as compared to other humidification towers. However, the water flow rate is restricted to a lower capacity because the thin film of water flows only on the inner perimeter of the tower. Wallis and Aull [35]used polypropylene made vertically hanging fleeces for their wetted wall humidifier. The thin film of the heated water was distributed and trickled downward along the inner perimeter of the fleeces to form a wetted surface. The dry air streamed upwards and came out saturated at the outlet of the humidifier. Orfi et al. [34] employed an improved heat and mass exchange design for a wetted wall humidifier. In their design, the water flowing velocity was reduced for better heat and mass exchange. The reduction in water flow velocity was ensured by covering the wooden vertical walls using the cotton wick. The wooden vertical walls were always kept wet using capillary force. This design improvement ensued higher humidifier performance and claimed to achieve around 100 % humidification efficiency.

The packed bed tower is a widely practiced humidification device in the HDH water desalination system owing to its better performance. It is similar to the spray towers in which water is sprayed in the form of droplets that fall under the force of gravity. However, in the packed bed tower, the packing material is used to improve the humidification efficiency. The use of packing material makes the water droplets more dispersed which

increases the area and time of contact between both water and air. However, this improvement leads to a higher pressure drop in the packed bed humidifier. Several factors affect the choice of the packing materials and their heat and mass transfer, e.g. pressure drop, durability, cost, and quality of water. Development of packing materials in the HDH systems were reported by Mirsky and Bauthier [36] and the performance of different packing materials in such systems were investigated by Aull and Krell [37]. Wallis and Aull [35] showed a gradual change of fills types in packed bed towers. Introduction of film fills caused a tremendous change by providing higher thermal performance by reducing pressure drop and increasing water to air contact area. However, older splash type fill packing is being used because all these benefits are lost pertaining to high fouling potential. In the humidifier, air comes in contact with water and humidified.

An innovative design approach is to use the bubble column humidifier. The choice of bubble column humidifier has been inspired due to higher rate of heat transfer in the liquid-gas dispersion that is usually 100 times higher as compared to single phase flow. In this humidifier, air is passed through perforated plate to form bubbles in hot water column. As the air bubbles propagate through hot water column, simultaneous heat and mass transfer take place and air comes out hot and humid at the outlet of humidifier. The bubble formation increases the time and surface of contact between air and water, which results in an improvement of humidification performance.

El-Agouz and Abugderah [38] carried out the experimental analysis of a single stage bubble column humidifier. An evaporator column of 500 mm x 250 mm square cross section was used in this experiment. The air stream is introduced by a 75 mm diameter PVC pipe having 32 holes of 10 mm diameter on both sides. The pipe was submerged in

the water and acted as a sparger to form bubbles in the pool of water. In this study, they considered the effect of different operating parameters on the vapor content difference in the air and humidifier efficiency. These operating parameters include water inlet temperature, the air inlet temperature, and the air inlet velocity. The results showed that the performance of bubble column humidifier is significantly affected by water inlet temperature and air inlet velocity. The air inlet temperature has a slight effect on vapor content difference in the air. The maximum humidification efficiency achieved for the bubble column humidifier was reported as 95 % with 222 g_w/kg_a at 75 °C of air and water temperatures.

El-Agouz [39] performed another experimental analysis of a single stage bubble column humidifier. An evaporator column of 400 mm x 300 mm square cross section was used in this experiment. The air stream is introduced by a 75 mm diameter copper pipe having 44 holes of 15 mm diameter on upper side. The pipe was submerged in the water and acted as a sparger to form bubbles in the pool of water. This experimental work aimed to analyze the effect of different operating parameters on the bubble column humidifier efficiency. These operating parameters include the water column height, the water column temperature, and the air flow rate. The results showed that the performance of bubble column humidifier is increased with the increase in water column temperature and air flow rate. The effect of water column height on the efficiency of bubble column humidifier is not significant. The maximum efficiency achieved for the bubble column humidifier was reported as 98 % at air flow rate of 14 kg/h and 85 °C of water temperatures.

Zhang et al. [40] performed the experiment on the single stage bubble column humidifier to analyze the effect of water level and air flow rate on the pressure drop and relative

humidity of air. A cylindrical column of 198 mm diameter was used as an evaporator chamber in this experiment. A sieve plate of 8 mm thickness having 91 holes of 1 mm diameter was used as sparger. This experimental work aimed to achieve the higher water content at the exit of humidifier with less pressure drop and less blower power consumption. The results showed that the increase in water level and air flow rate caused greater pressure drop and higher blower energy consumption. The moisture contents at the exit of humidifier were increased with the increase of water and air temperature. In the range of experimental operating conditions, the experimental results showed that the air reached the 100 % relative humidity.

In all the aforementioned experimental investigation of the bubble column humidifier, water is heated by an electric heater that limits the use of these devices in remote areas where electricity availability is scarce. Therefore, a novel bubble column humidifier is proposed that is operated through solar thermal energy as the main source of energy input. In this novel humidifier, the absorber plate and bubble column were incorporated in a single frame design, as shown in Figure 8. The absorber plate was painted black and titled to an angle equal to the latitude of Dhahran to absorb the maximum solar radiations. This design improvement has the following advantages:

- The tilted absorber plate acts as a sloped surface to create a thin film of water over the absorber plate. The minimum water depth over the absorber plate leads to a better heat transfer and a higher water temperature is achieved at the downstream of absorber plate. It also results in a significantly low pressure drop in the air-side.
- The hot humid air at the exit of the bubble column further passed over the thin film

of hot water flowing over absorber plate to absorb more moisture and higher vapor contents are achieved at the exit of humidifier. In other words, the humidifier heats both air and water simultaneously and air humidification process occurs throughout the full path of the air inside the humidifier.

- This proposed humidifier have a direct solar thermal heating. Subsequently, it can be located in remote areas, where there is a shortage in electricity.

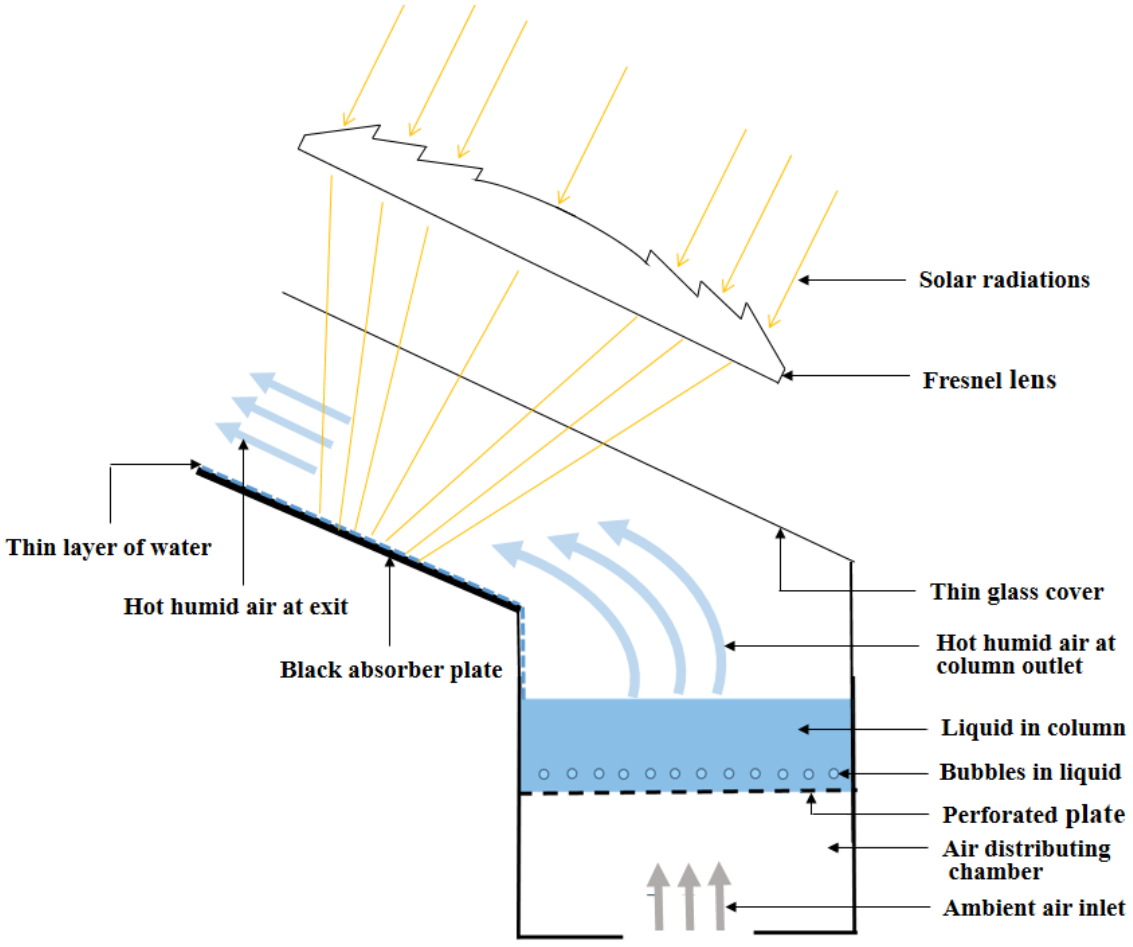

Figure 8 Bubble column humidifier incorporated with absorber plate.

CHAPTER 3

DESIGN OPTIMIZATION OF THE HUMIDIFIER

In HDH desalination systems, bubble column humidifier is not practiced for humidification purpose so far. There are very few studies that investigate the bubble column humidifier for HDH water desalination system. Therefore, there is a need to explore the potential of bubble column humidifier as an efficient decentralized small scale water desalination system. The best approach to analyze the bubble column humidifier is to build the experimental unit and examine it with different operating conditions. However, it is very important to perform the design optimization study before building the experimental setup because it will save time and cost. Therefore, theoretical modeling of the bubble column humidifier is performed in order to identify the influence of important operating parameters on the performance of the proposed humidifier design.

3.1 Theoretical modeling for bubble column

In the bubble column, air is passed through perforated plate to form bubbles in the hot water column as shown in Figure 9. As the air bubbles propagate through hot water column, simultaneous heat and mass transfer take place and air comes out hot and humid at the outlet of bubble column.

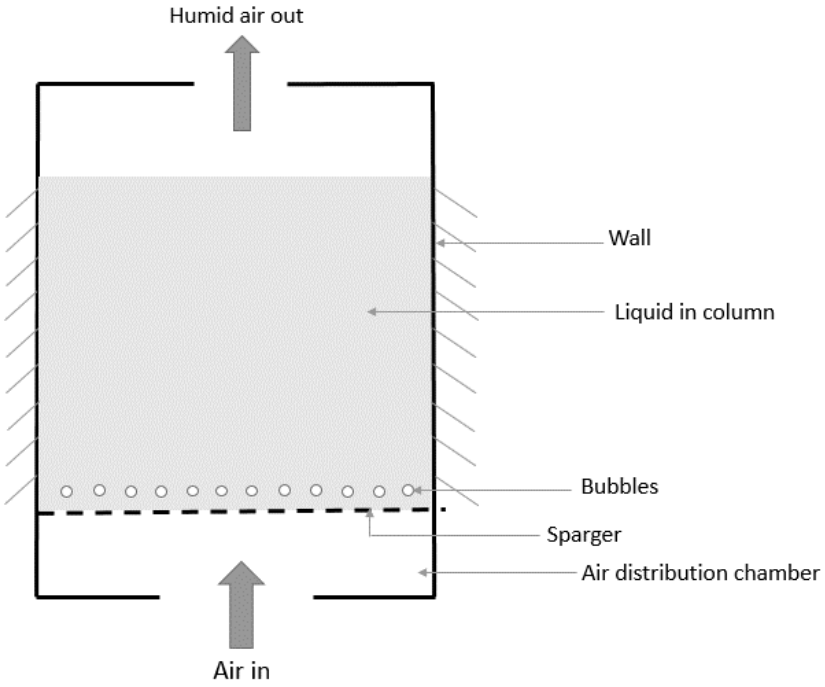

Figure 9 Air humidification in bubble column.

For the bubble column humidifier modeling, it is important to understate the mechanism of heat transfer in a bubble column. Heat transfer to the liquid-gas diffusion is studied by many researcher and they suggested different models to analyze the effect of heat transfer coefficient on different parameters. Kobel et al. [41] studies showed that the liquid properties and gas velocity have the main impact on heat transfer coefficient. Kast [42]

studied the effect of rising a bubble in the fluid and described that the fluid element in the front of the rising bubble moves toward the wall due to the radial momentum that it received by uprising the bubble. This radial momentum of the fluid breaks the boundary layer at the wall and the boundary layer assumption is not valid, especially in the case of high bubbles concentration. Conversely, the uprising bubble form a wake underneath it that sucks the fluid radially. The fast radial exchange flow due to uprising bubble results in a capacitive heat transfer. This mechanism is illustrated in Figure 10.

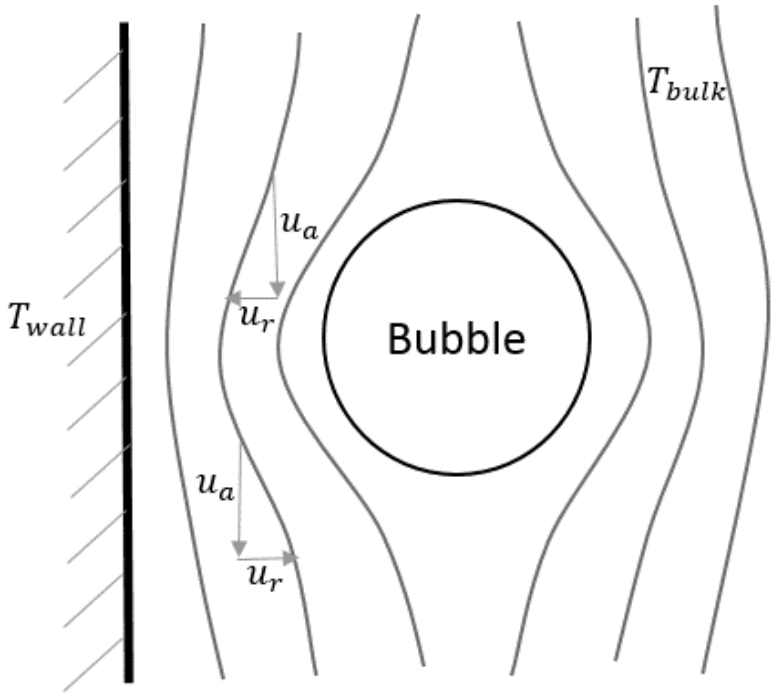

Figure 10 Flow around rising bubble.

3.2 Theoretical modeling for bubble column

The mathematical modelling for a direct contact heat and mass transfer in the bubble column humidifier includes the following assumptions:

- The water in a bubble column is at a uniform temperature, T_{bulk}.
- The liquid-gas interface in a water column experience the same temperature as the water bulk temperature.
- Bubbles experience a uniform temperature in the water column as the residence time of bubbles in water column is much lower than the required time to change the temperature of water.

The fluid will be in contact with the uprising bubble for a certain period of time. Hibbies Surface Renewal Theory explains the behavior of the uprising bubble with respect to time [43]. According to Hibbies Surface Renewal Theory, the mass is transported when it is in contact with water and the contact time (residence time) is equal roughly the same time required for the bubble to move one diameter further. Unsteady heat diffusion takes place adjacent to the surface in the fluid element that can be described as follow:

$$\frac{\partial T}{\partial t} = \alpha \frac{\partial^2 T}{\partial^2 x} \tag{10}$$

This problem is defined by the boundary conditions that corresponds the temperature T as the wall temperature at x = 0 for all values of time, the bulk (column) temperature as starting temperature for all values of x, and bulk temperature for all values of time when x = ∞. The last condition requires the infinite depth of the fluid and very short time of contact.

- $T=T_{wall}$ $x = 0$ $t \geq 0$
- $T=T_{bulk}$ $x > 0$ $t = 0$
- $T=T_{bulk}$ $x = \infty$ $t > 0$

Laplace transformation of equation (10) with boundary conditions results in instantaneous temperature profile that is used to get the following expression of heat flux:

$$q = \frac{2}{\sqrt{\pi}}\sqrt{\frac{k\rho C_p}{t}}(T_{wall} - T_{bulk}) \tag{11}$$

where, t is the renewal time calculated as

$$t = \frac{d_b}{V_c} \tag{12}$$

To calculate the surface renewal time, we need to evaluate the bubble diameter d_b and liquid circulation velocity V_c. The bubble diameter can be calculated by the following expression given by Miller DN [44]

$$d_b = \left\{\frac{6\sigma d_o}{(\rho_l - \rho_g).g}\right\}^{1/3} \tag{12}$$

Liquid circulation velocity can be calculated by the following expression suggested by Field and Rahimi [45]

$$V_c = 1.36\{gH(V_g - \varepsilon V_b)\} \tag{13}$$

where, ε is the volumetric gas holdup that can be calculated as follow:

$$\varepsilon = \frac{V_g}{0.3 + 2V_g} \tag{14}$$

Bubble velocity V_b, can be calculated from the following expression based on Mendelson's wave equation [46]:

$$V_b = \sqrt{\frac{2\sigma}{\rho_l d_b} + \frac{g d_b}{2}} \tag{15}$$

3.2.1 Heat and Mass Transfer

A thermal resistance model that includes both heat and mass transfer associated with air humidification in the bubble column is shown in Figure 11.

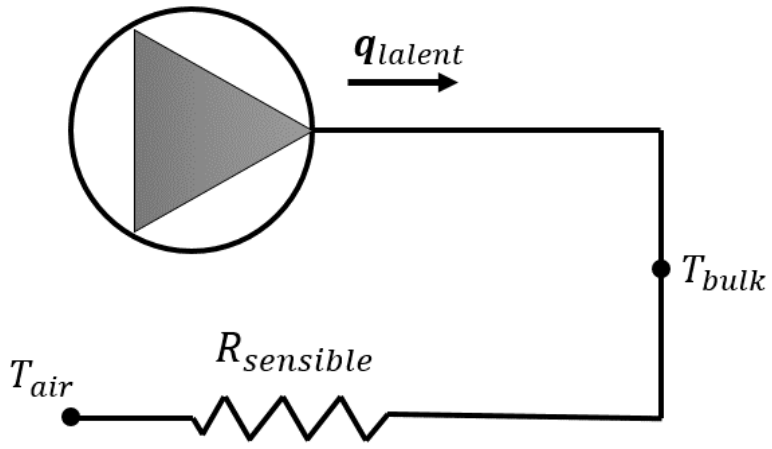

Figure 11 Thermal resistance model for bubbler humidifier.

The two temperature nodes in the thermal resistance model represents the average air temperature of the bubbles (T_{air}) and the bulk temperature of the liquid column (T_{bulk}).

Simultaneous heat and mass transfer is taking place between these two temperature nodes. The thermal resistance $R_{sensible}$ is responsible for the heat transfer and heat source q_{latent} symbolizes the mass transfer between the fluid and bubbles. The latent heat flux through diffusion of water vapors to bubbles and sensible heat flux via thermal resistance $R_{sensible}$ sum up to give overall heat flux *(q)* between the liquid and bubbles. It is defined as

$$q = q_{latent} + q_{sensible} \tag{16}$$

Heat flux due to evaporation is given by following equation

$$q_{latent} = j.h_{fg} \tag{17}$$

Where, *j* is the mass flux calculated as

$$j = \frac{\dot{m}_a}{A}(\omega_o - \omega_i) \tag{18}$$

The sensible heat flux ($q_{sensible}$) via thermal resistance $R_{sensible}$ is calculated as

$$q_{sensible} = \frac{T_{lmtd}}{R_{sensible}} \tag{19}$$

where, T_{lmtd} is the log mean temperature difference calculated as

$$T_{lmtd} = \frac{(T_{bulk} - T_{a,i}) - (T_{bulk} - T_{a,o})}{ln\left[\frac{(T_{bulk} - T_{a,i})}{(T_{bulk} - T_{a,o})}\right]} \tag{20}$$

$R_{sensible}$ is the thermal resistance associated with the sensible heat transfer from the liquid column to bubbles and can be calculated as

$$R_{sensible} = \frac{1}{h_t A} \tag{21}$$

where, h_t is the heat transfer coefficient linked with $R_{sensible}$ that can be calculated by introducing Lewis factor. Lewis factor linked the heat transfer to the mass transfer as follow:

$$h_t = Le_f\left(\rho c_p k_l\right)\frac{a_s vol}{A} \tag{21}$$

The area in the heat transfer coefficient expression is normalized by introducing specific interfacial area (a_s) of bubbles. The specific interfacial area (a_s),can be measured by the following expression presented by Miller DN [44]

$$a_s = \frac{6\varepsilon}{d_b} \tag{22}$$

Le_f is the Lewis factor calculated as

$$Le_f \cong Le^{2/3} \tag{23}$$

where, Le is Lewis number for air-water system and defined as

$$Le = \frac{\alpha}{D_{AB}} \tag{24}$$

k_l is the mass transfer coefficient linked with the latent heat and can be calculated as

$$\frac{1}{k_l} = \left(\frac{1}{k_{l,1}} + \frac{1}{k_{l,2}}\right)^{-1} \tag{25}$$

where, $k_{l,1}$ and $k_{l,2}$ are mass transfer resistences that can be calculated by the expressions presented by Narayan et al. [47] which are defined as

$$k_{l,1} = \frac{D_{AB}}{d_b/2} \tag{26}$$

$$k_{l,2} = \frac{2}{\sqrt{\pi}}\sqrt{\frac{D_{AB}}{t}} \tag{27}$$

3.3 Results and Discussion

The aforementioned equations are simultaneously solved using Engineering Equation solver (EES). The effect of some important parameters that include air superficial velocity, water column height, and perforated plate hole diameter on heat and mass transfer is analyzed. The influence of air superficial velocity on the heat transfer coefficient at different water column height is presented in Figure 12. The results showed that the air superficial velocity strongly influence the heat transfer coefficient in the bubble humidifier and heat transfer coefficient value increases as the air superficial velocity increases. The trend shows the remarkable resemblance with many researchers that investigate the effect of air superficial velocity on heat transfer coefficient in bubble column [48, 49]

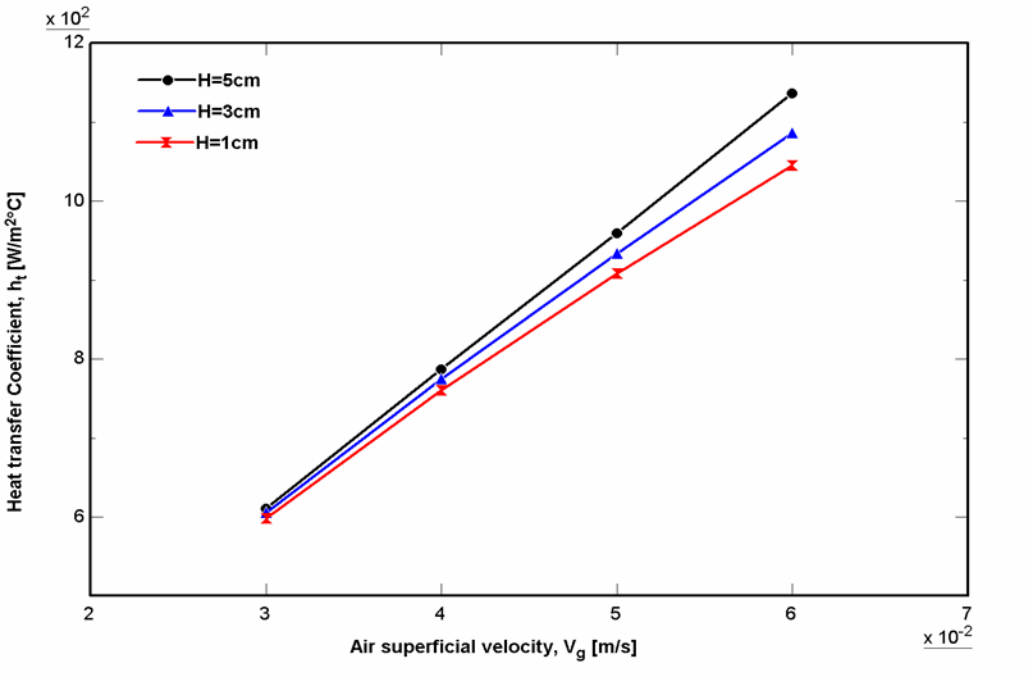

Figure 12 Influence of air superficial velocity on heat transfer coefficient.

In the heat transfer coefficient modeling, we introduced the Lewis factor that is used in governing equations of simultaneous heat and mass transfer. The influence of air superficial velocity on mass transfer coefficient is also analyzed along with the heat transfer coefficient and presented in Figure 13. Findings indicated that the increase in superficial velocity increases the mass transfer coefficient that is directly linked with the heat transfer coefficient via Lewis factor. Hence, both the heat and mass transfer coefficient are significantly increased as the air superficial velocity increases.

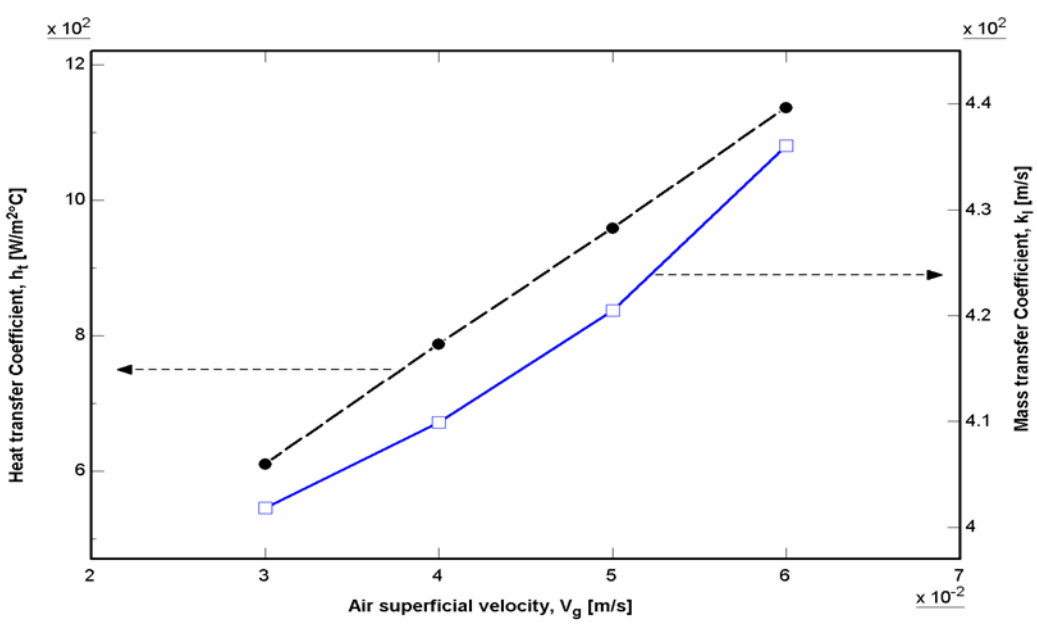

Figure 13 Influence of air superficial velocity on heat and mass transfer coefficient.

The total heat flux in the bubble column humidifier is the sum of the sensible heat flux that is linked with heat transfer coefficient and latent heat flux that is linked with mass transfer coefficient. The effect of perforated plate hole diameter and water column height on total heat flux is shown in Figure 14. The results showed that the increase in perforated plate hole diameter and water column height slightly decreases the heat transfer coefficient. Although, the influence of the perforated plate hole diameter and liquid column height on the total heat flux is not much significant but it is worth mentioning their trends as they provides vital information in designing the bubble column humidifier.

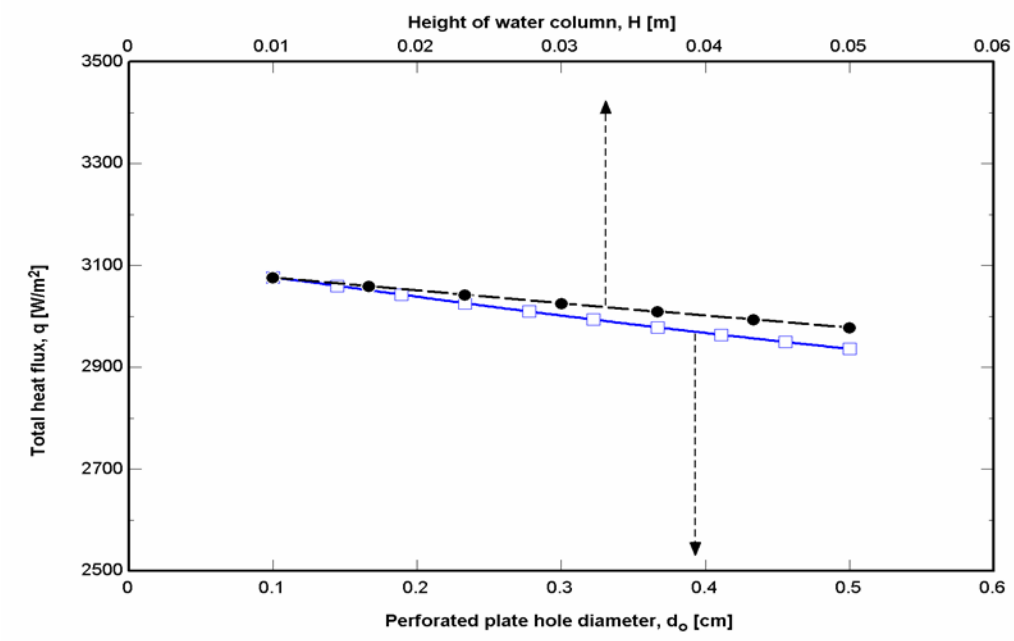

Figure 14 Influence of perforated plate hole diameter and water column height on total heat flux.

CHAPTER 4

EXPERIMENTAL INVESTIGATION OF THE HUMIDIFIER

4.1 Experimental Setup

A laboratory scale setup for the proposed bubble column humidifier is designed and built as shown in Figure 15.

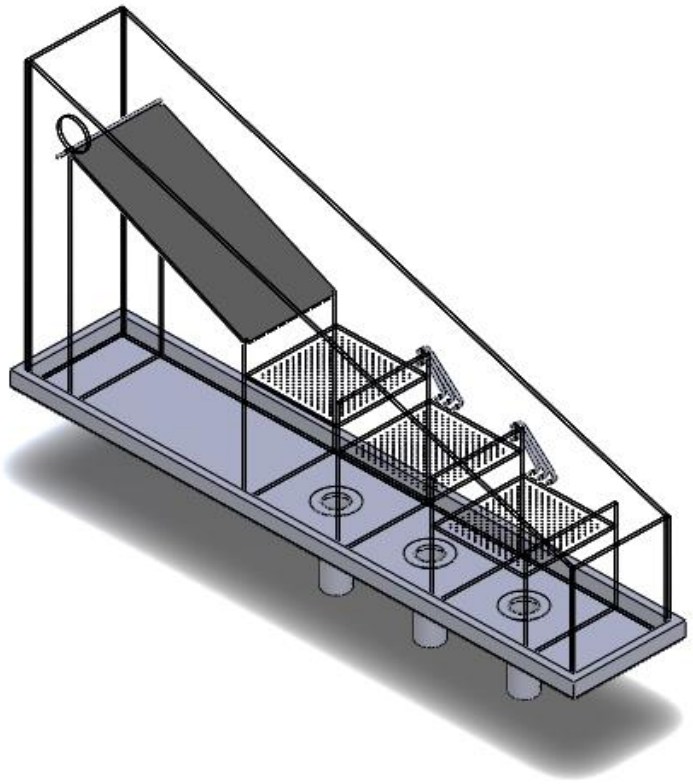

Figure 15 3-D design of the proposed multistage stepped bubble column humidifier.[5]

[5] Courtesy of Al-Hassan Qusay Mahmoud, an undergraduate student from ME department of KFUPM.

The frame of the experimental setup was constructed of 10 mm thick Plexiglas sheet. Plexiglas is a transparent thermoplastic material that has a thermal conductivity of 0.19 W/m.K. The use of such transparent material is advantageous in a sense that it allows the observer to see what is happening inside the unit while performing the experiment. Another advantage of using the Plexiglas is its low thermal conductivity that reduces the heat loses from the system. Plexiglas sheet is also used to build the bubble column of 300 mm x 300 mm cross section and 400 mm height. A perforated plate is used as a sparger to form the bubbles in a pool of hot water in the bubble column. The perforated plate is made of a 2 mm thick black acrylic Plexiglas 300 mm x 300 mm in cross section. The perforated plate splits the bubble column into lower and upper compartments. Air is introduced by a 400 W adjustable blower to the lower compartment of the bubble column through a 25 mm diameter CPVC pipe. The lower compartment of the bubble column is used to distribute the air stream uniformly through the perforated plate. The upper compartment of the bubble column is used as a pool for hot water. Figure 16 shows the constructed experimental setup and figure 17 shows the air bubbling in the water column.

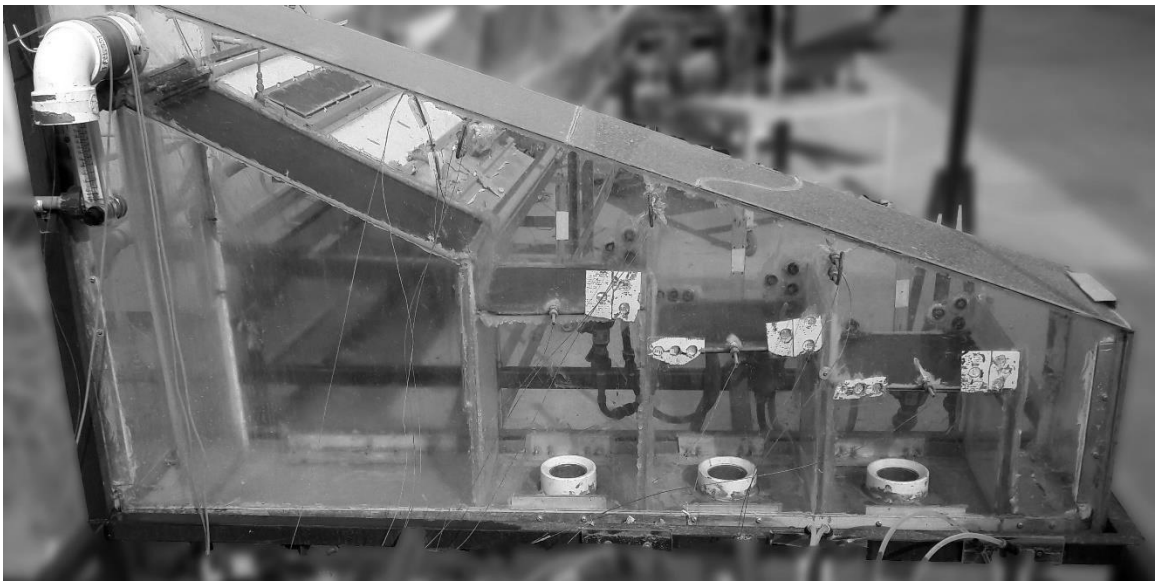

Figure 16 Photograph of the experimental setup.

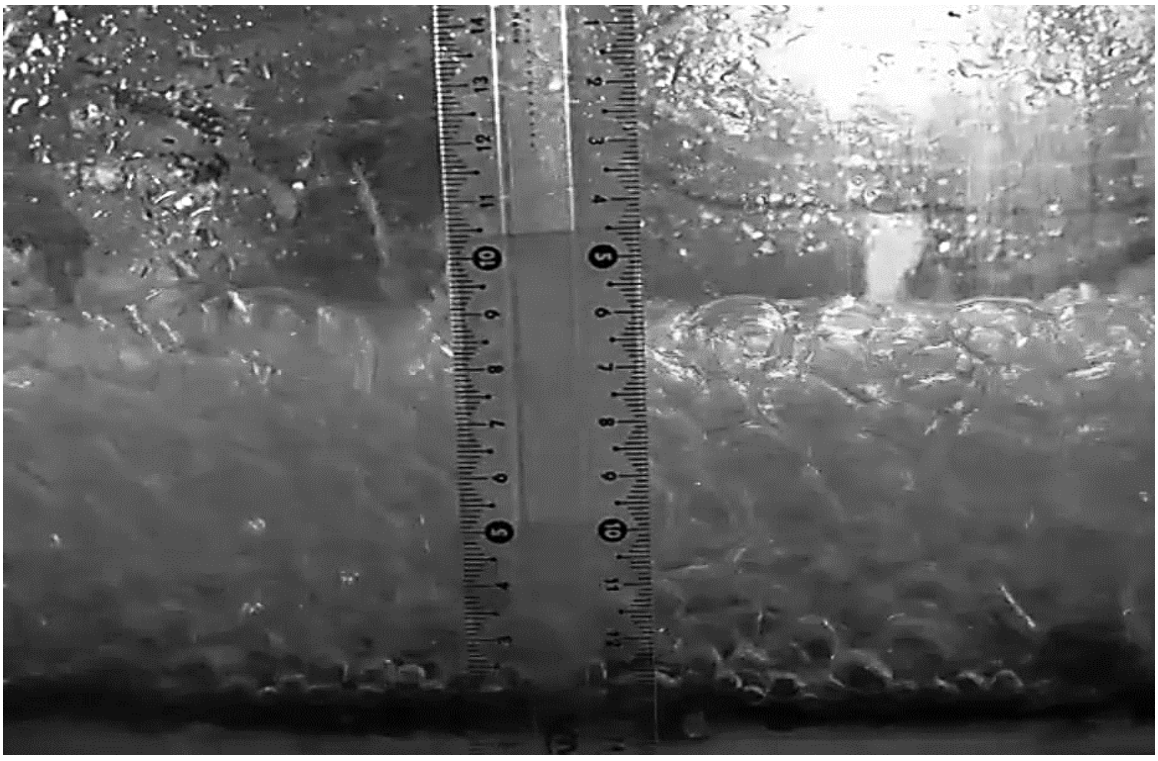

Figure 17 Air bubbling in the water column.

4.1.1 Experimental Procedure

The schematic diagram of the constructed multistage stepped bubble column humidifier along with the installed instrumentations is shown in Figure 18.

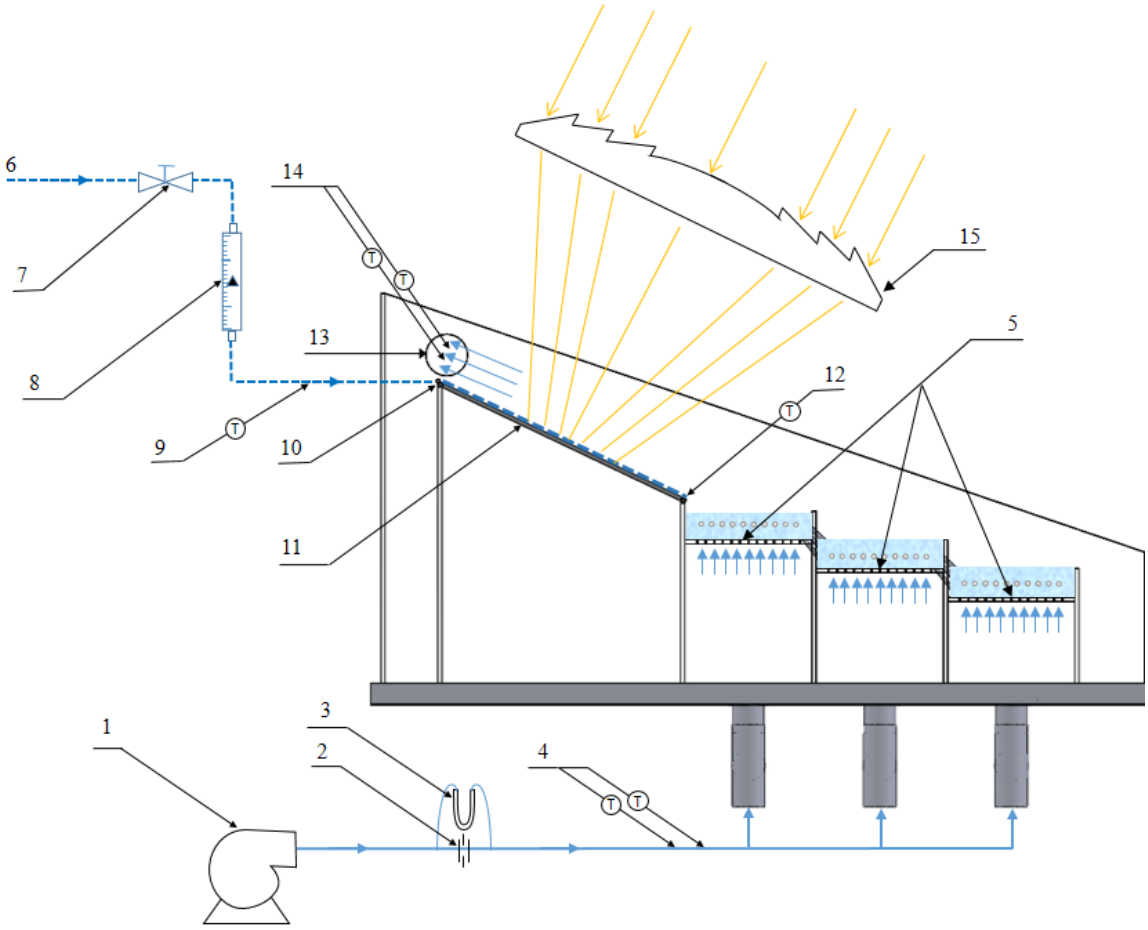

Figure 18 Schematic diagram of experimental setup.

(1) Air blower; (2) Orifice meter; (3) Manometer;
(4, 9, 12, 14) Thermocouple; (5) Perforated plate, (6) Water supply;
(7) Throttle valve; (8) Rotameter; (10) Water inlet;
(11) Absorber plate, (13) Air outlet; (15) Fresnel lens

4.2 Instrumentation

K-type thermocouples are used to measure water temperature as well as air dry-bulb/wet-bulb temperatures. Thermocouple probes are calibrated before installing them in the experimental setup. The volumetric flow rate of the water is measured by using FL5000 series rotameter of OMEGA. The volumetric flow rate of air is measured by an orifice meter connected to a manometer to read the pressure drop across the orifice plate. The orifice meter is designed and installed according to the ISO 5167 benchmark design recommendations [50]. The design of the orifice plate is shown in Figure 19.

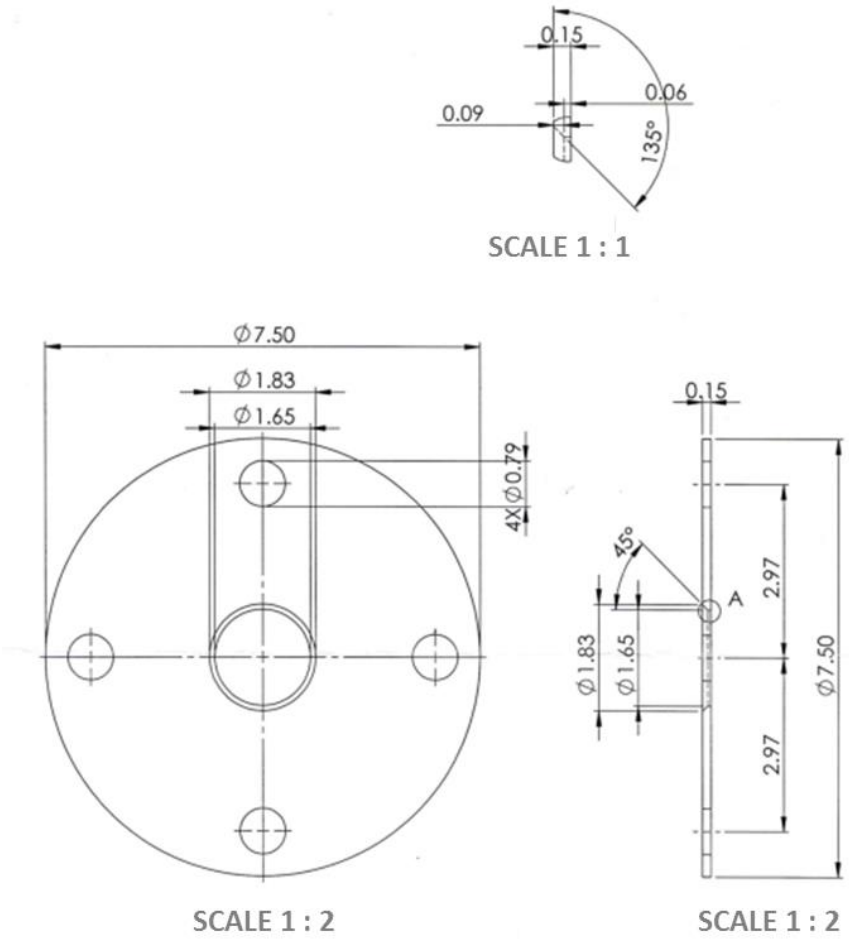

Figure 19 Design of the orifice plate.

4.2.1 Data Acquisition System

A data acquisition consisting of five NI 9213 thermocouple input modules installed in a NI cDAQ-9178 USB chassis is connected to a computer. Thermocouples measurements are displayed and stored using a Labview program. Real-time processed thermocouple readings are measured every 2 seconds and the average temperatures of every 5 minutes were recorded using the developed Labview program.

4.2.2 Error and Uncertainty

Thermocouple probes are calibrated before installing them in the experimental setup. Errors in the measurement devices is calculated as the ratio of the device least count to the minimum value of the output measured by that instrument. The uncertainty in the measurements is calculated as the root sum square of the fixed error of the instrumentation and the random error observed during different measurements [51]. The measurement devices along with their range, accuracy, and uncertainty are summarized in Table 4.

Table 4 Measurement devices along with their range, accuracy, and uncertainty.

Properties	Instruments	Range	Accuracy	Uncertainty
Temperature	NI cDAQ-9178, K-Type thermocouple	-267 – 316 °C	± 0.1 °C	± 0.05 °C
Relative humidity		0 - 100 % RH	± 0.1 % RH	± 0.93 %
Pressure	U-Tube manometer	0.1 - 50 cm H_2O	± 1 mm	± 0.1 cm H_2O
Water flow rate	Rotameter	1 - 7 LPM	± 5 % of full scale	± 0.2 LPM
Water column height	Graduate level	0.1 - 20 cm	± 1 mm	± 0.25 cm
Air superficial velocity	Orifice meter	10-50 cm/s	± 1 cm/s	± 0.79 cm/s
Solar radiations	Pyranometer	0-2000 W/m^2	± 5 % of full scale	± 1 W/m^2

4.3 Experimental investigation of single stage humidifier

The performance of the proposed humidifier design is investigated experimentally in a single stage configuration. The influence of important design and operating parameters on the performance of humidifier are discussed in details. The terminologies used in the performance analysis of the bubble column humidifier is defined as follow:

Air superficial velocity (Vsg) is defined as the ratio of volumetric flow rate of the air to the cross sectional area of the bubble column.

$$V_{sg} = \frac{Volumetric\ flow\ rate\ of\ air}{Area\ of\ the\ bubble\ column}$$

Open area ratio of the perforated plate is defined as the ratio of the perforation area to the plate area.

$$Open\ area\ ratio = \frac{Total\ area\ of\ holes}{Area\ of\ plate}$$

Vapor content difference is define as the difference of absolute humidity in the air between the inlet and exit state of the humidifier.

$$Vapor\ content\ differenec = \Delta\omega = \omega_{out} - \omega_{in}$$

The ratio of actual vapor content difference to maximum vapor content difference defined the humidification efficiency of the humidifier and is calculated as:

$$Humidification\ efficiency = \frac{\Delta\omega}{\Delta\omega^{ideal}} = \frac{\omega_{out} - \omega_{in}}{\omega_{out}{}^{sat} - \omega_{in}}$$

Where ω_{out} is the absolute humidity of the air at the exit of the humidifier; ω_{in} is the absolute humidity of the air at the inlet of the humidifier; and ${\omega_{out}}^{sat}$ is the saturated absolute humidity of the air at the outlet of the humidifier. The saturated absolute humidity corresponds to an ideal condition in which air at the outlet is saturated at water inlet temperature.

4.3.1 Influence of geometry of the perforated plate

The optimum design consideration of the perforated plate is an important aspect in the experimental investigation of the bubble column humidifier. In the design of the perforated plate, the perforations geometric configuration should be optimized to reduce air pressure drop. Another important aspect in the perforated design is to avoid water leakage through the perforations. Keeping in mind the aforementioned aspects, three different perforated plates were designed and tested to analyze the effect of perforation geometry on the performance of the bubble column humidifier. The geometric features of the three perforated plates used during the experimental work are listed in Table 5.

Table 5 Geometric features of different designs of perforated plate tested during experimentation.

	Number of holes	Hole Diameter (mm)	Pitch size (mm)	Open Area Ratio (%)
Design 1	105	3	25	0.77
Design 2	105	2	25	0.33
Design 3	149	2	20	0.49

Three different designs of perforated plates were tested at different air superficial velocities. Results are shown in Figure 20. The minimum pressure drop is achieved using design 1 due to the bigger hole diameter and higher open area ratio compared to the other two designs. However, water leakage was observed from the perforations during the

experiments that showed that this design is not useful. To overcome the problem of the water leakage, design 2 was tested with the same number of holes as in design 1, i.e., 105 holes; but the hole diameter was reduced from 3 mm to 2 mm. Design 2 was successful in preventing water leakage from the perforations but the pressure drop was high. The high pressure drop is due to the low open area ratio in design 2. Therefore, design 3 was tested with 149 holes with 2 mm hole diameter. The higher number of holes increased the open area ratio and reduced the pressure drop compared to design 2. Moreover, no leakage was observed with design 3 during the experiment. Therefore, design 3 was selected as the best choice for our experimental setup. The perforated plate dimensions and hole geometry of design 3 are shown in Figure 21. The perforated plate is 300 mm x 300 mm in cross section and it consists of 149 holes, 2 mm-diameter each. The holes are made in equilateral triangular configuration where the distance between any two adjacent holes is 20 mm. The holes are distributed 40 mm away from the boundary of the perforated plate to avoid the shear stresses near the wall of the bubble column.

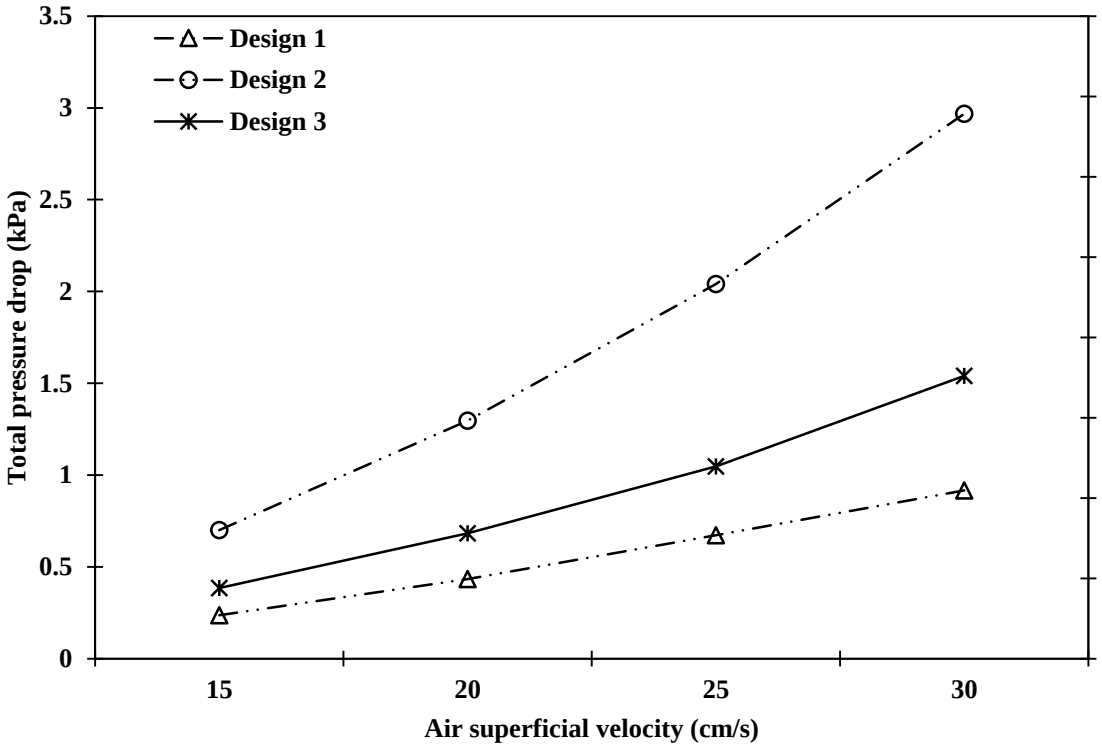

Figure 20 Influence of air superficial velocity on the dynamic pressure drop under different design considerations of perforated plate.

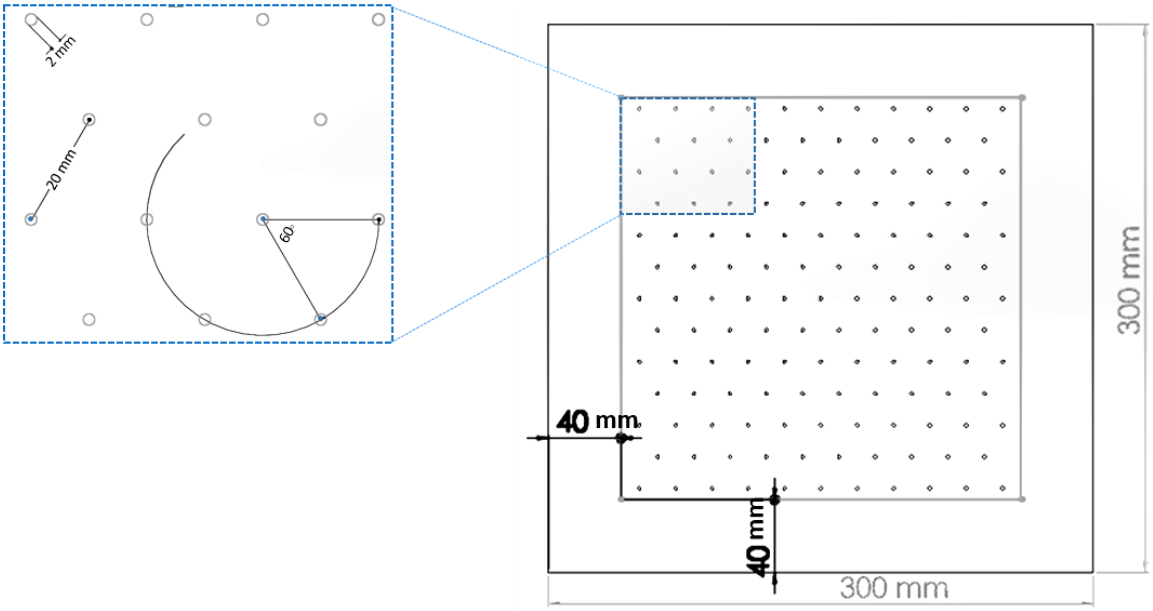

Figure 21 Dimensioning and geometric features of the selected perforated plate.

Figure 22 shows the effect of water column height on the total air pressure drop at different air superficial velocities. The figure shows that the minimum pressure drop is attained at the lowest water column height of 1 cm and with 15 cm/s air superficial velocity. Increasing water column height to 3 cm and then to 5 cm while keeping the air superficial velocity at 15 cm/s results in a significant increase in the pressure drop. Furthermore, the air superficial velocity at 15 cm/s is not sufficient to completely overcome the static pressure head of the 5 cm water column height such that some water leaked through the perforations. Therefore, air superficial velocity at 15 cm/s is not taken into consideration for further investigations. The maximum pressure drop is monitored with a higher air superficial velocity of 30 cm/s. On contrary to the air superficial velocity of 15 cm/s, there is a slight increase in the pressure drop at higher water column heights.

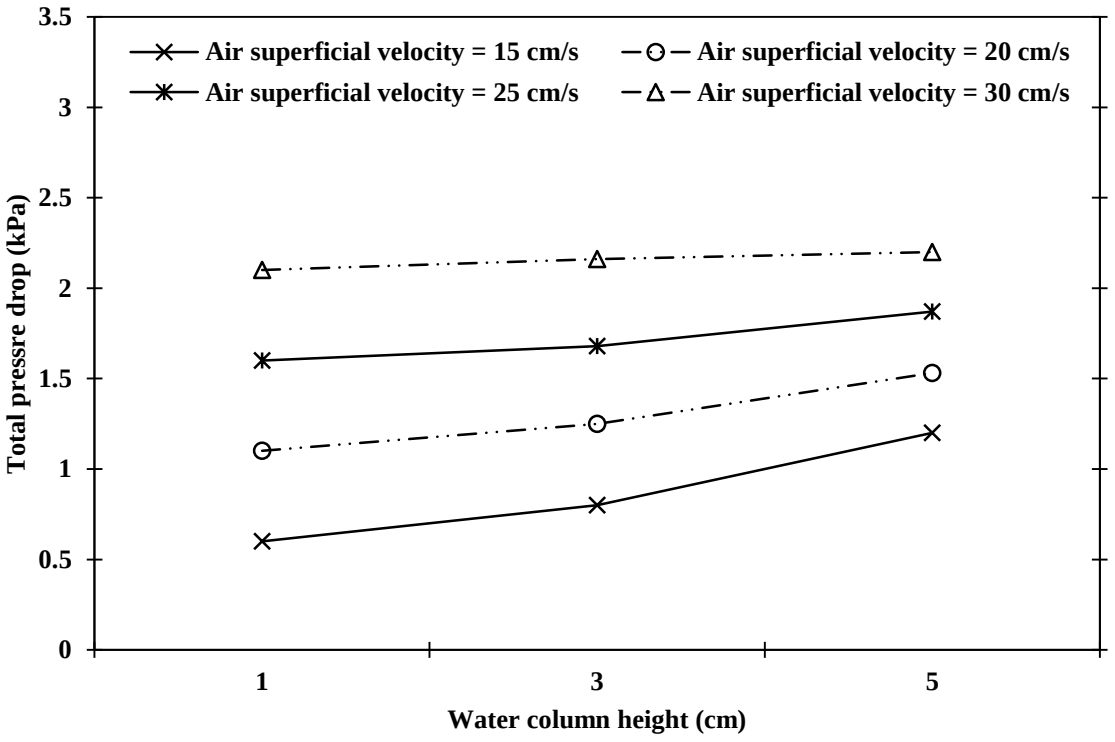

Figure 22 Effect of water column height on the total pressure drop at different air superficial velocities.

4.3.2 Influence of Air Superficial Velocity

The investigation of varying air superficial velocity is one of the major operating parameters to optimize the performance of bubble column humidifier. As the core objective of the humidifier is to effectively humidify the air, the amount of vapor contents in the moist air (absolute humidity) at the exit of humidifier was investigated at different air superficial velocities. Figure 23 shows the absolute humidity of air at the inlet of the proposed humidifier design, exit of the bubble column, and outlet of the proposed humidifier design at different air superficial velocities. The air is induced to the humidifier with the help of the blower that sucks the air from the atmosphere. The absolute humidity of the inlet air is dependent on the real time atmospheric conditions and it is almost constant during the particular experimental analysis. However, the absolute humidity of the moist air at the exit of the bubble column and outlet of the humidifier is increased with the increase in the air superficial velocity. The reason of higher absolute humidity at higher air superficial velocity is attributed to the formation of more bubbles of comparatively larger size that provides larger interfacial area. Consequently, better heat and mass transfer takes place in the bubble column part of the humidifier.

Findings also reveal that the absolute humidity of the air significantly increased at the exit of the bubble column as compared to its condition at the inlet. The significant increase in the absolute humidity is attributed to the higher rate of heat and mass transfer in the bubble column. The humid air at the exit of the bubble column further passed over the thin film of hot water flowing over the absorber plate to absorb some moisture and, consequently, the absolute humidity is further slightly increased. The slight increase in the absolute humidity is due to the lower available potential of the moist air to absorb more moisture as the moist

air at the exit of the bubble column is enriched with moisture contents and close to its saturation point. The moist air reaches the water inlet temperature and comes out saturated at the exit of the humidifier.

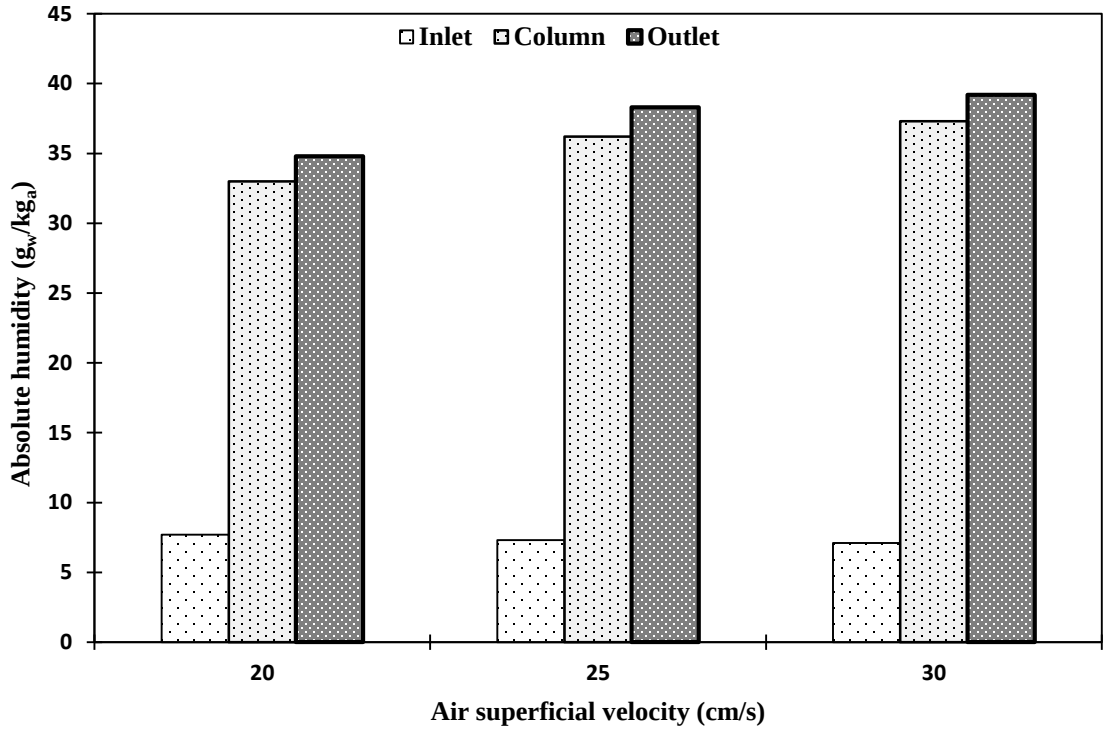

Figure 23 Influence of air superficial velocity on the absolute humidity.[6]

[6] Measurment taken on 10 June, 2015 at 11 am at water column height of 3 cm.

4.3.3 Influence of Solar Radiations

The proposed humidifier design is novel in terms of its ability to have a direct solar thermal heating. In this humidifier, the absorber plate and bubble column were incorporated in a single frame design. The absorber plate was painted black and titled to an angle equal to the latitude of Dhahran to absorb the maximum solar radiations. Moreover, the tilted absorber plate also acts as a sloped surface to create a thin film of water over the absorber plate. The minimum water depth over the absorber plate leads to a better heat transfer and a higher water temperature that is achieved at the exit of absorber plate. However, this design improvement is highly influenced by the availability of the solar radiations. Figure 24 shows the performance of the humidifier in terms of the absolute humidity at the exit of the bubble column and the outlet of the proposed humidifier design at different solar irradiances. Results indicate that the absolute humidity of air is increased at higher solar radiations. Higher solar radiations provide greater amount of the heat to black absorber plate and increase the water temperature. The increase in the water temperature enhances the moisture absorption ability of air and, consequently, higher humidity ratio is achieved at the outlet of humidifier.

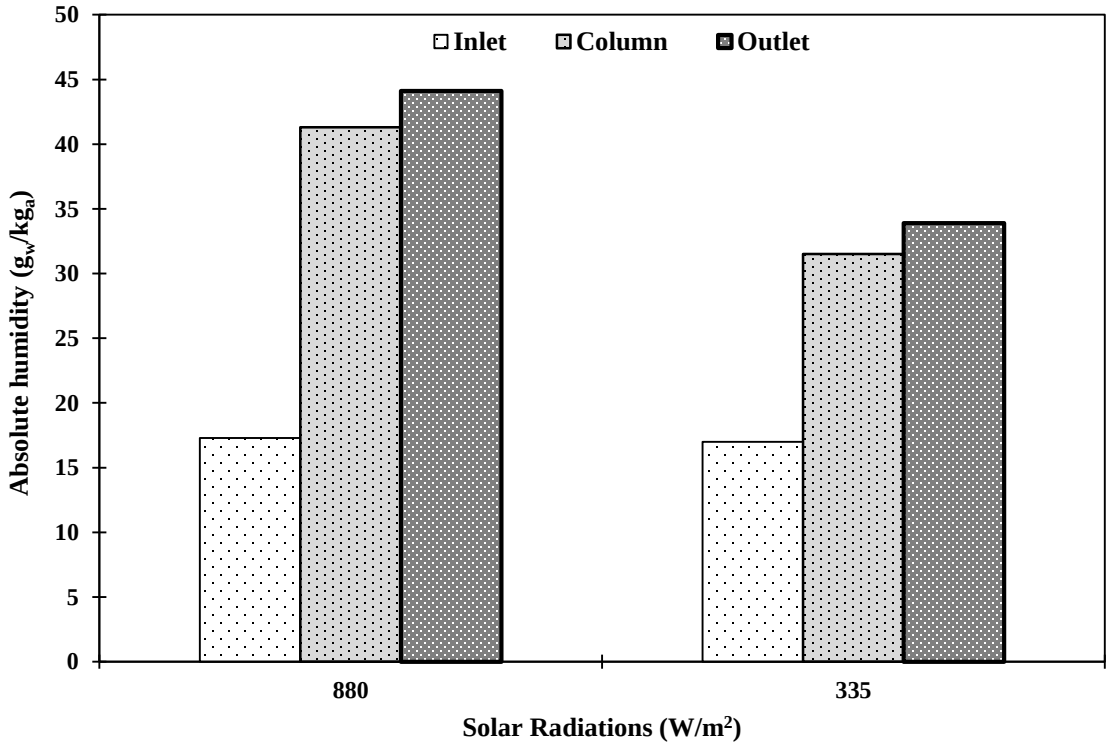

Figure 24 Influence of solar radiations on the absolute humidity.[7]

[2] Measurment taken on 8 August, 2015 at 11 am and 4 pm at water colum height of 3 cm and air superficial velocity of 30 cm/s.

4.3.4 Influence of inlet Relative Humidity

The influence of the inlet air relative humidity on the performance of humidifier is an important aspect as it signpost the optimum performance operating conditions for its possible integration with a dehumidifier. Therefore, the performance of the proposed humidifier design was analyzed at different relative humidity of the inlet air. Experiments were performed in the month of June and August to have the real time climatic variations in the relative humidity of the inlet air. Figure 25 shows the influence of relative humidity of the inlet air on the performance of the humidifier design in terms of humidification efficiency and absolute humidity achieved at the exit of the humidifier. Findings reveal that the absolute humidity of the moist air at the exit of bubble column and the outlet of the humidifier is almost same in the month of June and August. However, the absolute humidity of the air at the inlet is less in June as compared to August. This is due to the lower relative humidity of the inlet air in the month of June as compared to August. Although, the absolute humidity of the moist air at the exit of the bubble column and the outlet of the humidifier is almost same, the air vapor content difference between the outlet and inlet of the humidifier is higher in the month of June as compared to August. The reason of attaining a higher vapor content difference in the month of June is the lower relative humidity of the inlet air that provide more potential to absorb moisture as compared to the air with high relative humidity. This higher potential of absorbing moisture leads to a higher humidification efficiency. This analysis is very useful for optimizing the performance of HDH system under close air or open air configuration. In close air HDH system, the air follow the close loop in which the air at the exit of dehumidifier is again

introduced into the humidifier. The analysis signposts the importance of highly efficient dehumidifier that can extract the maximum amount of water vapors out of the moist air and provides dry air at the exit of a dehumidifier. This dry air is feed back to the humidifier and has more potential to absorb moisture as compared to the moist air. This higher potential of absorbing moisture leads to a higher humidification efficiency and, consequently, an improved HDH system is obtained. This study also provide useful information aimed at optimum operating conditions for an open air HDH systems. In this configuration, fresh air is introduced at the inlet of the humidifier for each HDH cycle and discharged to the surroundings from the exit of dehumidifier. In an open air system, the air should be dried before feeding it to the humidifier for improved humidification process.

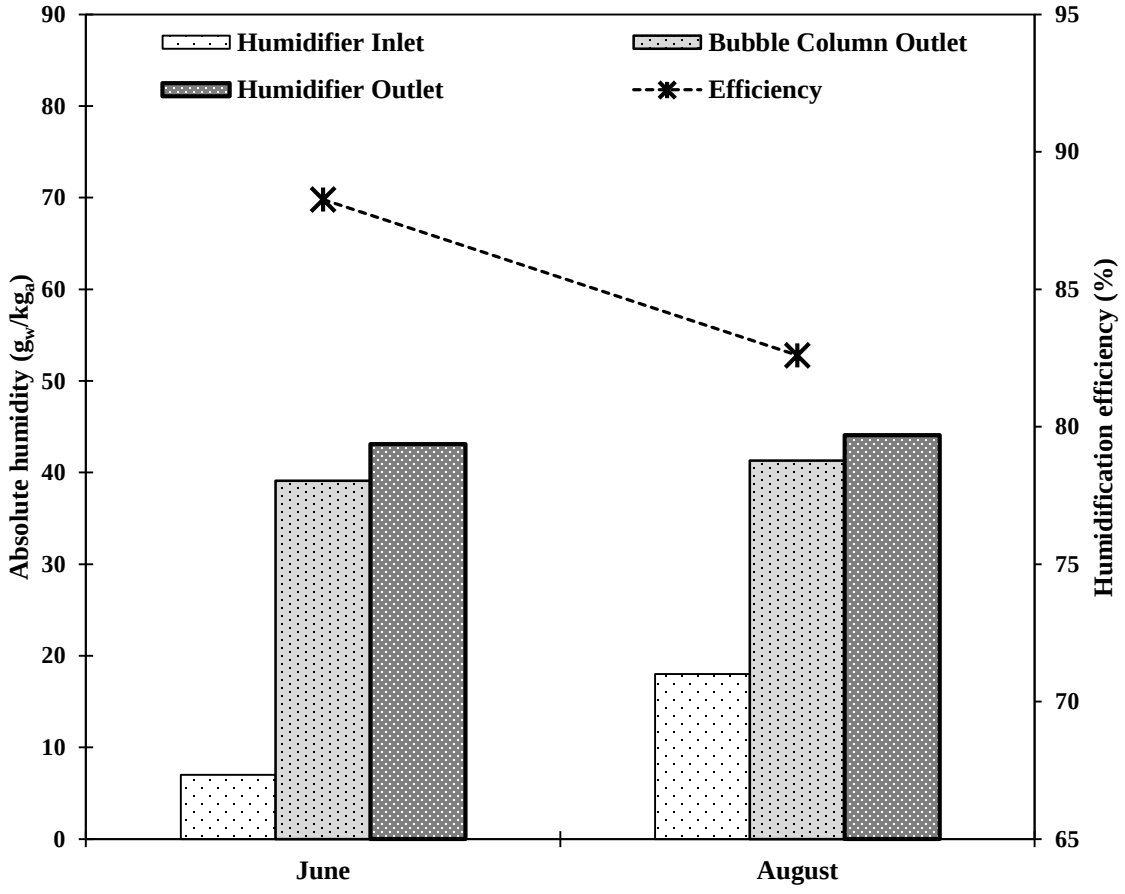

Figure 25 Influence of relative humidity on the absolute humidity and humidification efficiency.[8]

[8] Measurment taken on 10 June and 8 August, 2015 at 11 am at water column height of 3 cm and air superficial velocity of 30 cm/s.

4.3.5 Influence of Water Temperature

The major advantage of the proposed humidifier is its ability to have direct solar thermal heating, the day round performance of the system was tested under climatic conditions of Dhahran, Saudi Arabia. The system was operated with and without Fresnel lens between 7 am to 5 pm in the month of June and August. The system performance with and without Fresnel lens was analyzed in terms of the absolute humidity of the moist air at the exit of the humidifier. Figure 26 and Figure 27 shows the solar radiations on the tilted absorber plate, air and water inlet temperatures, and the water temperature achieved at the exit of absorber plate with and without the use of Fresnel lens for the particular day in the month of June and August, respectively. It can be seen from both figures that the solar radiation and ambient air temperature rise in the morning hours, reach their maximum values around mid-day, and then decrease in the afternoon. Water temperature followed the same trend since it is directly influenced by the solar radiations. The black absorber plate was heated by solar radiation. Accordingly, water temperature was increased as it flows over the absorber plate. A higher water temperature was achieved by using Fresnel lens that concentrates the solar radiations on the absorber plate and, consequently, heats the water to a higher temperature.

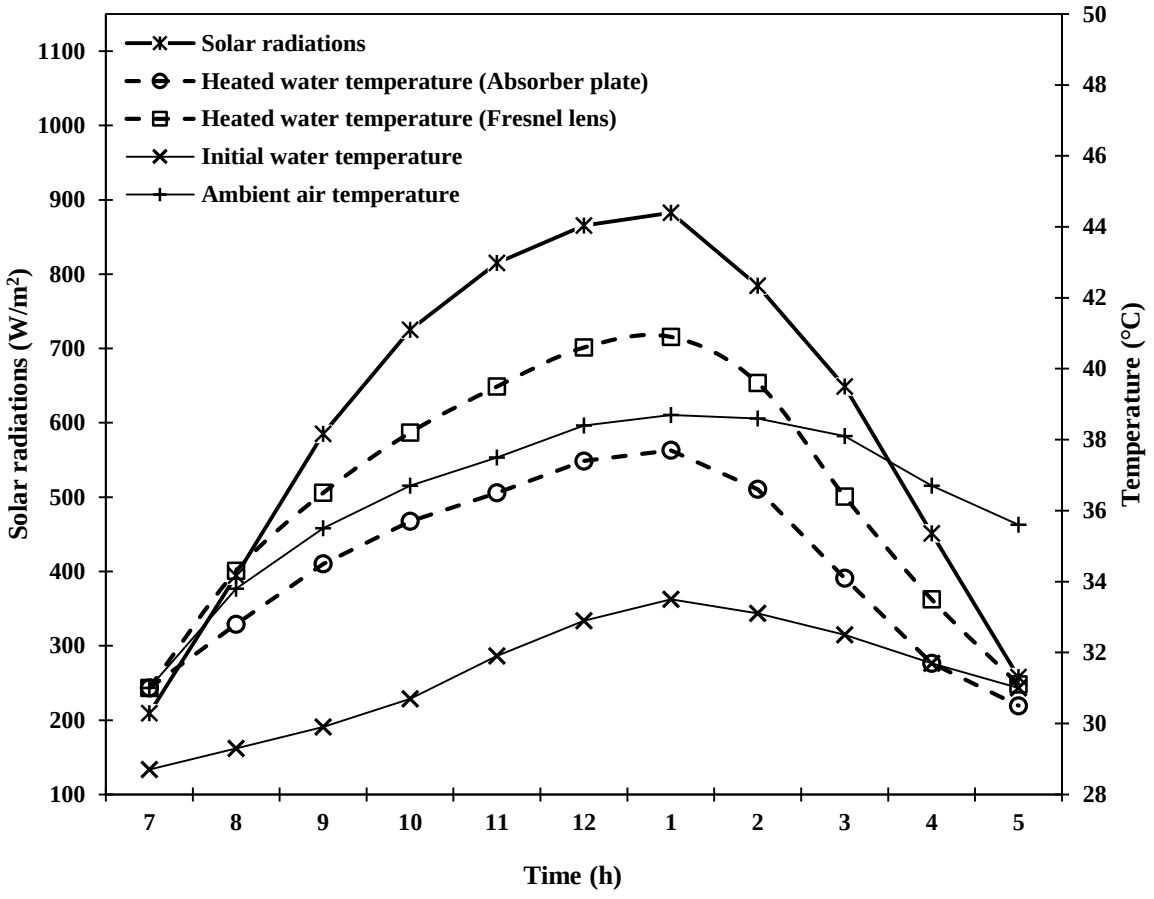

Figure 26 Influence of solar radiations on the water temperature in the bubble column humidifier in the month of June (14 June 2015).

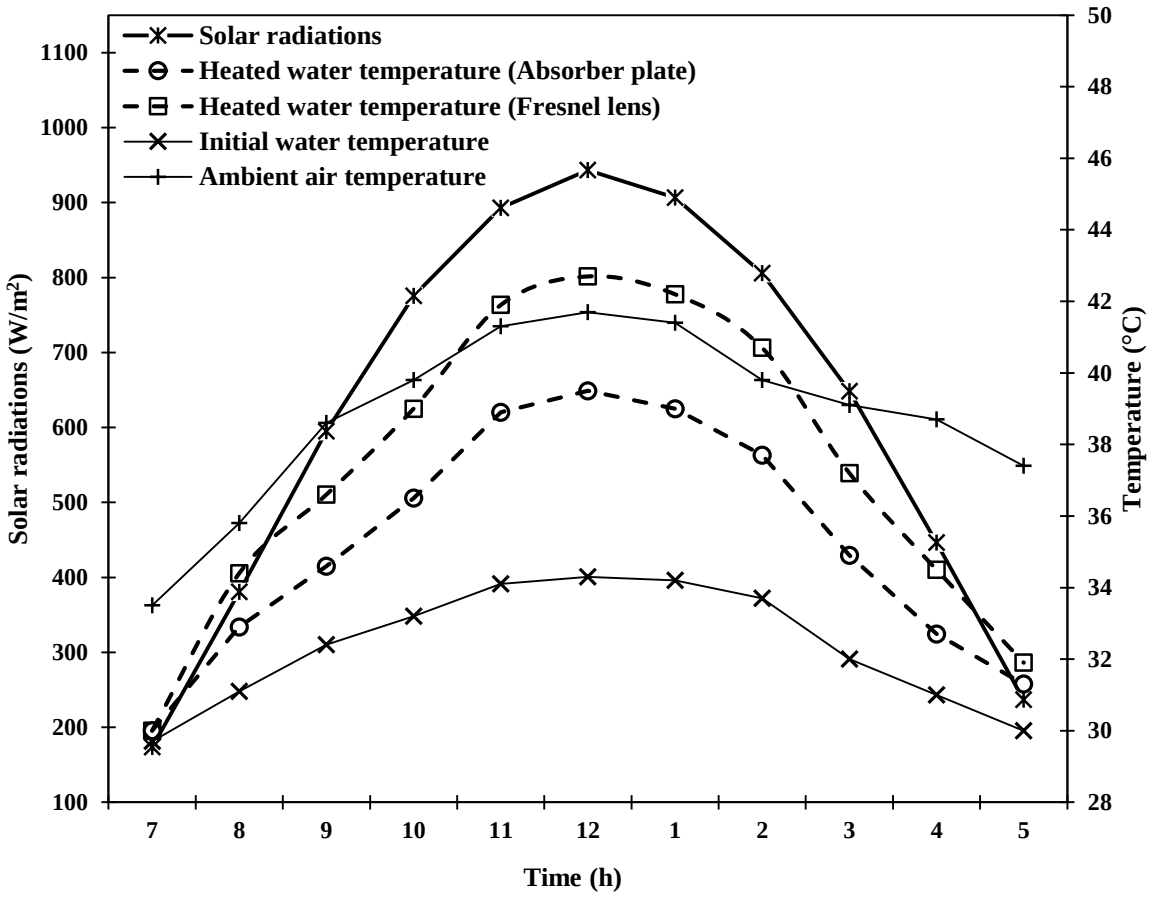

Figure 27 Influence of solar radiations on the water temperature in the bubble column humidifier in the month of August (10 August 2015).

Since the core objective of the bubble column humidifier is to effectively humidify the air, the day round performance of the proposed design is analyzed in terms of the absolute humidity of the moist air at the exit of the humidifier. Initially, the humidifier design was operated without the integration of Fresnel lens and water is heated by passing it over the absorber plate that was painted black and titled to an angle equal to the latitude of Dhahran to absorb the maximum solar radiations. The water temperature difference achieved in the humidifier and its influence on the air absolute humidity was investigated at different air superficial velocities. The investigated day round performance of the humidifier in the month of June and August are summarized in Figure 28 and Figure 29.

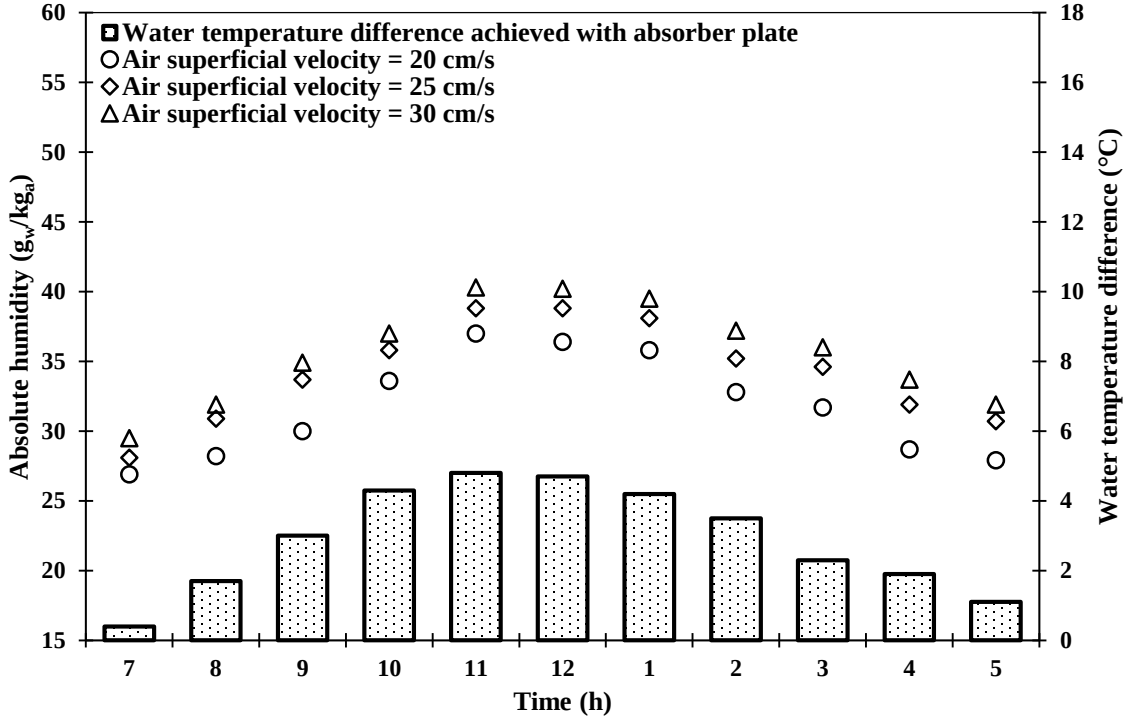

Figure 28 Influence of water temperature and air superficial velocity on the absolute humidity of the moist air at the exit of humidifier in the month of June.

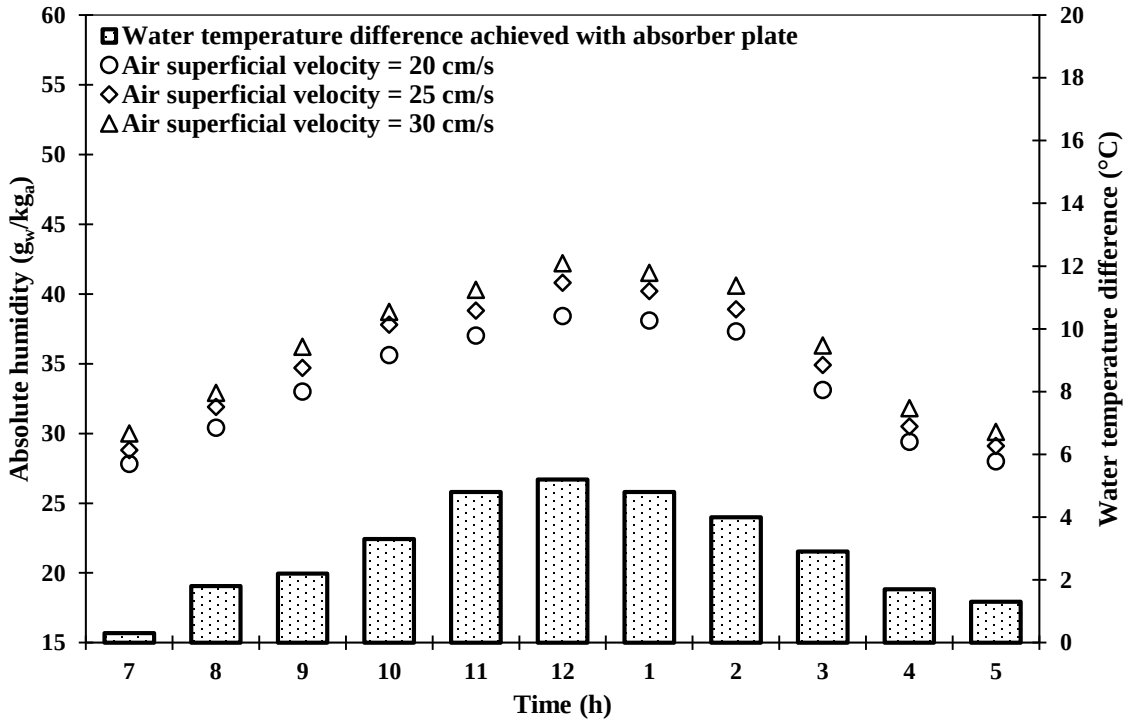

Figure 29 Influence of water temperature and air superficial velocity on the absolute humidity of the moist air at the exit of humidifier in the month of August.

Figure 28 shows that the absolute humidity and water temperature difference rises in the morning hours, reaches their maximum values around mid-day, and then decrease in the afternoon. Figure 29 shows the similar trend with slightly different values that were caused by the variations in the climatic conditions. The maximum value of absolute humidity around mid-day is due to the highest achievable water temperate at that time. As the increase in water temperature enhances the ability of the air to absorb more moisture, the proposed humidifier design is integrated with Fresnel lens to achieve the higher water temperature at the inlet of bubble column humidifier. The achieved absolute humidity and water temperature difference with Fresnel lens integration in the proposed humidifier design are shown in Figure 30 and Figure 31 for the month of June and August respectively. Results indicate that the absolute humidity is increased by 7.9 % with the integration of Fresnel lens in the proposed design. The integration of Fresnel lens increased the concentration of solar radiation on the absorber plate and heated the water to a higher temperature. The increase in the water temperature enhanced the ability of the air to absorb more moisture and, consequently, a higher absolute humidity is achieved at the outlet of the humidifier with the integration of Fresnel lens. The influence of air superficial velocity on the day round performance of the humidifier was also investigated under the aforementioned experimental conditions. Results indicate that the absolute humidity is increased by 7.9 % and 12.3 % when the air superficial velocity is increased from 20 cm/s to 25 cm/s and 30 cm/s respectively. The increase in air absolute humidity with the increase in the superficial velocity of the air is attributed to the formation of bigger air bubbles. Moreover, the number of air bubbles increases with the increase in air superficial velocity and, consequently, provides a higher interfacial area for better heat and mass transfer.

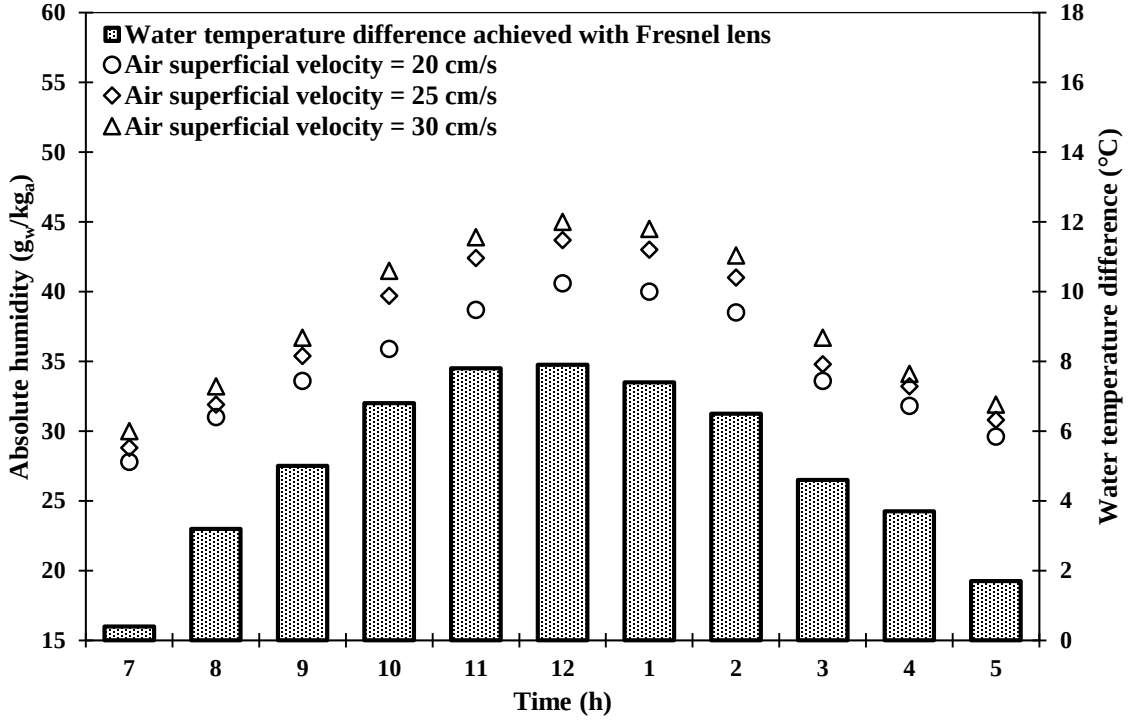

Figure 30 Fresnel lens integration in the proposed design to increase the absolute humidity of the moist air at the exit of humidifier in the month of June.

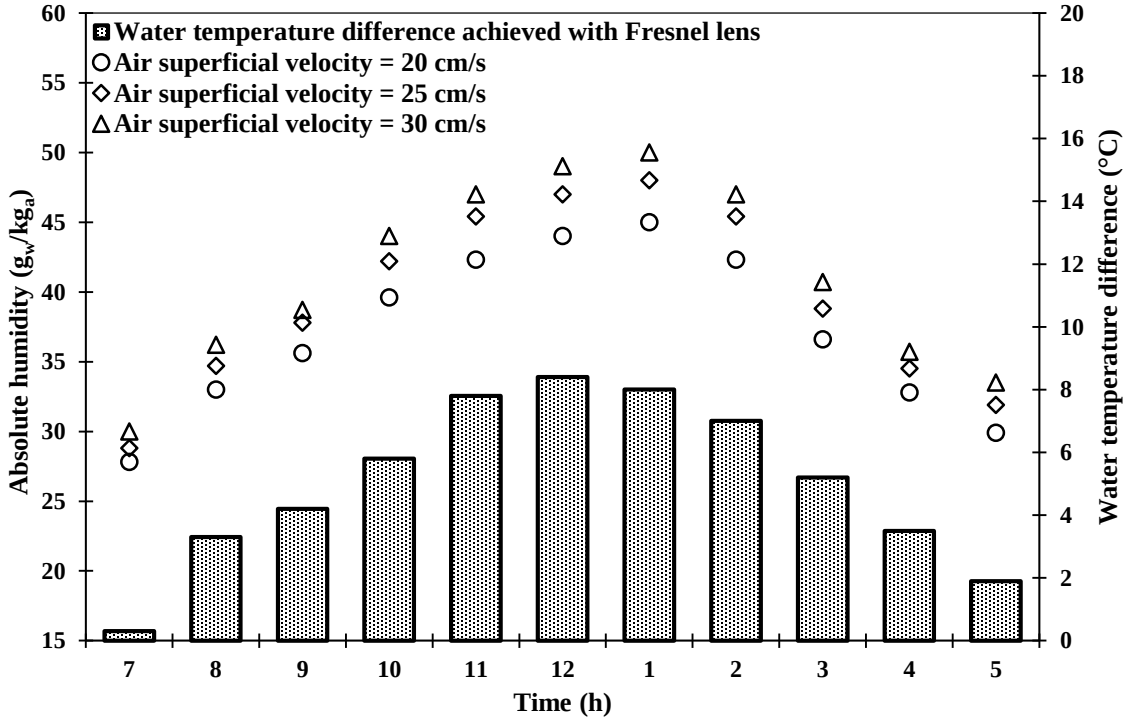

Figure 31 Fresnel lens integration in the proposed design to increase the absolute humidity of the moist air at the exit of humidifier in the month of August.

The influence of the inlet air relative humidly on the day round performance of the humidifier was investigated at different air superficial velocities. Experiments were performed in the month of June and August to have the real time climatic variations in the relative humidity of the inlet air. The investigated results under the real climatic conditions of Dhahran in the month of June and August are summarized in Figure 32 and Figure 33 respectively. Results in both figures show that the humidification efficiency increases with the increase in air superficial velocity irrespective of the inlet air relative humidity. However, the average day round humidification efficiency of the proposed humidifier design is 7.14 % higher in the month of June as compared to August. This is due to the higher vapor content difference between the outlet and inlet of the humidifier in the month of June as compared to the August. The reason of attaining higher vapor content difference in the month of June is the lower relative humidity of the inlet air that ranged between 13-22 % as compared the month of August when the inlet air relative humidity varies between 35-44 %. The air at a lower relative humidity has more potential to absorb moisture as compared to the air with a high relative humidity. This information is of pivotal importance to understand the optimum operating conditions of the humidifier for its possible integration with the dehumidifier. Consequently, an improved HDH system is obtained.

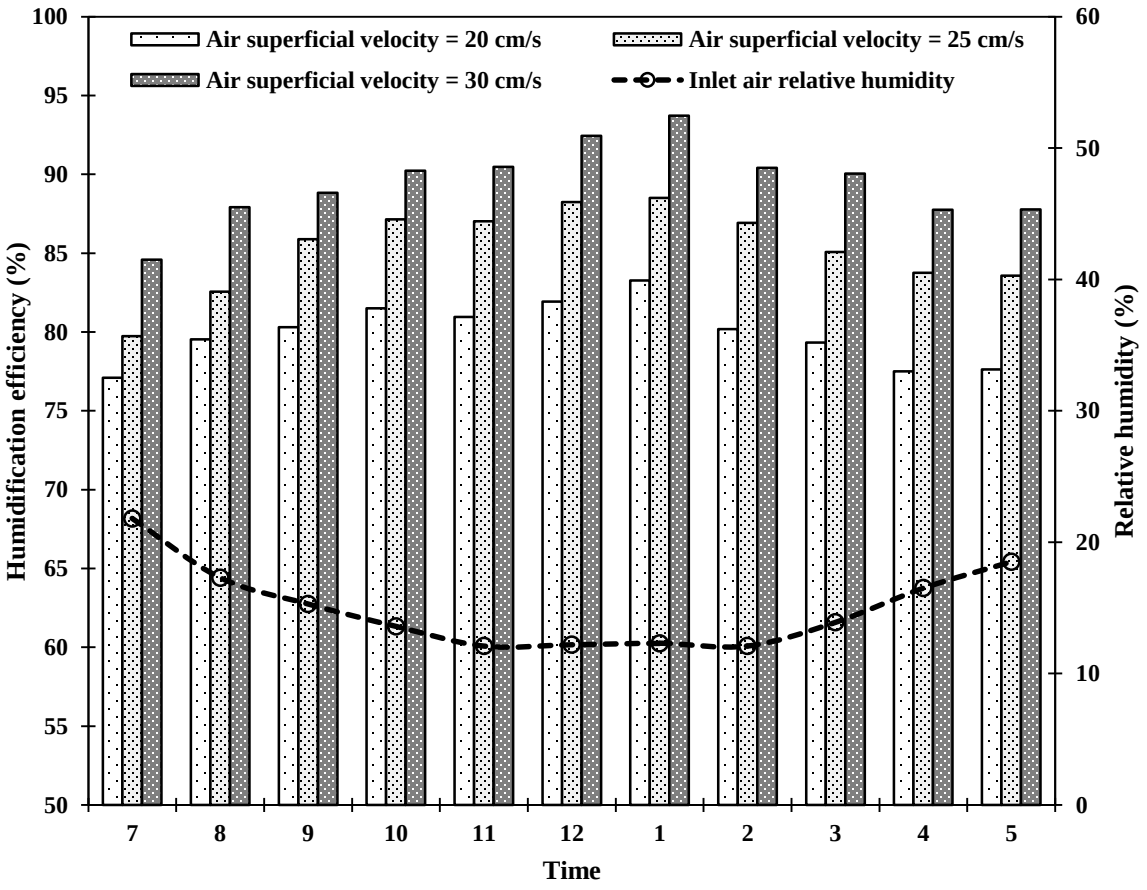

Figure 32 Humidification efficiency of the proposed humidifier design in the month of June.

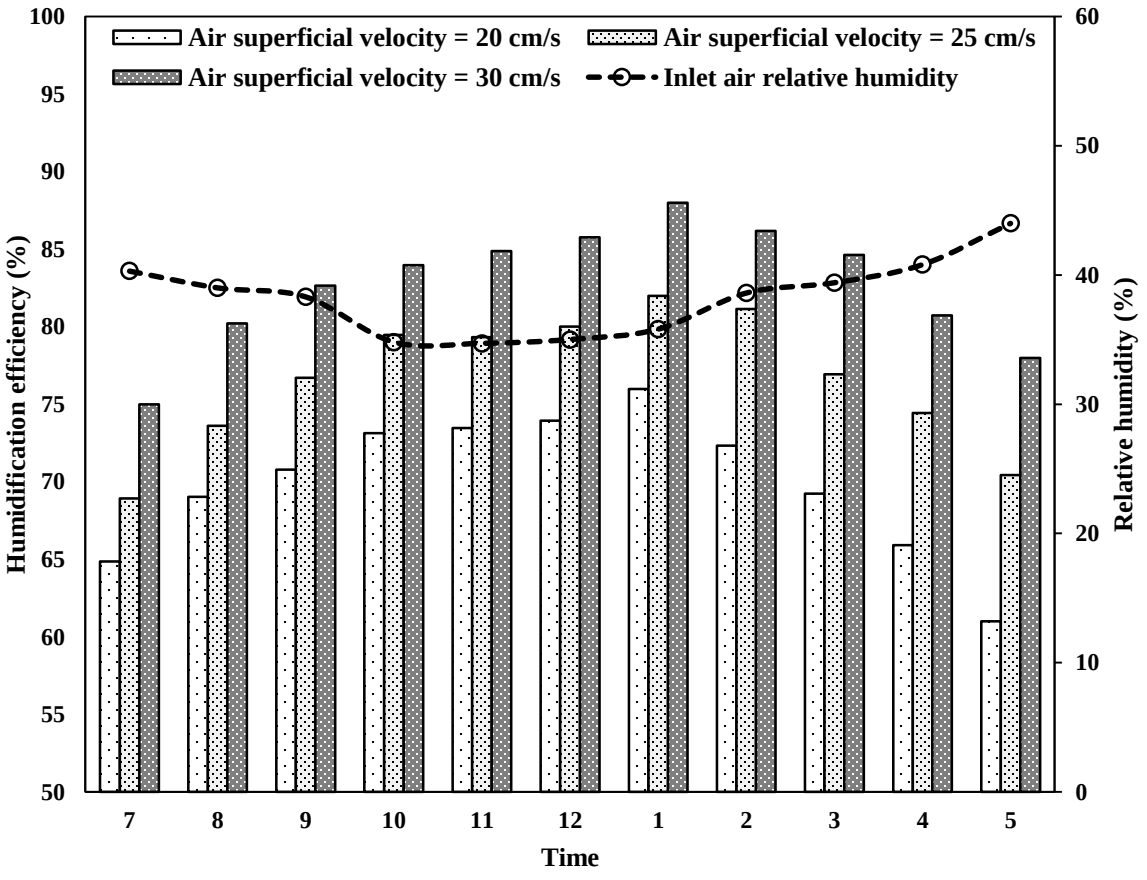

Figure 33 Humidification efficiency of the proposed humidifier design in the month of August.

4.3.6 Electric Heater Integration in Single Stage Bubble Column Humidifier

Careful analysis of aforementioned experimental results inferred that the humidifier performance is dependent on many factors like geometric features of the perforated plate, air superficial velocity, water column height, and water inlet temperature. However, the water temperature at the inlet of the humidifier is the most dominant factor contributing toward the better performance of the humidifier. Therefore, this part of the study is focused on analyzing the performance of the humidifier at different water temperature at the inlet of the humidifier. The influence of increasing water temperature on the absolute humidity is analyzed at different water column heights with varying air superficial velocities. The water temperature at the inlet of humidifier is varied in the range of 35 °C to 75 °C. The desired temperature of the water is achieved by using 4 electrically heated elements of 1.2 kW power each. These heating elements are incorporated with thermostat for the constant availability of the water at the desired temperature. K-type thermocouples are used to measure water temperature as well as air dry-bulb/wet-bulb temperatures. A data acquisition consisting of two NI 9213 thermocouple input modules installed in a NI cDAQ-9178 USB chassis is connected to a computer. Thermocouples measurements are displayed and stored using a Lab-view program. Real-time processed thermocouple readings are measured every 2 seconds and the average temperatures of every 5 minutes were recorded using the developed Lab-view program. The air superficial velocity at the inlet of humidifier is varied in the range of 20 cm/s to 30 cm/s. The desired air superficial velocity is achieved and control by the adjustable blower. The blower is adjustable for the desired volumetric flow rate of the air stream that is measured by an orifice meter connected to a manometer to measure the pressure drop across the orifice plate and hence calculate air

flow rate. The volumetric flow rate of the water is measured and adjusted to the desired value by using rotameter. The water level in the bubble column is varied in the range of 1 cm to 5 cm. The desired water level in the bubble column is maintained by using the control valve that are installed at different water column heights.

The influence of water inlet temperature, air superficial velocity, and water column height on the performance of the humidifier is analyzed in terms of absolute humidity. Figure 34 shows the influence of water temperature at different air superficial velocities when the water column height is maintained at 1 cm. Results show that the absolute humidity significantly increased with the increase in water temperature at the inlet of the humidifier. The increasing trend of the absolute humidity is more prominent in higher temperature range. This means that the performance of the humidifier is dominantly influenced with the increase of water temperature in higher temperate range. The reason of attaining higher absolute humidity in higher temperature range is attributed to the ability of air to absorb more moisture at higher temperature range. The influence of varying air superficial velocity on the amount of vapor contents in the moist air (absolute humidity) at the exit of humidifier is also presented in figure 34. The air is induced to the humidifier with the help of the blower that sucks the air from the atmosphere. The absolute humidity of the inlet air is dependent on the real time atmospheric conditions and it is almost constant during the particular experimental analysis. However, with the increase of water inlet temperature to 75 °C, the absolute humidity of the moist air at the exit of the humidifier is increased from 227 g_w/kg_a to 249 g_w/kg_a with the increase in the air superficial velocity from 20 cm/s to 25 cm/s. Further increase in the air superficial velocity from 25 cm/s to 30 cm/s results in a slight decrease of absolute humidity from the value of 249 g_w/kg_a to 238 g_w/kg_a under the

same prevailing conditions. Therefore, the optimum air superficial velocity at the water column height of 1cm is found out to be 25 cm/s.

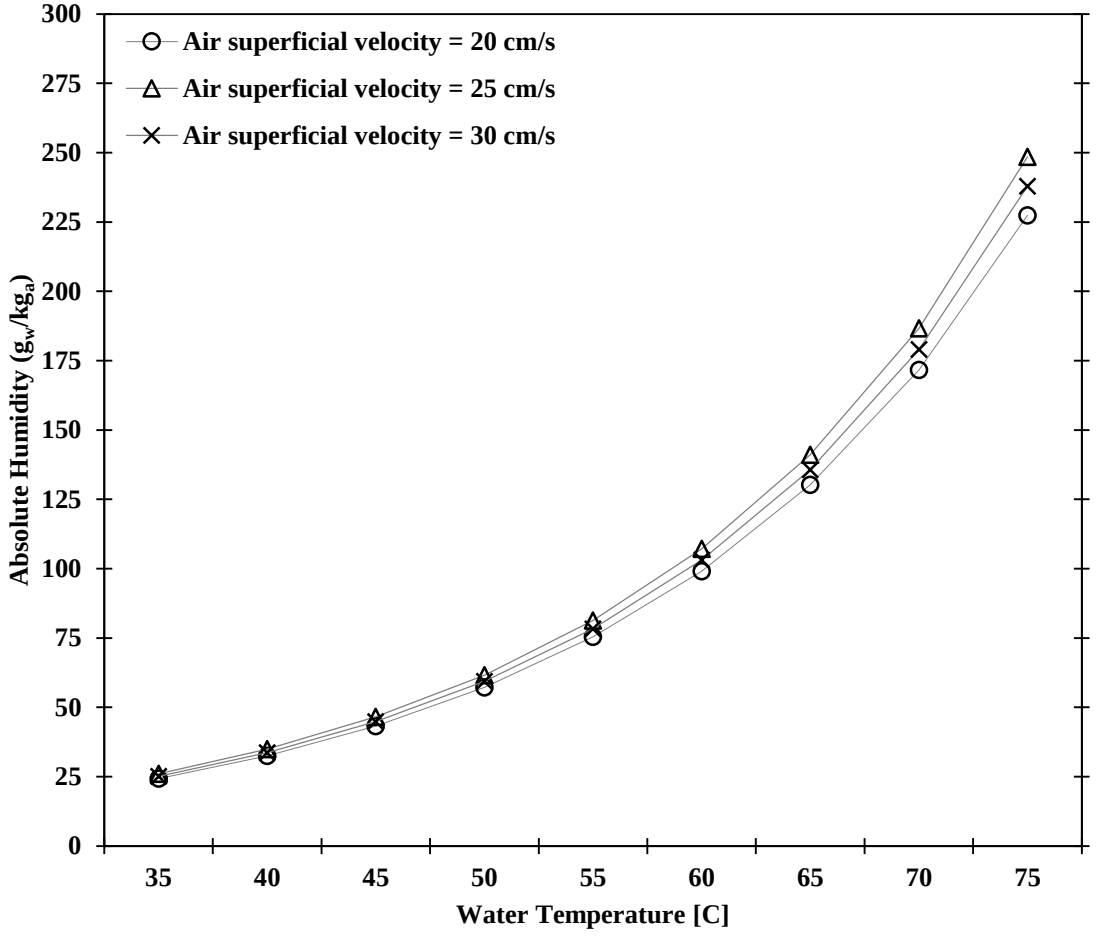

Figure 34 Influence of water temperature at different air superficial velocities at 1cm water column height.

The same experimental procedure is adopted to analyze the performance of humidifier under the influence of increasing water temperature and varying air superficial velocities when the water column height is maintained at 3 cm. Findings are summarized in Figure 35 that indicate the similar increasing trend of absolute humidity with the increase in water temperature as observed in Figure 34. Results also show the increase in absolute humidity

with the increase in air superficial velocity. At inlet water temperature of 75 °C, the absolute humidity is increased from 217 g_w/kg_a to 227 g_w/kg_a when the air superficial velocity is increased from 20 cm/s to 25 cm/s. On contrary to the results of 1 cm water column height, the absolute humidity is further increased from 227 g_w/kg_a to 248 g_w/kg_a when the air superficial velocity is increased from 25 cm/s to 30 cm/s. Therefore, the optimum air superficial velocity at the water column height of 3 cm is found out to be 30 cm/s.

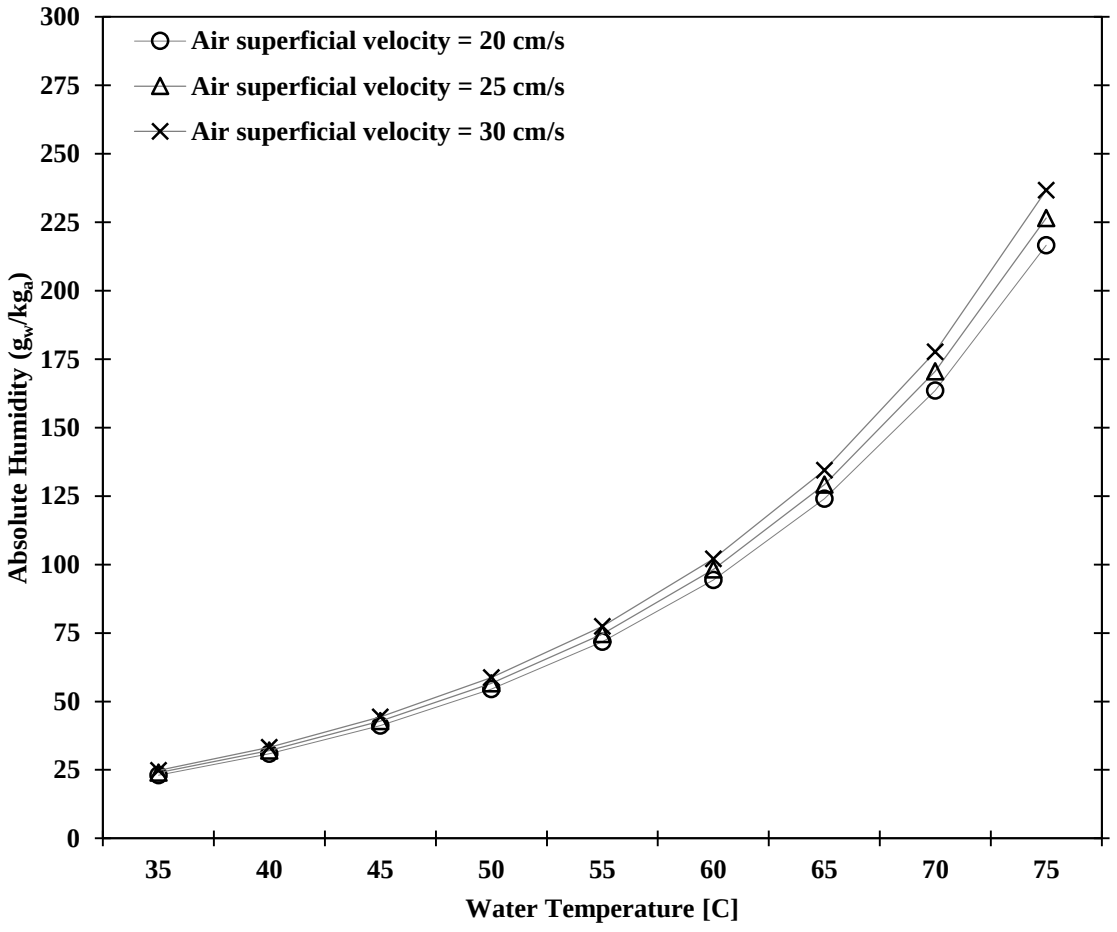

Figure 35 Influence of water temperature at different air superficial velocities at 3 cm water column height.

Figure 36 shows the influence of water temperature at different air superficial velocities when the water column height is maintained at 5 cm. Results indicate the similar increasing trend of absolute humidity with the increase in water temperature and air superficial velocity as observed in figure 35. However, the maximum achievable absolute humidity at 20 cm/s and 25 cm/s is 173 g_w/kg_a and 192 g_w/kg_a respectively that is 20.15 % and 23.6 % less as compared to the results obtained at 3 cm water column height under the same prevailing conditions. The best results for water column height of 5 cm are obtained at air superficial velocity of 30 cm/s for which absolute humidity reached upto 236 g_w/kg_a when the water temperature at the inlet of the humidifier is increased to 75 °C. Comparing the performance of humidifier in terms of absolute humidity, the best results are obtained at the water column height of 1 cm with the air superficial velocity of 25 cm/s and the water column height of 3 cm with the air superficial velocity of 30 cm/s. The increase in air absolute humidity at lower water column height with an optimum value of air superficial velocity is recognized to the higher number of air bubbles formation of relatively bigger size that provides a higher interfacial area for better heat and mass transfer.

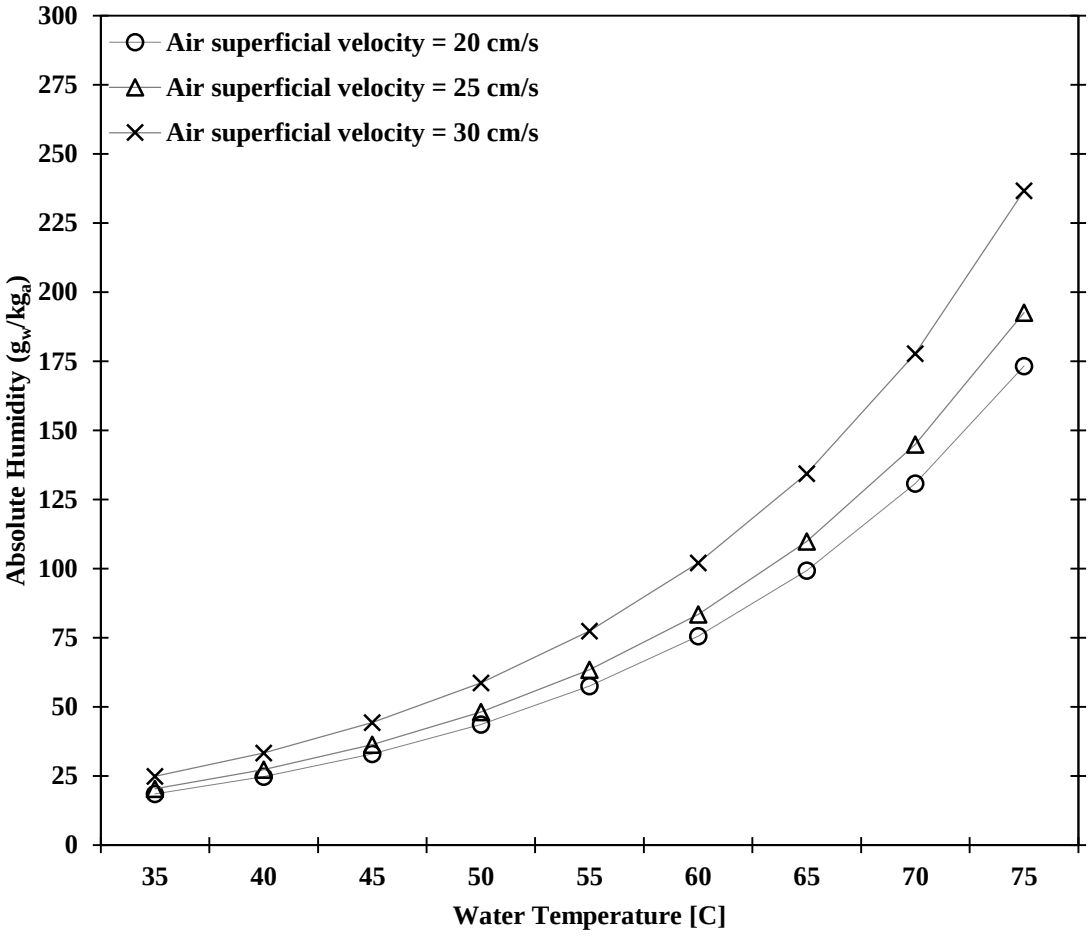

Figure 36 Influence of water temperature at different air superficial velocities at 5 cm water column height.

4.3.7 Effectiveness of Single Stage Bubble Column Humidifier

Careful review of previous literature studies show that the researchers describe various effectiveness definition for simultaneous heat and mass transfer. These definitions are used for a specific heat and mass exchanger device under the limited boundary conditions. Various effectiveness definitions along with their applicability range are summarized in Table 6.

Table 6 Various effectiveness definitions along with their applicability range.

Type	Definition	Applicability range
Temperature based effectiveness [52],[53]	$\varepsilon_T = \frac{\Delta T}{\Delta T^{ideal}}$	Humidifiers and Cooling towers (HCR ≥ 1)
Humidity based effectiveness [38-40], [54]	$\varepsilon_\omega = \frac{\Delta \omega}{\Delta \omega^{ideal}}$	Humidifier, dehumidifiers and cooling coils (HCR ≤ 1)
Air stream enthalpy based effectiveness [54]	$\varepsilon_h = \frac{\Delta h_a}{\Delta h_a^{ideal}}$	Humidifier, dehumidifiers and cooling coils (HCR ≤ 1)
Energy based effectiveness [55]	$\varepsilon_E = \frac{\Delta \dot{H}}{\Delta \dot{H}_{max}}$	All simultaneous heat and mass exchanger devises, all situations

In all the experimental investigation of the bubbler humidifier [38-40], the humidification efficiency was evaluated by using the humidity based effectiveness that is defined as:

$$\varepsilon_{\omega} = \frac{\Delta\omega}{\Delta\omega^{ideal}} = \frac{\omega_{out} - \omega_{in}}{{\omega_{out}}^{sat} - \omega_{in}}$$

Where $\omega_{out} and\ \omega_{in}$ are the humidity ratio of the moist air at the inlet and outlet of the humidifier. The ${\omega_{out}}^{sat}$ is the outlet moist air absolute humidity at saturation.

As the core objective of the direct contact humidifier is to attain higher vapor contents in the moist air at the outlet, the efficiency of the humidifier can be represented in terms of the humidity of moist air at its inlet and outlet states. However, this approach is not appropriate as the effect of water temperature is not taken into consideration. Narayan et al. [56] proved that an energy based effectiveness is a more suitable approach to evaluate the performance of heat and mass exchanger devices like humidifier. The effectiveness of direct contact heat and mass exchanger humidifier can be calculated by the expression proposed by Narayan et al., which is defined as

$$\varepsilon_{E} = \frac{\Delta\dot{H}}{\Delta\dot{H}_{max}}$$

where $\Delta\dot{H}_{max}$ is defined separately for water and air stream. In the case of air passing through the hot water column, the ideal condition for air at the exit can be achieved when it is saturated at water inlet temperature. Similarly, the ideal condition for the water is to achieve air wet bulb temperature at the exit of the humidifier. The effectiveness definition of water heated direct contact heat and mass transfer humidifier can be defined as

For $\Delta\dot{H}_{max,w} < \Delta\dot{H}_{max,a}$

$$\varepsilon_E = \frac{m_{w,i}h_{w,i} - m_{w,o}h_{w,o}}{m_{w,i}h_{w,i} - m_{w,o}h_{w,o}^{ideal}}$$

For $\Delta\dot{H}_{max,w} > \Delta\dot{H}_{max,a}$

$$\varepsilon_E = \frac{h_{a,o} - h_{a,i}}{h_{a,o}^{ideal} - h_{a,i}}$$

where $h_{w,o}^{ideal} and\ h_{a,o}^{ideal}$ is calculated at air inlet wet bulb temperature and water inlet temperature in the humidifier.

Based on the aforementioned effectiveness definitions extracted from literature, the various effectiveness definitions are implemented on the experimentally obtained data of the proposed bubble column humidifier. Figure 37 shows the temperature based effectiveness(ε_T) and energy based effectiveness(ε_E) of the proposed humidifier design when the heat capacity ratio is greater than or equal to one (HCR ≥ 1). Results shows that the energy based effectiveness(ε_E) and temperature based effectiveness (ε_T) follow the similar trend in the range of 45 °C to 75 °C. The minimum effectiveness is obtained at 45 °C. The reason of lower effectiveness at 45 °C is attributed with the heat capacity ratio at that point which is equal to one (HCR=1). At heat capacity ratio equal to unity, the water and air stream have equal heat capacity that limits the driving potential of heat and mass transfer between two streams. This effect of heat capacity ratio is explained in details by Naryan et al. both theoretically [55] and experimentally [58]. The maximum energy based effectiveness achieved in a single stage is equal to 49 %. The air stream enthalpy based effectiveness(ε_h), and humidity based effectiveness (ε_ω) are not considered under these

experimental results (HCR ≥ 1) due to the applicability range of the enthalpy based effectiveness(ε_h), and humidity based effectiveness (ε_ω) that is valid only when the heat capacity ratio is less than or equal to one (HCR ≤ 1).

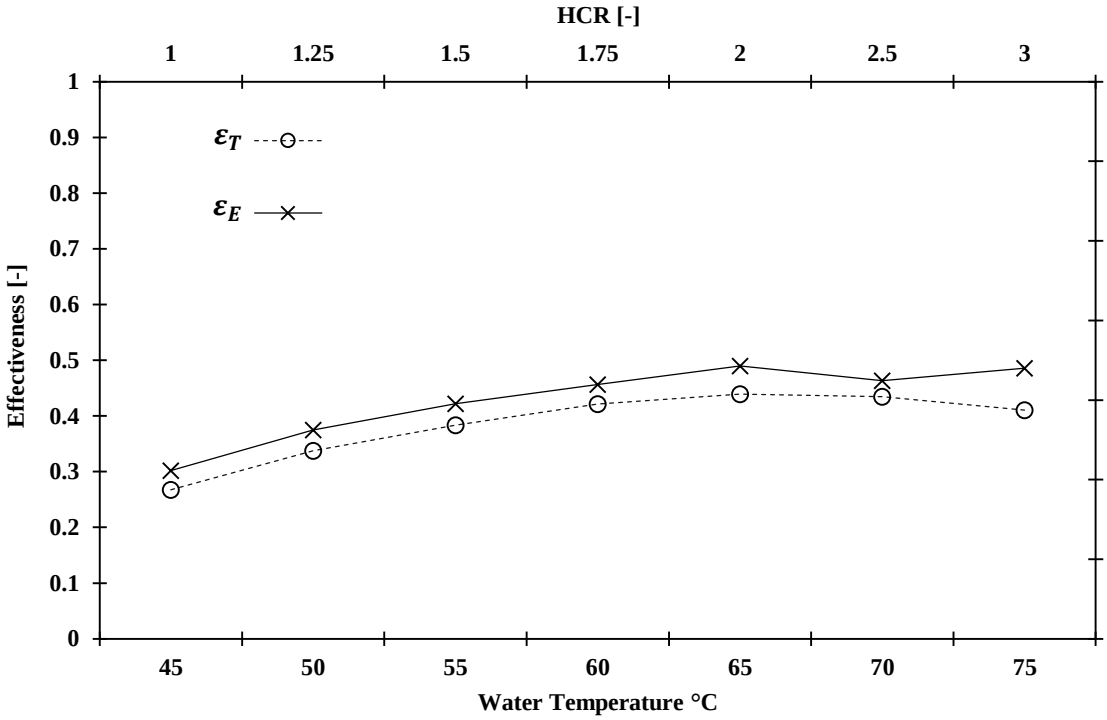

Figure 37 Effectiveness of single stage humidifier configuration at HCR ≥ 1.

4.4 Experimental investigation of Multi Stage Bubble Column Humidifier

The proposed humidifier design take the advantage of its multi-stage stepped configuration that allows the water stream to run through stages under the force of gravity. It also help to maintain a minimum desirable water column depth that results in minimum pressure drop in the air-side. Another advantage of multi stage configuration is the segmentation of the water and air stream path to provide the lower temperature difference in each stage that decrease the irreversibility in the system. The schematic representation of segmented water and air stream along the steps of proposed humidifier design is shown in Figure 38.

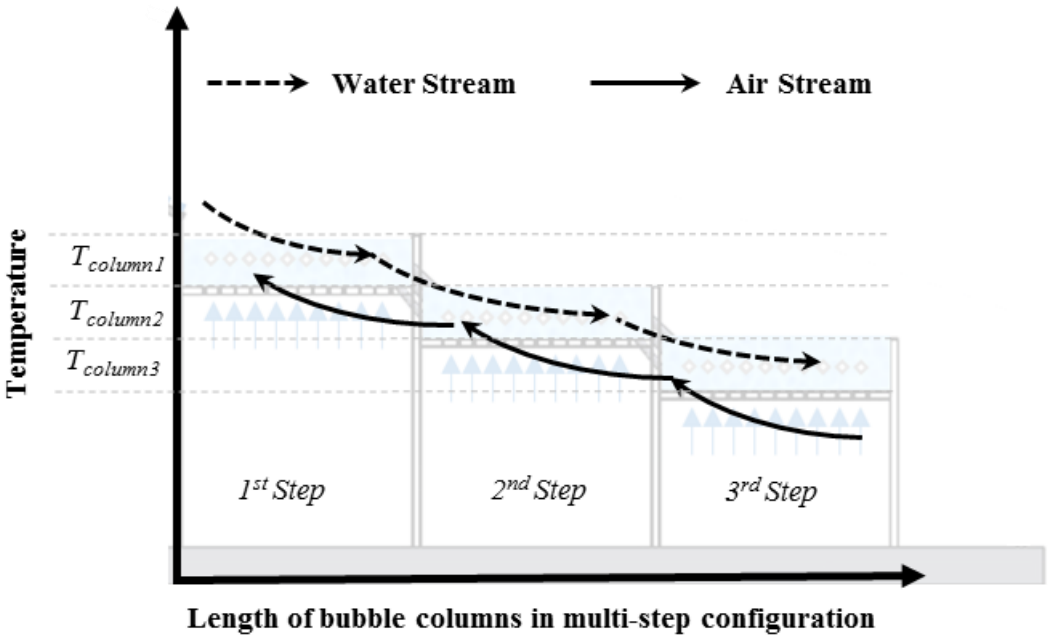

Figure 38 Segmented water and air stream along the steps of multistage humidifier design.

Figure 39 represents the air humidification process in the proposed humidifier operated in single stage, two stage, and three stage configuration. The experiments were performed at inlet water temperature of 60 °C and inlet air temperature of 32 °C with 50 % relative humidity. The points B, B', and B'' on the psychometric chart represent the exit state of the air at the exit of the humidifier operated in single stage, two stage, and three stage configuration, respectively. Results shows that the absolute humidity is increased with the increase in number of stages.

The air humidification process in a single stage humidifier configuration is represented by line A-B on the psychometric chart. In a single stage humidifier configuration, the water and air stream homogeneously mixed in the bubble column and experience a large temperature difference that increase the irreversibility in the system. The air humidification process in a two stage humidifier configuration is represented by line A-2' for second stage and line 2'-B' for the first stage on the psychometric chart. As we increase the number of stages from 1 to 2, hot humid air at the exit of second bubble column stage (represented by point 2' on the psychometric chart) further passed over the neighboring first bubble column stage (represented by line 2'-B' on psychometric chart) that is operating at higher temperature as compared to second stage. This allows the air to absorb more moisture and higher absolute humidity is achieved at the exit of humidifier operated in two stage configuration. Similarly, when the proposed design is operated in 3 stages, the air at the exit of third bubble column stage (represented by point 3'' on the psychometric chart) further passed over the neighboring second bubble column stage (represented by line 3''-2'' on the psychometric chart) and first bubble column stages (represented by line 2''-B''

on the psychometric chart). This allows more time for heat and mass transfer and air comes out more hot and humid at the exit of humidifier operated in three stage configuration.

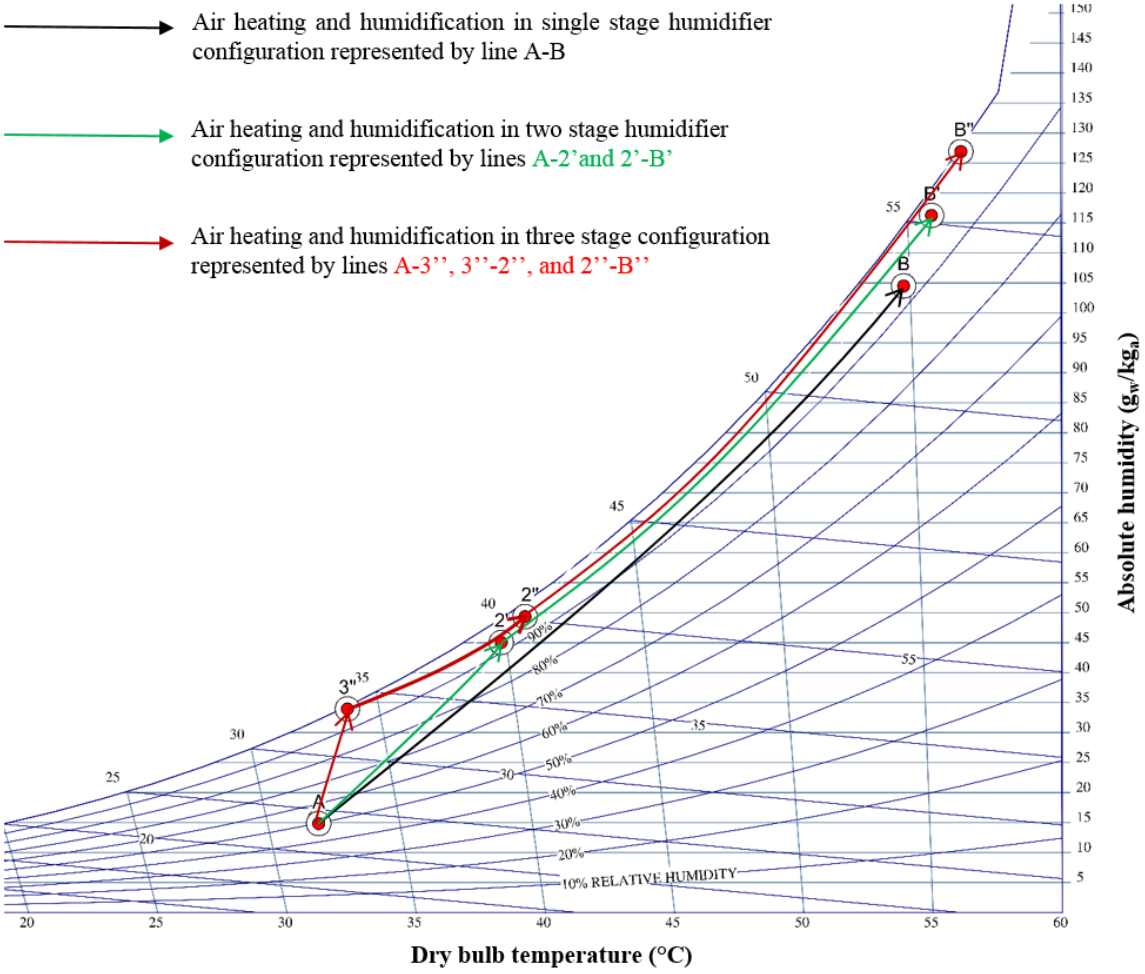

Figure 39 Psychometric chart for air humidification process in the proposed humidifier operated in single stage, two stage, and three stage configuration.[9]

[9] The experiments were conducted at the water column height of 3 cm, inlet water temperature of 60 °C, inlet air temperature of 32 °C, inlet air relative humidity of 50 %, and air superficial velocity of 25 cm/s.

The optimum values of air superficial velocity and water column height obtained from single stage investigation (section 4.3.6) are further analyzed in terms of pressure drop in the multi stage bubble column humidifier. Figure 40 shows the total pressure drop in the all three stages under the obtained optimum values of water column height of 1 cm with air superficial velocity of 25 cm/s and water column height of 3 cm with air superficial velocity of 30 cm/s. Results show that the higher pressure losses are experienced at water column height of 3 cm with air superficial velocity of 30 cm/s as compared to water column height of 1 cm with air superficial velocity of 25 cm/s. Therefore, water column height of 1 cm with air superficial velocity of 25 cm/s is considered to be an optimum balance for higher system performance with lower pressure drop.

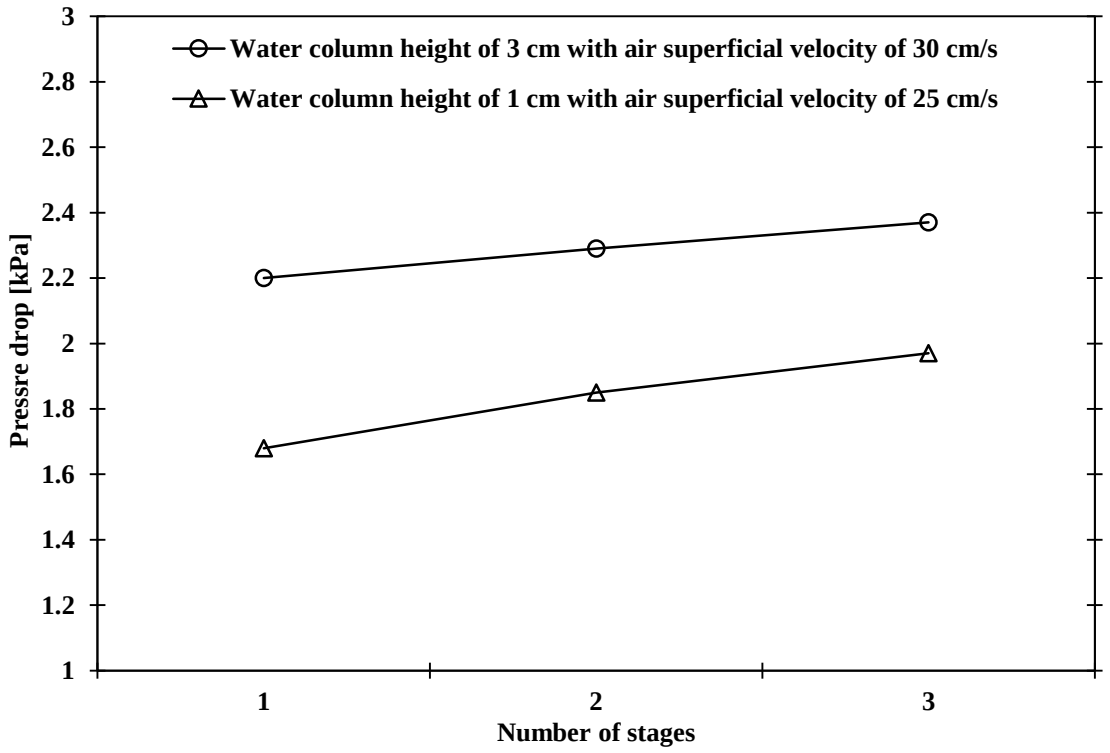

Figure 40 Influence of water column height on total pressure drop under varying air superficial velocity.

The major advantage of the proposed humidifier is its ability to have direct solar thermal heating, therefore, the day round performance of the system was tested under climatic conditions of Dhahran, Saudi Arabia. The system was operated between 7 am to 5 pm in the month of June. The system performance was analyzed in terms of the absolute humidity of the moist air at the exit of the humidifier. Figure 41 shows the solar radiations on the tilted absorber plate, air and water inlet temperatures, and the water temperature achieved at the exit of absorber plate for the particular day in the month June.

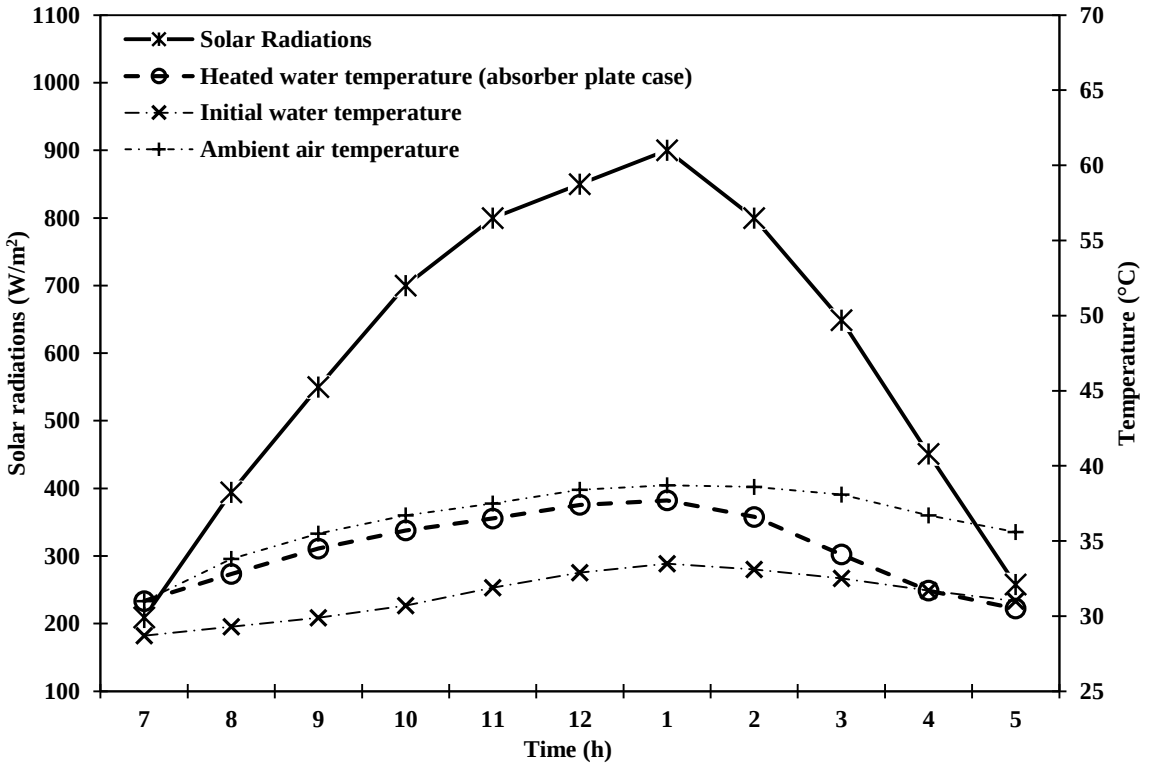

Figure 41 Solar radiations, air and water inlet temperatures, and the water temperature achieved at the exit of absorber plate on 17 June.

The day round performance of the multistage design is analyzed in terms of the absolute humidity of the moist air at the exit of the humidifier. The experiments are performed at the optimum air superficial velocity of 25 cm/s and water column height of 1 cm/s. The absolute humidity of the air at the exit of humidifier in single stage, two stage, and three stage configuration is summarized in in Figure 42. Figure 42 shows that the maximum value of absolute humidity is achieved around mid-day (1 pm) that is due to the highest achievable water temperate at that time. Findings show that the average day round absolute humidity is 9 % higher in two stages as compared to single stage. Similarly the average day round absolute humidity increased by 23 % when the humidifier is operated in three stages as compared to single stage.

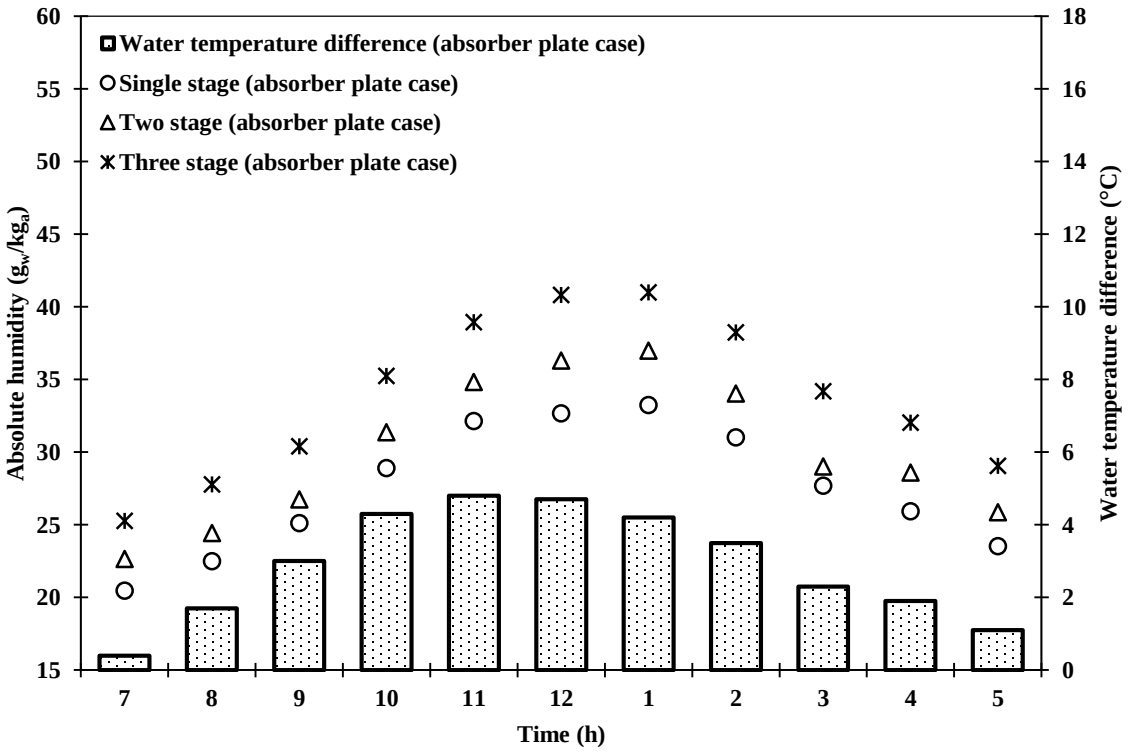

Figure 42 Water temperature difference achieved using absorber plate during 7 am to 5 pm and corresponding absolute humidity in single stag, two stage, and three stage configuration.

As the increase in water temperature enhances the ability of the air to absorb more moisture, the humidifier is integrated with Fresnel lens to achieve the higher water inlet temperature. The day round performance of the system was tested with the integration of Fresnel lens under climatic conditions of Dhahran, Saudi Arabia. Figure 43 shows the solar radiations on the tilted absorber plate, air and water inlet temperatures, and the water temperature achieved at the exit of absorber plate with the integration of Fresnel lens for the particular day in the month of June. It can be seen from figure that a higher water temperature was achieved by using Fresnel lens that concentrates the solar radiations on the absorber plate and, consequently, heats the water to a higher temperature.

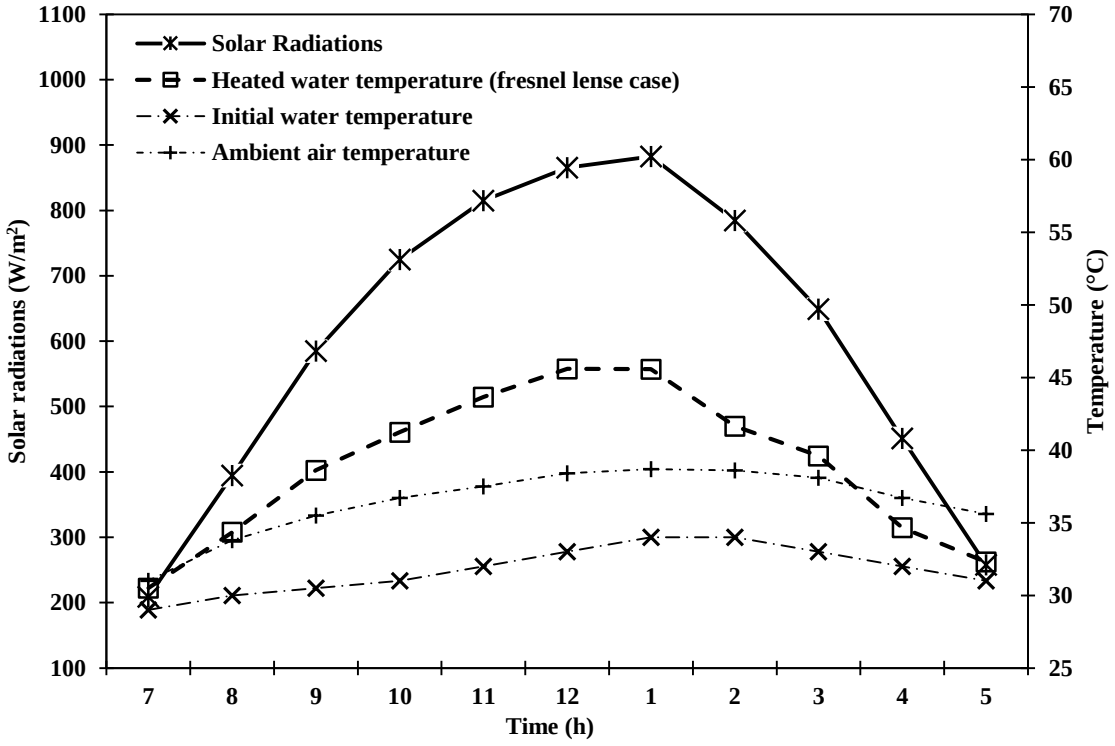

Figure 43 Solar radiations, air and water inlet temperatures, and the water temperature achieved at the exit of absorber plate with the integration of Fresnel lens on 18 June.

The achieved absolute humidity with Fresnel lens integration is shown in Figure 44. Results indicate the similar increasing trend of absolute humidity with the increase in number of stages. However, the achievable absolute humidity using Fresnel lens is 25-26 % higher as compared to the results obtained without the integration of Fresnel lens under the same prevailing conditions.

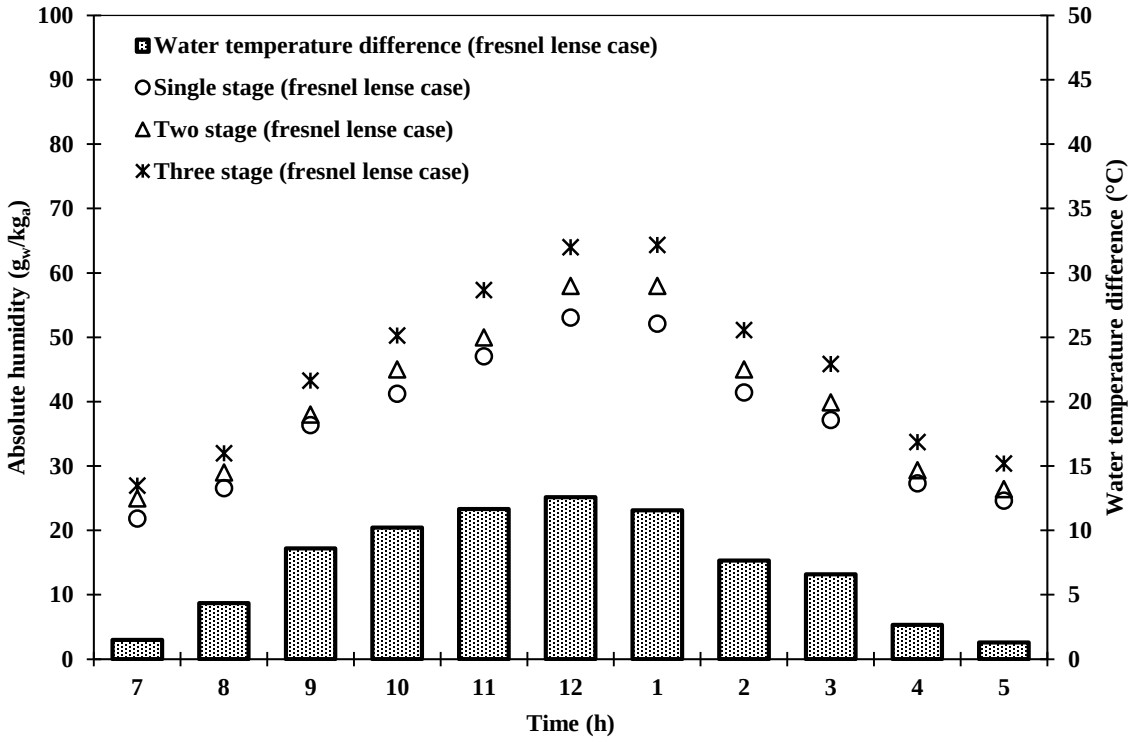

Figure 44 Water temperature difference achieved using Fresnel during 7 am to 5 pm and corresponding absolute humidity in single stag, two stage, and three stage configuration.

The influence of the inlet air relative humidity on the performance of humidifier is an important aspect as it signpost the optimum performance operating conditions for its possible integration with a dehumidifier. Therefore, the performance of the humidifier was tested in the month of August to experience the humidifier performance under the climatic variations in the relative humidity of the inlet air. The day round solar radiations, air and water inlet temperatures, and the heated water temperature for absorber plate case and Fresnel lens case are shown in Figure 45 and Figure 46 respectively. Both figures show nearly same solar radiation and ambient air temperature profile during the day round experimental investigation. However the heated water temperature value reached up to 47 °C around mid-day for Fresnel lens case that is 19 % higher than the highest value achieved for heated water temperature in case of absorber plate.

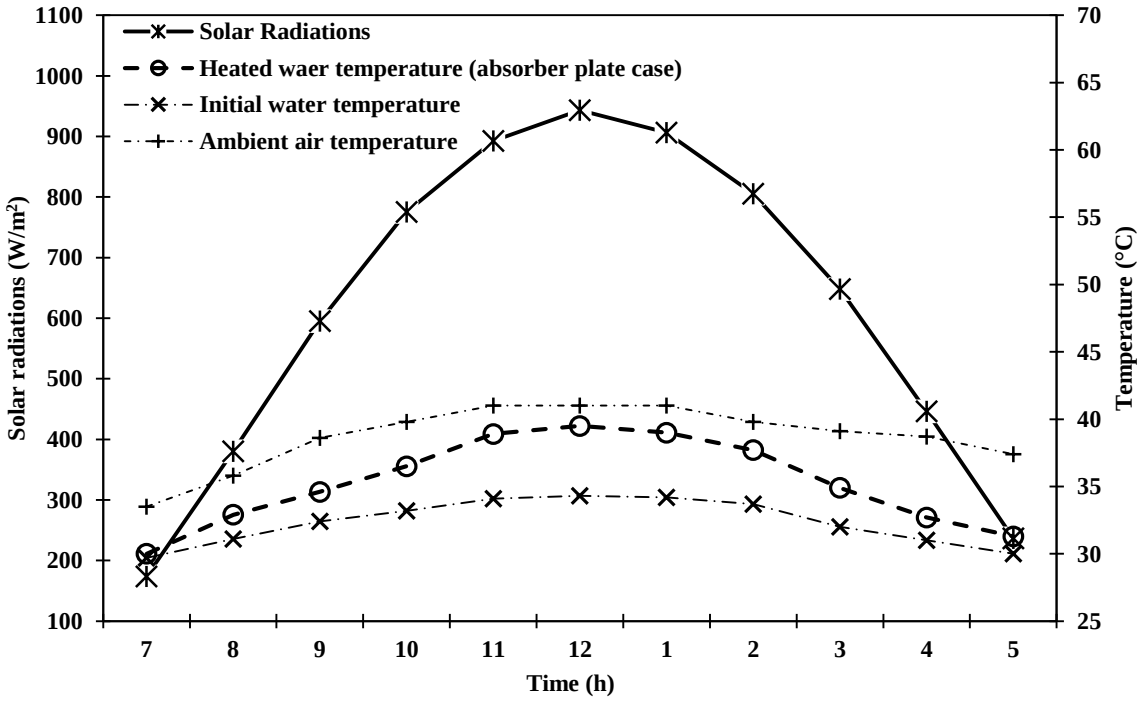

Figure 45 Solar radiations, air and water inlet temperatures, and the water temperature achieved at the exit of absorber plate on 14 August.

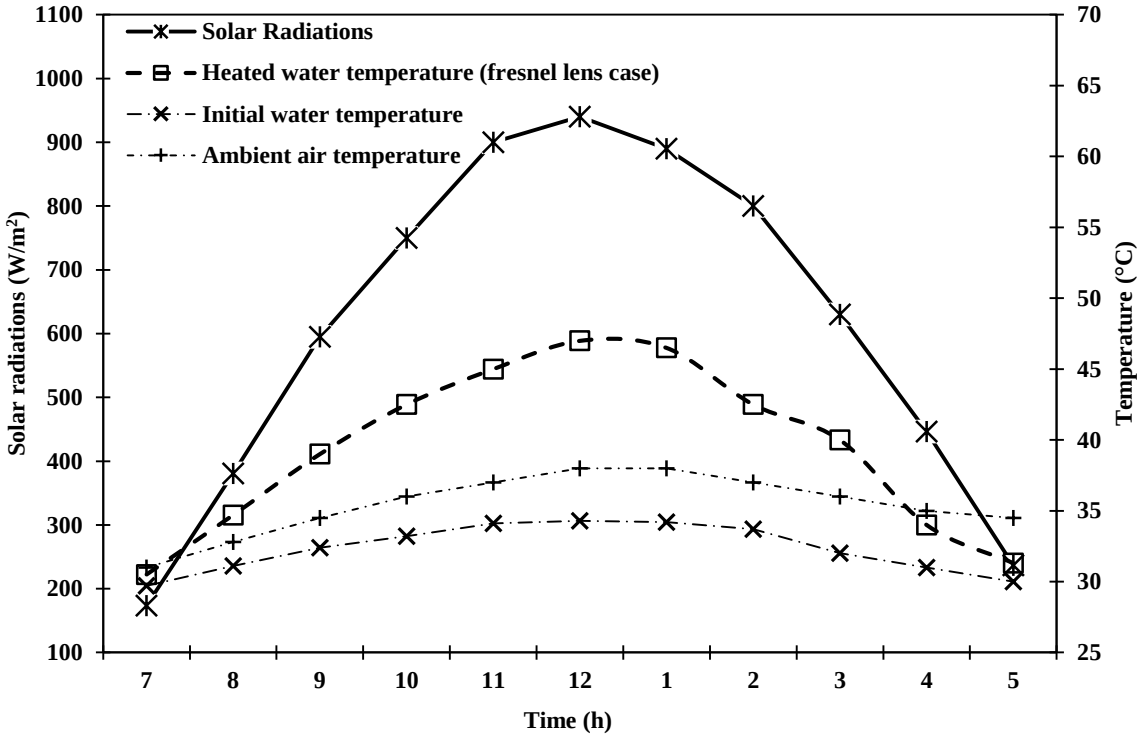

Figure 46 Solar radiations, air and water inlet temperatures, and the water temperature achieved at the exit of absorber plate with the integration of Fresnel lens on 15 August.

The day round performance of the multistage humidifier is investigated in terms of vapor content difference achieved by the moist air between the inlet and exit state of humidifier. The vapor content difference achieved in single stag, two stage, and three stage configuration in the month of June and August are shown in Figure 47 and Figure 48 respectively. Findings reveals that the vapor content difference between of the moist air between the outlet and inlet of the humidifier is higher in the month of June as compared to August. The reason of attaining a higher vapor content difference in the month of June is the lower relative humidity of the inlet air that provide more potential to absorb moisture as compared to the air with high relative humidity. This higher potential of absorbing moisture leads to a higher humidification efficiency.

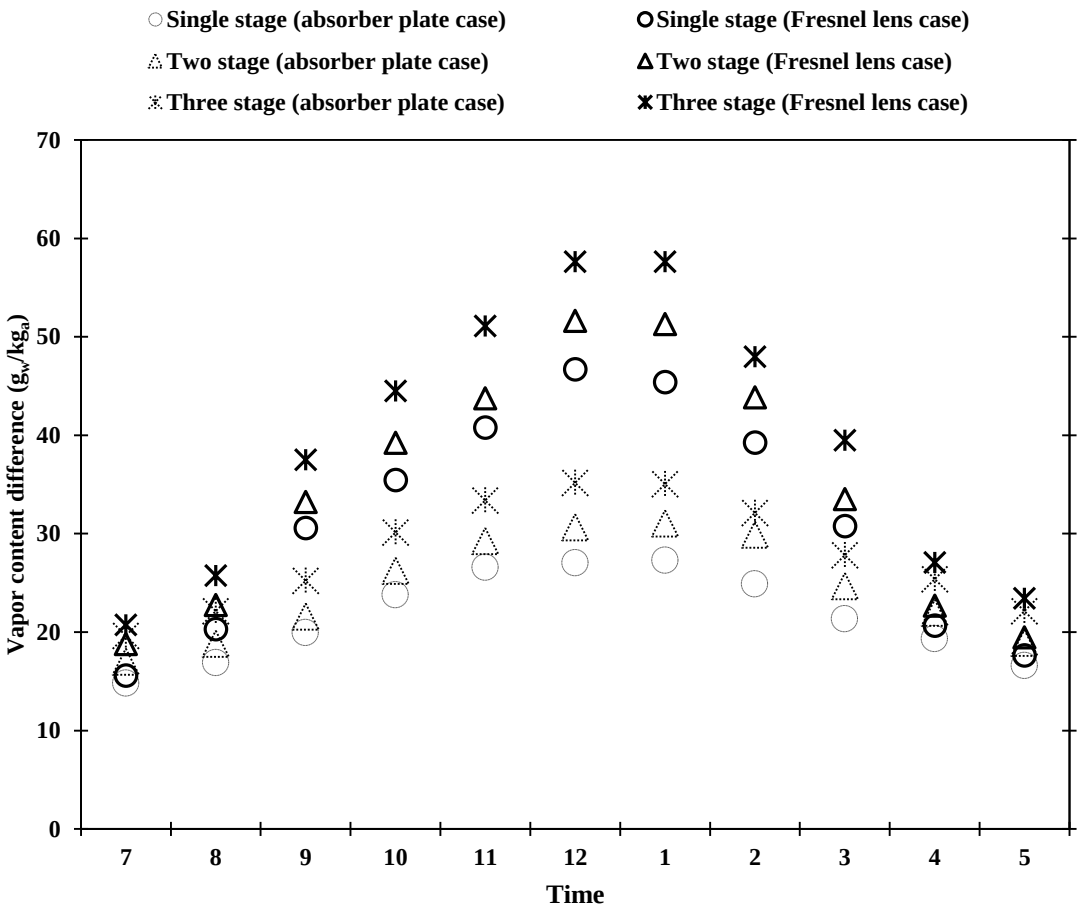

Figure 47 Vapor content difference achieved in single stage, two stage, and three stage configuration with and without integration of Fresnel lens in the month of June.

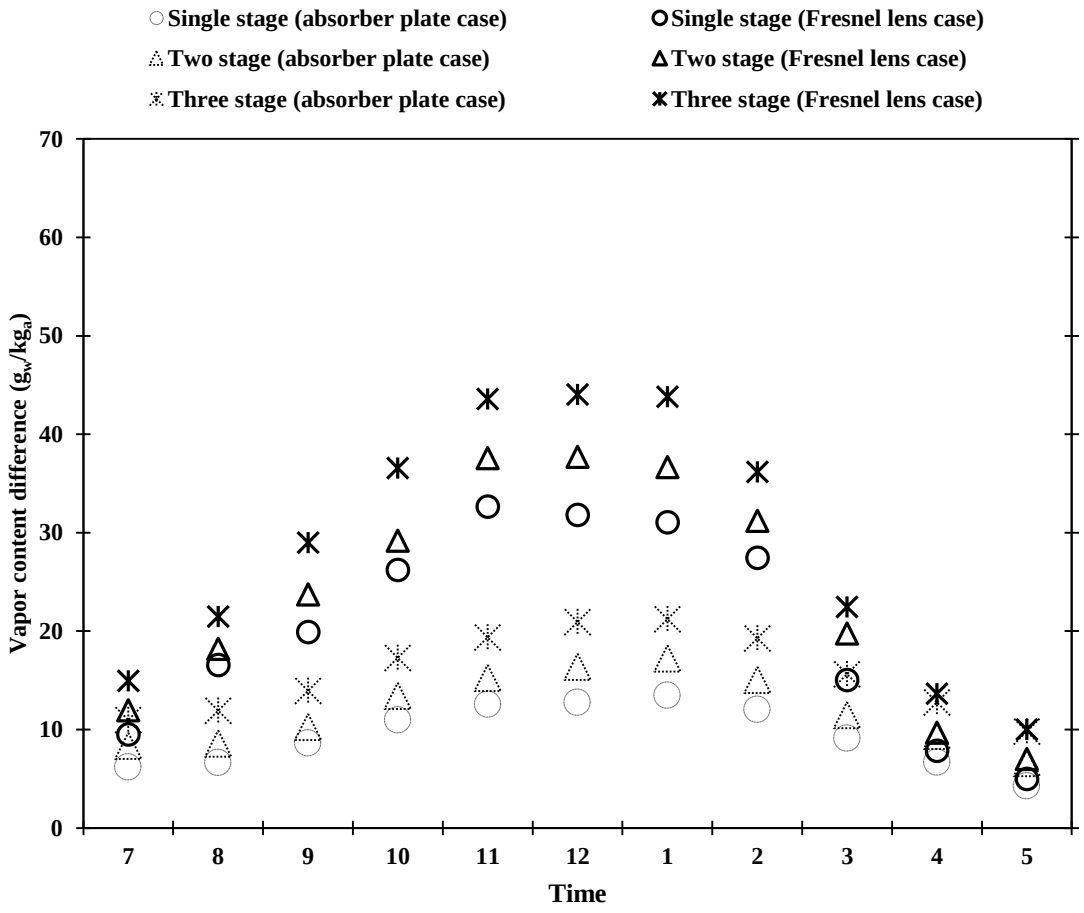

Figure 48 Vapor content difference achieved in single stage, two stage, and three stage configuration with and without integration of Fresnel lens in the month of August.

Figure 49 shows the day round humidification efficiency along with the relative humidity of the inlet air during a particular day of June. The humidifier is tested for its single stage, two stage, and three stage configuration with and without the integration of the Fresnel lens. Findings indicate the increase in humidification efficiency with the increase in number of stages. This is due to the higher residence time of the moist air in the humidifier that increase the contact interval between liquid-gas interfaces. Therefore, more heat and mass transfer take place and air comes out more hot and humid at the exit of humidifier. The humidification efficiency ranged from 82-96 % with maximum value was achieved with three stage configuration during the mid-day. Figure 50 shows the day round humidification efficiency of a single stage, two stage, and three stage humidifier along with the relative humidity of the inlet air during a particular day of August. Similar increasing trend of humidification efficiency is observed with the increase of number of stages as observed in Figure 49. However the achieved humidification efficiency ranged from 77-90 % that is lower as compared to the efficiency experienced in Fig. 16. Hence, the system performed better in the month of June. The reason of attaining higher humidification efficiency in the month of June is attributed to the lower relative humidity of the inlet air that varied between 13-22 % as compared to the month of August when the relative humidity of the inlet air varied in the range of 34- 47 %.

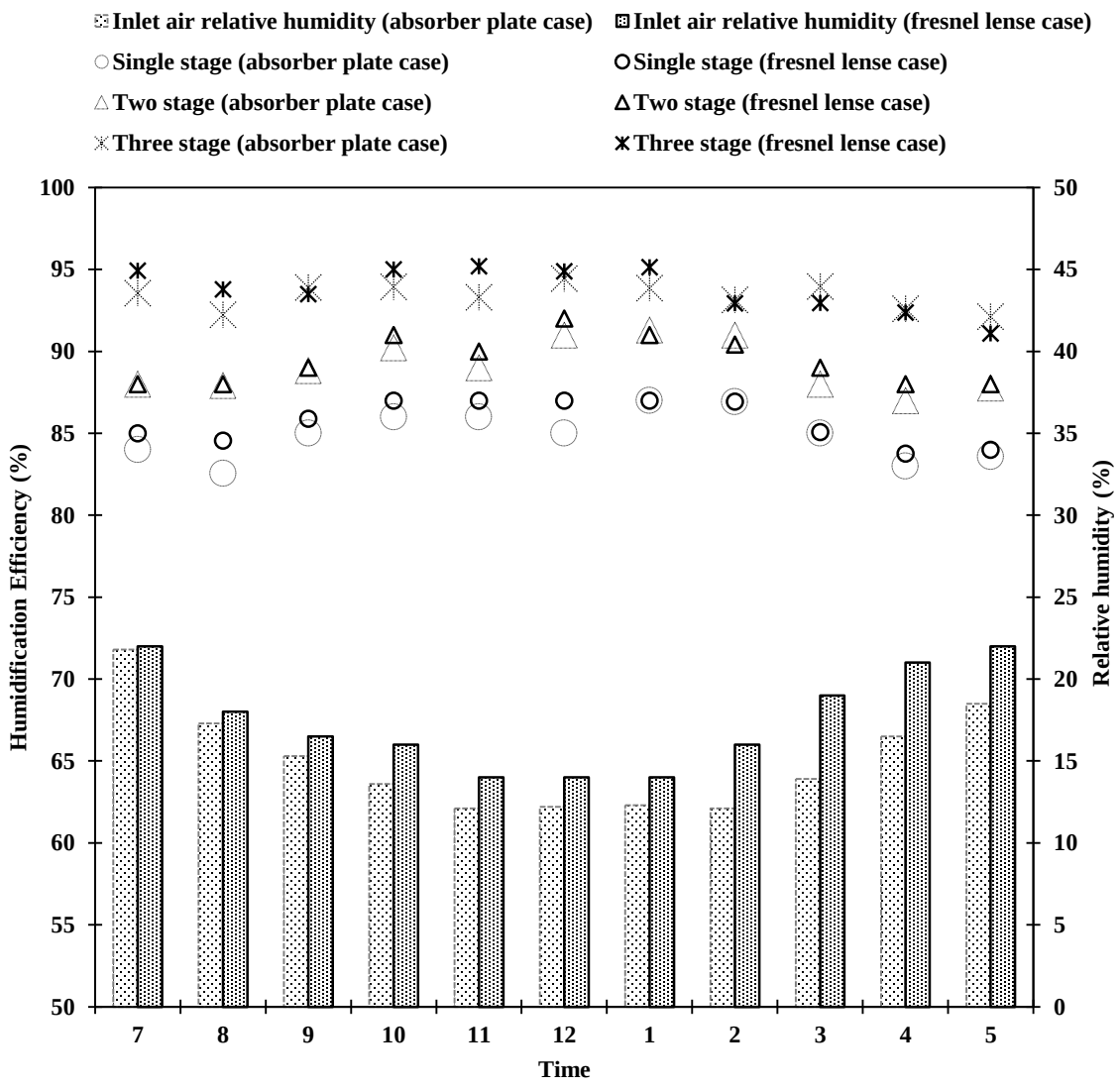

Figure 49 Humidification efficiency in single stage, two stage, and three stage configuration with and without integration of Fresnel lens in the month of June.

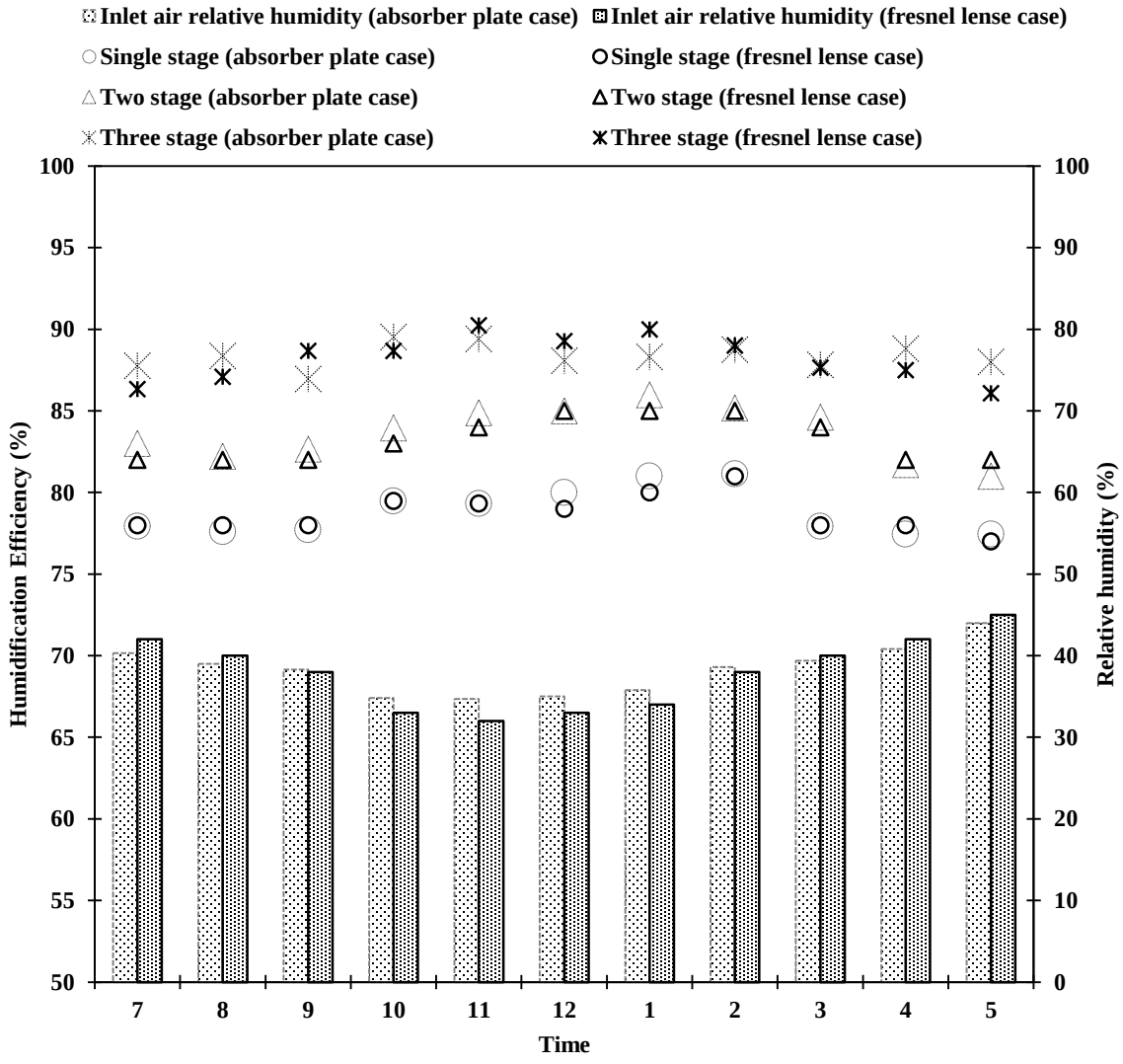

Figure 50 Humidification efficiency in single stage, two stage, and three stage configuration with and without integration of Fresnel lens in the month of August.

4.4.1 Electric Heater Integration in Multi Stage Bubble Column Humidifier

The water temperature at the inlet of the humidifier is the leading factor contributing towards the better performance of the humidifier. The proposed humidifier design take the advantage of direct solar thermal heating by using absorber plate and Fresnel lens. However, the maximum achievable temperature under the prototype design constrains is limited to 50 °C. Therefore, an electric heater is installed to analyze the performance of the multistage bubble column humidifier at higher water inlet temperature.

The performance of single stage, two stage, and three stage bubble column humidifier is analyzed and compared at different water inlet temperature. The performance is analyzed in terms of absolute humidity when the water temperature at the inlet of humidifier is varied in the range of 50 °C to 75 °C. The water column height is maintained at 1 cm and air is introduced at a superficial velocity of 25 cm/s. The results are shown in Figure 51 which indicate that the absolute humidity increased with the increase in water inlet temperature. The absolute humidity follow the exponentially increasing trend with the increase in water inlet temperature irrespective of the number of stages. However, the increase in number of stages provide more residence time to the moist air for further heating and humidification. Consequently, higher absolute humidity is achieved at the exit of the humidifier. The maximum achieved absolute humidity at 75 °C is found to be 248 g_w/kg_a for single stage, 267 g_w/kg_a for two stages, and 289g_w/kg_a for three stages of the proposed humidifier design.

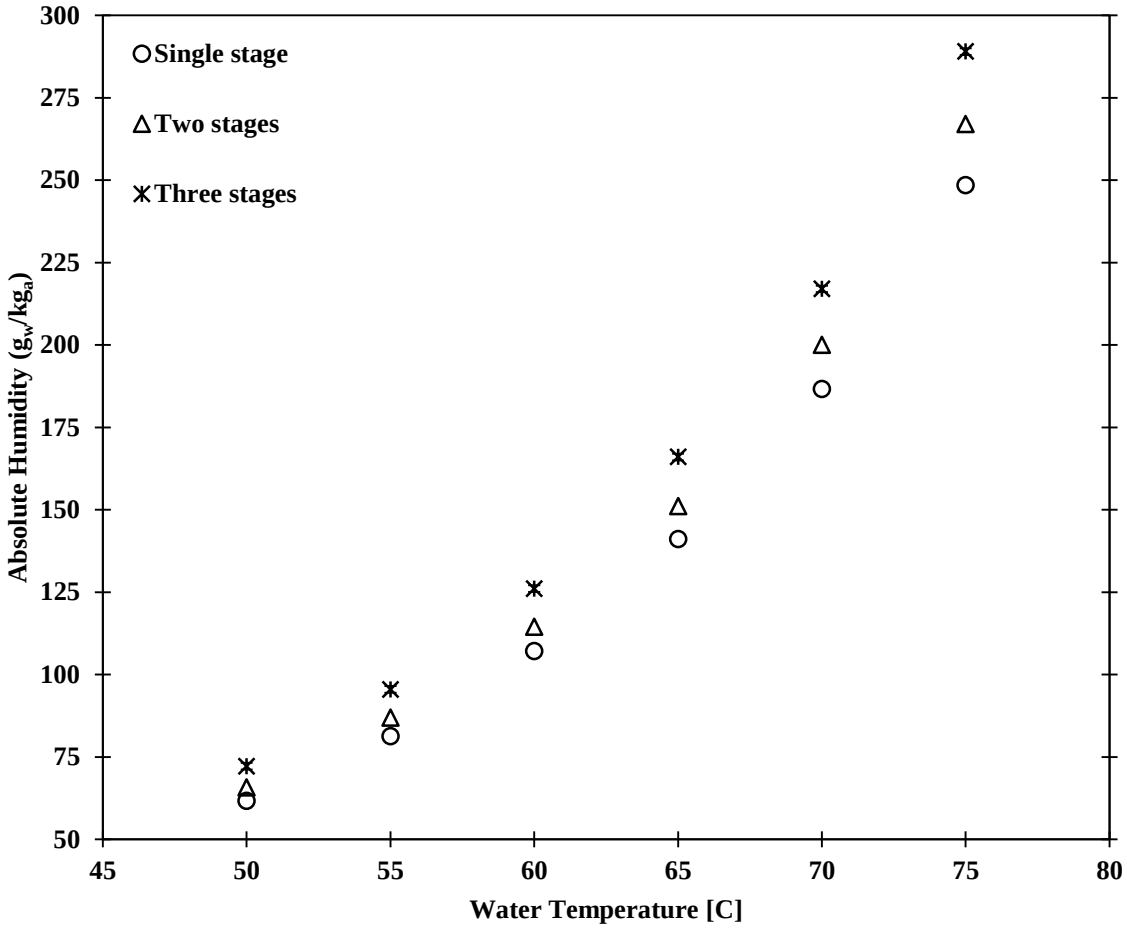

Figure 51 Comparison of absolute humidity achieved in single stage, two stages, and three stages of the humidifier under varying inlet water temperature.

The percentage increase in the absolute humidity achieved by two stage and three stage configuration of the humidifier at different water inlet temperature is shown in Figure 52. Results indicate that the absolute humidity of two stage bubble column humidifier is 6-8 % higher as compared to single stage bubble column humidifier. Similarly, the absolute humidity is increased in the range of 13-15 % in three stage configuration as compared to the single stage humidifier.

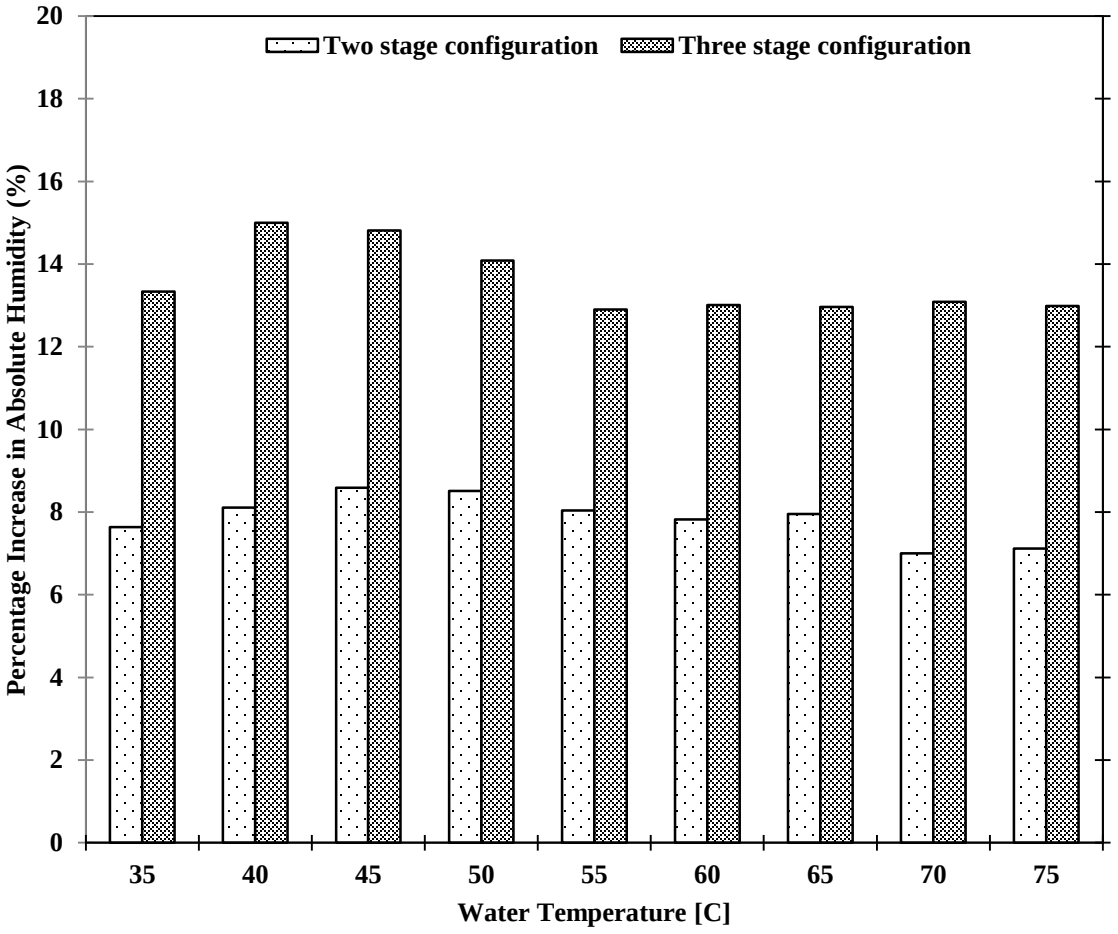

Figure 52 Percentage increase in absolute humidity with two stage and three stage configuration as compared to single stage configuration.

4.4.2 Effectiveness of Multi Stage Bubble Column Humidifier

The effectiveness of two stage and three stage humidifier is analyzed at different values of inlet water temperature. The proposed humidifier design is operated in two stage and three stage configuration under the optimized value of water column height (1 cm) and air superficial velocity (25 cm/s). The temperature is varied in the range of 45 °C to 75 °C. The effectiveness of two stage and three stage configuration of the humidifier design is shown in Figure 53 and Figure 54 respectively. Results show that the energy based effectiveness(ε_E) and temperature based effectiveness (ε_T) follow the similar trend and remain in good agreement with each other. The minimum values of energy based effectiveness(ε_E) and temperature based effectiveness (ε_T) is obtained at 45 °C. The reason of lower effectiveness at 45 °C is recognized by the heat capacity ratio at that point which is equal to one (HCR=1). At heat capacity ratio equal to unity, the water and air stream have equal heat capacity that limits the driving potential of heat and mass transfer between two streams. The maximum energy based effectiveness achieved is 60 % for two stage configuration and 81 % for three stage configuration of the humidifier. The particular experimental results correspond to the situation in which heat capacity ratio is equal to or greater than one (HCR $\geq$ 1). Therefore, air side enthalpy based effectiveness(ε_h) and humidity based effectiveness (ε_ω) are not considered under these experimental conditions due to their applicability range that is valid only when the heat capacity ratio is less than or equal to one (HCR $\leq$ 1).

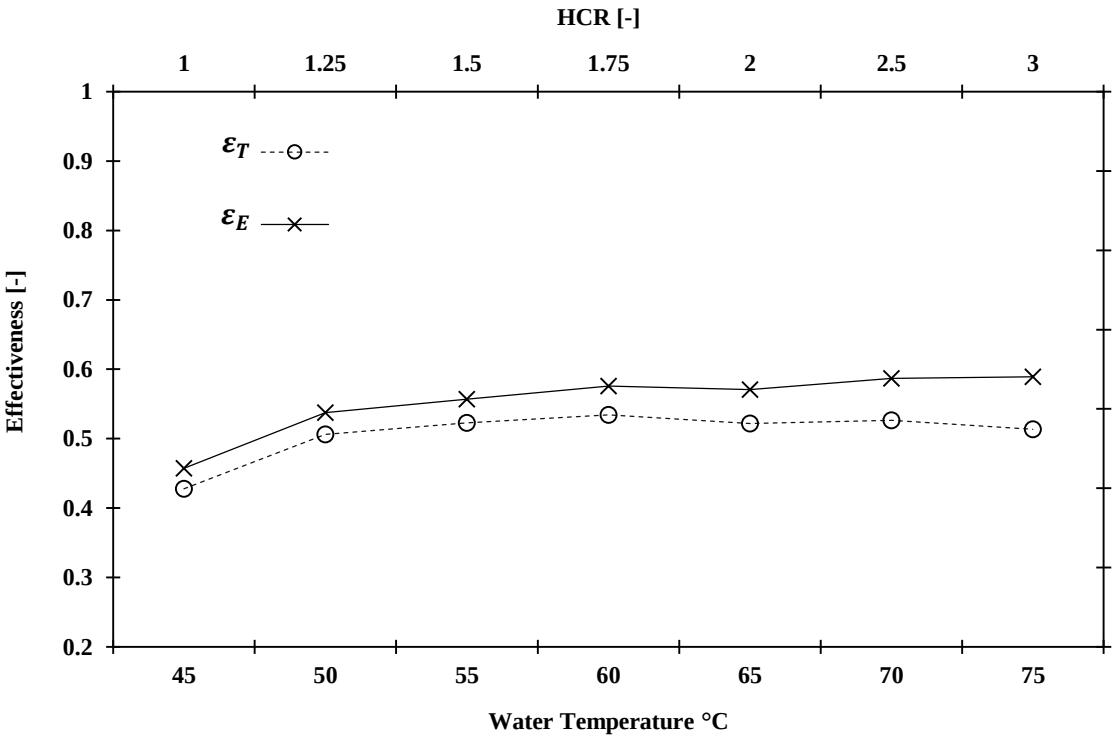

Figure 53 Effectiveness of two stage humidifier configuration at HCR ≥ 1.

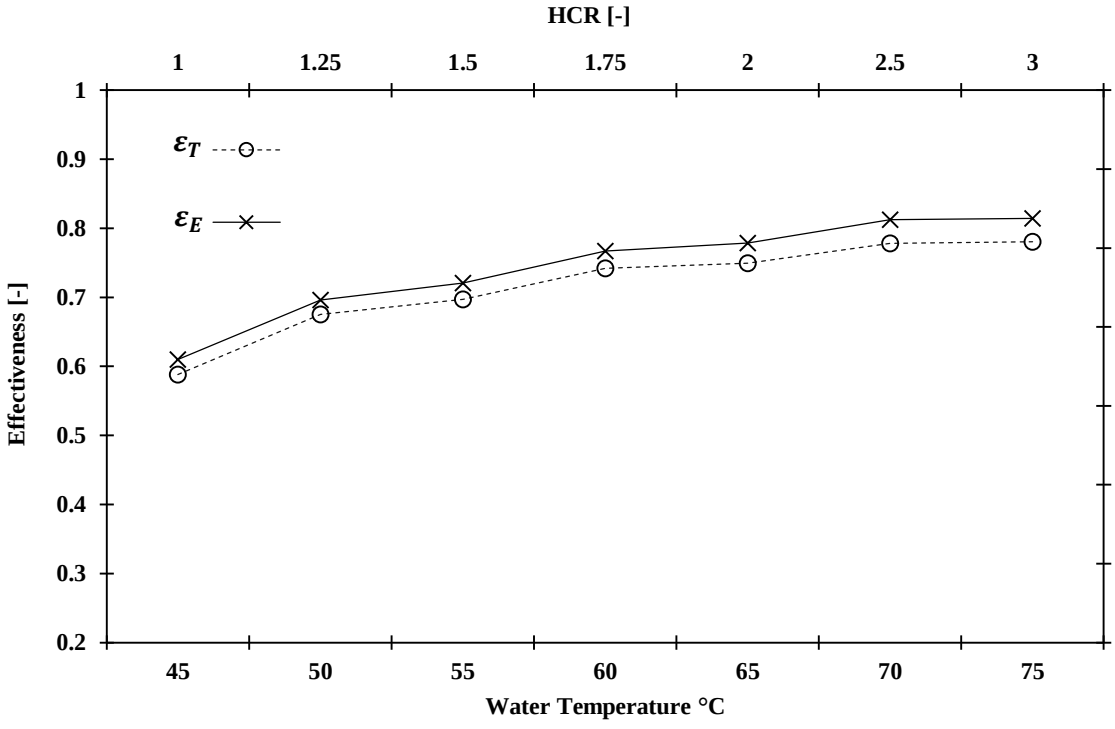

Figure 54 Effectiveness of three stage humidifier configuration at HCR ≥ 1.

Figure 55 summarize the energy based effectiveness results of single stage, two stage, and three stage configuration of the humidifier. Results clearly demonstrate the advantage of multistage configuration of the proposed humidifier design. The effectiveness increases with the increase in number of stages for all temperature values of the inlet water. The maximum effectiveness value achieved is 49 % for single stage configuration, 60 % for two stage configuration, and 81 % for three stage configuration of the humidifier.

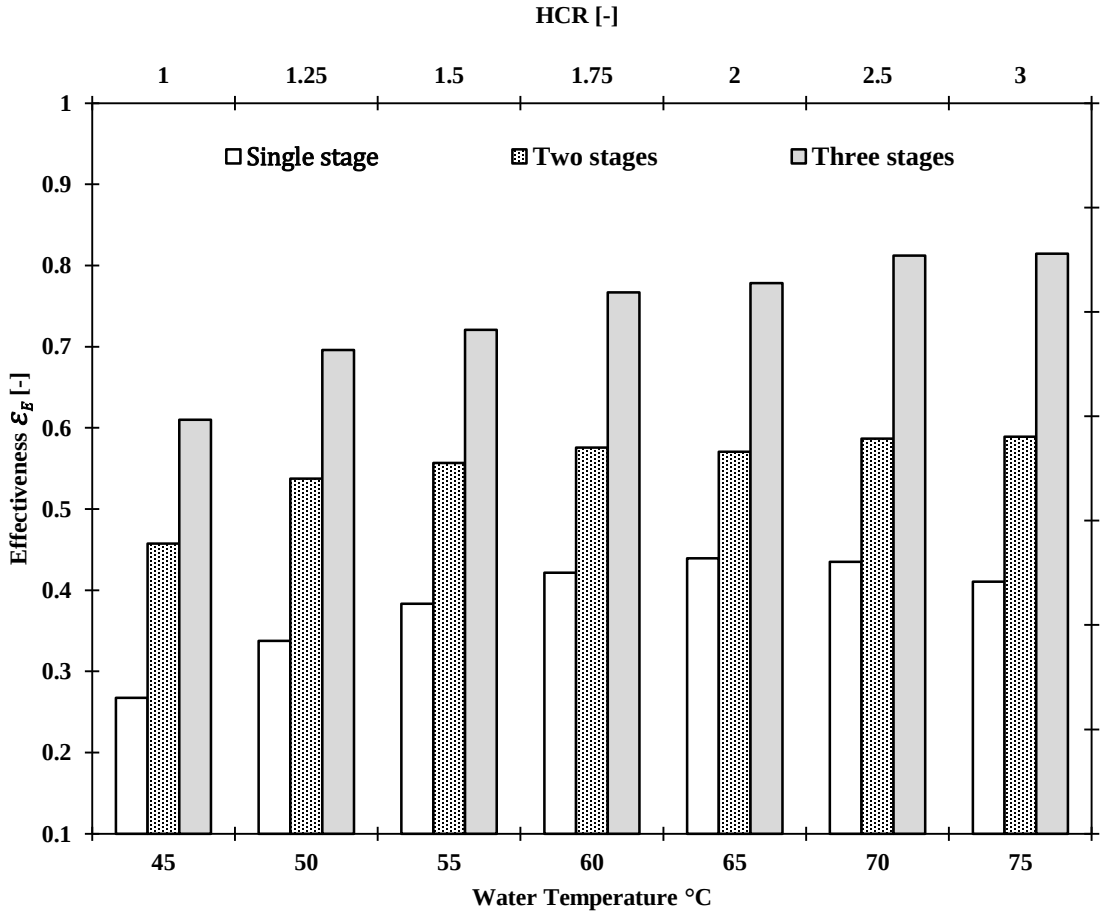

Figure 55 Energy based effectiveness results of single stage, two stage, and three stage configuration of the proposed humidifier.

4.5 Comparison of Results with Literature

Careful review of previous literature studies on HDH system indicate the use of multi-satge humidification technique to improve the performance of the system. This technique consists of several steps of air heating and humidification and leads to high vapor concentration in the airflow. These studies reported the achieved vapor content difference ($\Delta\omega$) of the moist air between the inlet and exit stage of the humidifier. Garg et al. [10] performed the experimental and numerical study on multi-effect humidification dehumidification solar desalination system. The reported vapor content difference value is 66 g_w/kg_a at 70 °C. The vapor content difference reported by Chafik [56] is 75 g_w/kg_a at 55 °C after four stages of air heating and humidification process. Amara et al. [18] reported that the achieved vapor content difference after eight stages of heating and humidification is approximately 110 g_w/kg_a at 60 °C. Dai and Zhang [22] stated the use of falling film humidification chamber with larger surface area and forced convection. The study concluded that the system performed better in the higher temperature range (70°C - 90°C) and reported the achieved vapor content difference value of 174 g_w/kg_a at 85 °C. Agouz and Abugerah [38] studied the performance of bubble column humidifier and reported the achieved vapor content difference value of 85 g_w/kg_a and 110 g_w/kg_a at the water temperature of 55 °C and 60 °C respectively.

The performance of the proposed humidifier design in terms of vapor content difference achieved at different water inlet temperature is compared with the published data. Figure 56 shows the comparison of achieved absolute humidity in present study with some published results. Results clearly shows the advantage of using bubble column as a

humidification device. The vapor content difference achieved in present study under the optimized single stage configuration is 92 g_w/kg_a at 55 °C and 121 g_w/kg_a at 60 °C that is much higher than the results stated by Garg at al. [10] and Dai and Zhang [22]. The present single stage results are in good agreement with the published results of Agouz and Abugerah [38]. However the obtained vapor content difference for 3 stage configuration is significantly higher than the results obtained by Agouz and Abugerah. The achieved vapor content difference with three stage configuration is 139 g_w/kg_a at 60 °C that is comparable to the results stated by Chafik [57] after fifteen stages of air heating and humidification.

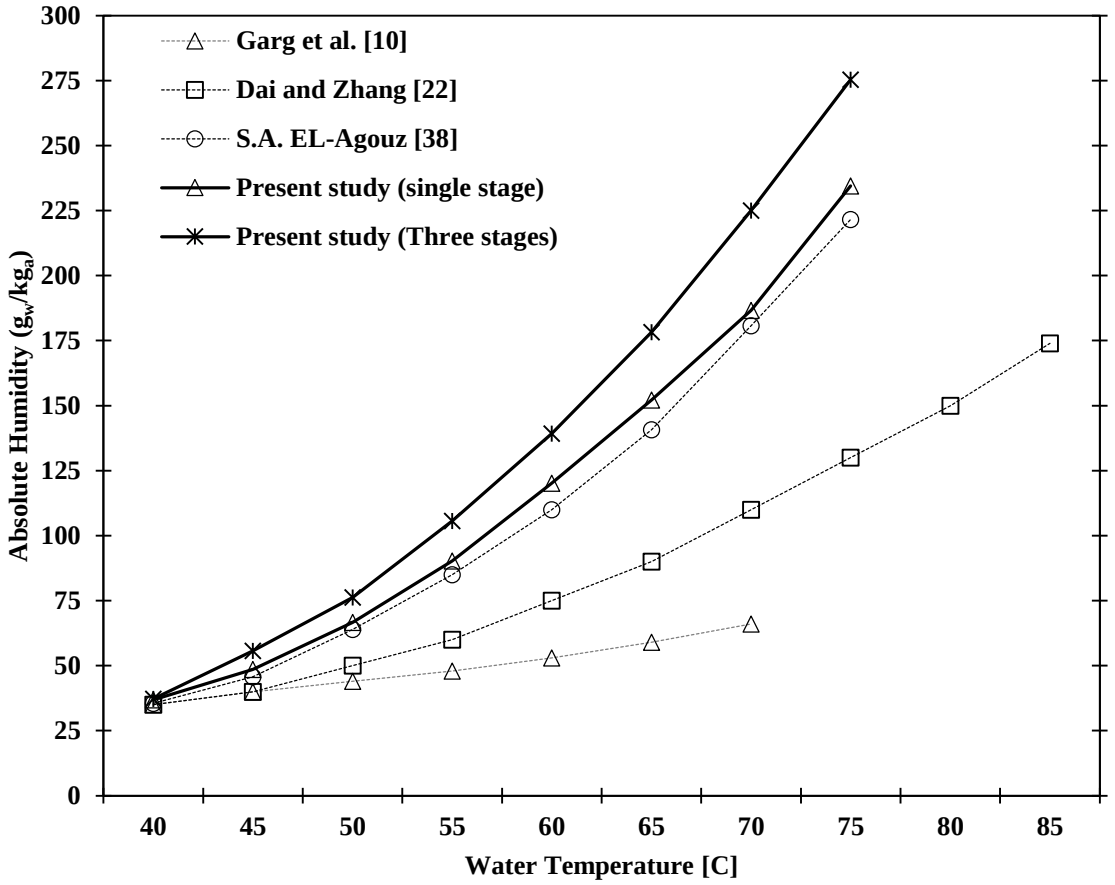

Figure 56 Comparison of present work with literature.

CHAPTER 5

CONCLUSIONS AND FUTURE SCOPE

5.1 Conclusions

Humidification-dehumidification (HDH) is a carrier gas based thermal technique that is ideal for a small scale decentralized water desalination system. An innovative design approach is to use the bubble column humidifier to enhance the performance of the HDH water desalination system. Therefore, a novel solar heated multi-stage bubble column humidifier is designed and tested. The study aimed to explore the optimum operating conditions of the new humidifier design proposed and signpost the following underscored findings:

1. The proposed humidifier design take the benefit of its tilted absorber plate for water heating and stepped configuration of bubble column for air humidification. This design improvement has the following advantages:

    - The tilted absorber plate acts as a sloped surface to create a thin film of water over the absorber plate. The minimum water depth over the absorber plate leads to a better heat transfer and a higher water temperature is achieved at the downstream of absorber plate. It also results in a significantly low pressure drop in the air-side.

- The hot humid air at the exit of the bubble column further passed over the thin film of hot water flowing over absorber plate to absorb more moisture and higher vapor contents are achieved at the exit of the humidifier. In other words, the humidifier heats both air and water simultaneously and air humidification process occurs throughout the full path of the air inside the humidifier.
- This proposed humidifier have a direct solar thermal heating. Subsequently, it can be located in remote areas, where there is a shortage in electricity.

2. The optimum design for the perforated plate is an important aspect in the experimental investigation of bubble column humidifier. Different design configurations of the perforated plate were tested in order to achieve the lower pressure drop in the system. Findings revealed that the minimum pressure drop was experienced at a lower water column height and a lower air superficial velocity. However, the water column height and air superficial velocity should be optimized according to the geometry of the perforated plate in order to avoid water leakage through the perforations. Experiments were performed to find out the optimum values of air superficial velocity and water column height. The water column height of 1 cm with air superficial velocity of 25 cm/s reflected the optimum balance for higher system performance with lower pressure drop.

3. The day round performance of humidifier was analyzed in terms of the absolute humidity of the moist air at the exit of humidifier. The experiments were performed for single stage, two stage, and three stage configuration at the optimized balance of air superficial velocity and water column height. Findings reveal that the maximum value of absolute humidity was achieved in three stage configuration around mid-day when

highest water heating temperature was attained. The comparison of single stage with multistage configuration shows that the absolute humidity is 9 % higher for two stage configuration and 23 % higher for three stage configuration as compared to single stage humidifier.

4. The proposed design of the bubble column humidifier was integrated with the Fresnel lens in order to achieve a higher water temperature. The increase in water temperature enhanced the ability of air to absorb more moisture and consequently higher absolute humidity is achieved at the outlet of bubble column humidifier. The integration of the Fresnel lens increased the absolute humidity up to 26 % as compared to the results obtained without the integration of the Fresnel lens under the same prevailing conditions.

5. The day round performance of the humidifier was tested in single stage, two stage, and three stage configuration in two different months (June and August) to experience the effect of varying relative humidity of the inlet air. Results indicate that the humidification efficiency ranged from 82-96 % in the month of June with maximum value was achieved with three stage configuration during the mid-day. The lower humidification efficiency was experienced in the month of August that ranged from 77-90 %. Hence, the system performed better in the month of June when the inlet air relative humidity varied between 13-22 % as compared to 34- 47 % in the month of August during the experiments. The reason of achieving better performance in the month of June is attributed to the higher potential of the air to absorb moisture at a lower relative humidity as compared to the air with a high relative humidity.

6. The performance of the proposed humidifier design was analyzed in terms of energy

based effectiveness to anticipate its true potential as an effective mean of heat and mass exchange. Findings signpost the significant performance improvement when the proposed humidifier design is operated in multistage configuration.

7. The comparison of the proposed humidifier design with the published results show the dominating performance of bubble column as a humidification device. The vapor content difference achieved in present study under the optimized single stage configuration is 92 g_w/kg_a at 55 °C and 121 g_w/kg_a at 60 °C that is much higher than the results stated by Garg at al. [26] and Dai and Zhang [28]. The present single stage results are in good agreement with the published results of Agouz and Abugerah [20]. However, the obtained vapor content difference for three stage configuration is significantly higher than the results obtained by Agouz and Abugerah. The achieved vapor content difference with 3 stage configuration is 139 g_w/kg_a at 60 °C that is comparable to the results stated by Chafik [29] after fifteen stages of air heating and humidification.

8. The proposed design is original in its stand-alone/off-grid functionality in electricity scarce remote areas. The results of this work will be a valuable reference for both researchers and engineers in the area of water desalination. It will also alleviates the sustainability concerns of conventional energy based water desalination systems by balancing the potable water requirements through renewable energy. Moreover, it will provide the prospects of reducing the clean water scarcity in remote areas.

5.2 Future Scope

- Incorporating the heat storage system for a longer operation of the humidifier.
- Improving the system effectiveness at balance condition (HCR=1) by increasing the number of stages.
- Integration of the new design with the dehumidifier to analyze the performance of the overall HDH system.

References

[1] G. Fiorenza, V. K. Sharma, and G. Braccio, "Techno-economic evaluation of a solar powered water desalination plant," Energy Conversion and Management, vol. 44, pp. 2217-2240, 2003.

[2] 2030 water resourse group, “Charting our water future,” 2009. Retreived from http://www.2030waterresourcesgroup.com /water_full/.

[3] J. E. Miller, "Review of water resources and desalination technologies," Sandia National Labs Unlimited Release Report SAND-2003-0800, 2003.

[4] S. Kalogirou, "Use of parabolic trough solar energy collectors for sea-water desalination," Applied Energy, vol. 60, pp. 65-88, 1998.

[5] Dabbagh et al. "Desalination an Emergent Option", Water in the Arab World: Perspectives and Prognoses, Harvard University Press, 1994.

[6] G. P. Narayan, M. H. Sharqawy, E. K. Summers, J. H. Lienhard, S. M. Zubair, and M. A. Antar, "The potential of solar-driven humidification–dehumidification desalination for small-scale decentralized water production," Renewable and Sustainable Energy Reviews, vol. 14, pp. 1187-1201, 2010.

[7] S. Al-Hallaj, M. M. Farid, and A. Rahman Tamimi, "Solar desalination with a humidification-dehumidification cycle: performance of the unit," Desalination, vol. 120, pp. 273-280, 1998.

[8] H. B. Bacha, T. Damak, M. Bouzguenda, and A. Y. Maalej, "Experimental validation of the distillation module of a desalination station using the SMCEC principle," Renewable Energy, vol. 28, pp. 2335-2354, 2003.

[9] M.M. Farid, A.W. Al-Hajaj, Solar desalination with humidifica- tion–dehumidification cycle, Desalination 106 (1996) 427–436.

[10] H. Garg, R. Adhikari, and R. Kumar, "Experimental design and computer simulation of multi-effect humidification (MEH)-dehumidification solar distillation," Desalination, vol. 153, pp. 81-86, 2003.

[11] A. Nafey, H. E. Fath, S. El-Helaby, and A. Soliman, "Solar desalination using humidification–dehumidification processes. Part II. An experimental investigation," Energy Conversion and Management, vol. 45, pp. 1263-1277, 2004.

[12] H. MÜLler-Holst, "SOLAR THERMAL DESALINATION USING THE MULTIPLE EFFECT HUMIDIFICATION (MEH)-METHOD," in Solar Desalination for the 21st Century, L. Rizzuti, H. Ettouney, and A. Cipollina, Eds., ed: Springer Netherlands, 2007, pp. 215-225.

[13] Y. Li, J. F. Klausner, R. Mei, and J. Knight, "Direct contact condensation in packed beds," International Journal of Heat and Mass Transfer, vol. 49, pp. 4751-4761, 2006.

[14] M. A. Younis, M. A. Darwish, and F. Juwayhel, "Experimental and theoretical study of a humidification-dehumidification desalting system," Desalination, vol. 94, pp. 11-24, 1993.

[15] G. P. Narayan, R. K. McGovern, S. M. Zubair, and J. H. Lienhard V, "High-temperature-steam-driven, varied-pressure, humidification-dehumidification system coupled with reverse osmosis for energy-efficient seawater desalination," Energy, vol. 37, pp. 482-493, 2012.

[16] E. Chafik, "Design of plants for solar desalination using the multi-stag heating/humidifying technique," Desalination, vol. 168, pp. 55-71, 2004.

[17] I. Houcine, M. BenAmara, A. Guizani, and M. Maâlej, "Pilot plant testing of a new solar desalination process by a multiple-effect-humidification technique," Desalination, vol. 196, pp. 105-124, 2006.

[18] M. Ben Amara, I. Houcine, A. Guizani, and M. Mâalej, "Experimental study of a multiple-effect humidification solar desalination technique," Desalination, vol. 170, pp. 209-221, 2004.

[19] C. Yamalı and İ. Solmus, "A solar desalination system using humidification–dehumidification process: experimental study and comparison with the theoretical results," Desalination, vol. 220, pp. 538-551, 2008.

[20] J. Orfi, M. Laplante, H. Marmouch, N. Galanis, B. Benhamou, S. B. Nasrallah, C. T. Nguyen, "Experimental and theoretical study of a humidification dehumidification water desalination system using solar energy," Desalination, vol. 168, pp. 151-159, 2004.

[21] G. Al-Enezi, H. Ettouney, and N. Fawzy, "Low temperature humidification dehumidification desalination process," Energy Conversion and Management, vol. 47, pp. 470-484, 2006.

[22] Y. J. Dai and H. F. Zhang, "Experimental investigation of a solar desalination unit with humidification and dehumidification," Desalination, vol. 130, pp. 169-175, 2000.

[23] M. Khedr, "Techno-Economic investigation of an air humidification-dehumidification desalination process," Chemical Engineering & Technology, vol. 16, pp. 270-274, 1993.

[24] "Thermal design of humidification dehumidification systems for affordable and small-scale desalination", Thesis (Ph. D.)--Massachusetts Institute of Technology, Dept. of Mechanical Engineering, 2012, http://hdl.handle.net/1721.1/78176.

[25] H. T. A. El-Dessouky, "Humidification-dehumidification desalination process using waste heat from a gas turbine," Desalination, vol. 71, pp. 19-33, 1989.

[26] M. S. Abdel-Salam, M. M. Hilal, A. F. El-Dib, and M. Abdel Monem, "Experimental Study of Humidification-Dehumidification Desalination System," Energy Sources, vol. 15, pp. 475-490, 1993/07/01 1993.

[27] H. Müller-Holst, M. Engelhardt, and W. Schölkopf, "Small-scale thermal seawater desalination simulation and optimization of system design," Desalination, vol. 122, pp. 255-262, 1999.

[28] K. Bourouni, M. T. Chaibi, and L. Tadrist, "Water desalination by humidification and dehumidification of air: state of the art," Desalination, vol. 137, pp. 167-176, 2001.

[29] R. H. Xiong, S. C. Wang, L. X. Xie, Z. Wang, and P. L. Li, "Experimental investigation of a baffled shell and tube desalination column using the humidification-dehumidification process," Desalination, vol. 180, pp. 253-261, 2005.

[30] J. Klausner, Y. Li, and R. Mei, "Evaporative heat and mass transfer for the diffusion driven desalination process," Heat and Mass Transfer, vol. 42, pp. 528-536, 2006/04/01 2006.

[31] Y. Li, J. F. Klausner, and R. Mei, "Performance characteristics of the diffusion driven desalination process," Desalination, vol. 196, pp. 188-209, 2006.

[32] G. P. Narayan, M. H. Sharqawy, S. Lam, S. K. Das, and J. H. Lienhard, "Bubble columns for condensation at high concentrations of noncondensable gas: Heat-transfer model and experiments," AIChE Journal, vol. 59, pp. 1780-1790, 2013.

[33] Treybal, R.E., 1980. Mass Transfer Operation, McGraw-Hill, NewYork.

[34] J. Orfi, M. Laplante, H. Marmouch, N. Galanis, B. Benhamou, S. B. Nasrallah, and C. T. Nguyen, "Experimental and theoretical study of a humidification-dehumidification water desalination system using solar energy," Desalination, vol. 168, pp. 151-159, 2004.

[35] Wallis, J.S., & Aull, R.J. (1999). Improving Cooling Tower Performance. Hydrocarbon Engineering, 92-95.

[36] Mirsky, G.R., & Bauthier, J. (1993). Evolution of Cooling Tower Fill. CTI Journal, 14(1), 12-19.

[37] Aull, R.J., & Krell, T. (2000). Design Features of Cross-Fluted Film Fill and Their Effect on Thermal Performance. CTI Journal, 21(2), 12-33.

[38] S. A. El-Agouz and M. Abugderah, "Experimental analysis of humidification process by air passing through seawater," Energy Conversion and Management, vol. 49, pp. 3698-3703, 2008.

[39] S. A. El-Agouz, "Desalination based on humidification–dehumidification by air bubbles passing through brackish water," Chemical Engineering Journal, vol. 165, pp. 413-419, 2010.

[40] L. Zhang, G. Cheng, and S. Gao, "Experimental study on air bubbling humidification," Desalination and Water Treatment, vol. 29, pp. 258-263, 2011/05/01 2011.

[41] H. Kolbel, W. Siemes, R. Maas, and K. Muller, "Wärmeübergang an Blasensäulen," Chemie Ingenieur Technik, vol. 30, pp. 400-404, 1958. English translation: Heat transfer in bubble columns. Retrieved from:

http://www.fischer-tropsch.org/DOE/DOE_reports/89012412/de89012412_toc.htm

[42] W. Kast, "Analyse des wärmeübergangs in blasensäulen," International Journal of Heat and Mass Transfer, Vol. 5, pp. 329-336, 1962.

[43] Higbie R, "The rate of absorption of a pure gas into a still liquid during a short time of exposure," Transactions of the American Institute of Chemical Engineers, 1935.

[44] D. N. Miller, "Scale-up of agitated vessels gas-liquid mass transfer," American Institute of Chemical Engineers journal, vol. 20, pp. 448-453, 1974.

[45] R. W. Field and R. Rahimi, "Hold-up heat-transfer in bubble columns," In: Fluid Mixing III. Amarousion-Pefki, Greece: European Federation of Chemical Engineering, 1988.

[46] H. D. Mendelson, "The prediction of bubble terminal velocities from wave theory," American Institute of Chemical Engineers journal, 1967.

[47] G. P. Narayan, M. H. Sharqawy, S. Lam, S. K. Das, and J. H. Lienhard, "Bubble columns for condensation at high concentrations of noncondensable gas: Heat-transfer model and experiments," AIChE Journal, vol. 59, pp. 1780-1790, 2013.

[48] Y. J. Cho, K. J. Woo, Y. Kang, and S. D. Kim, "Dynamic characteristics of heat transfer coefficient in pressurized bubble columns with viscous liquid medium," Chemical Engineering and Processing: Process Intensification, Vol. 41, pp. 699-706, 2002.

[49] S. C. Saxena, N. S. Rao, and A. C. Saxena, "Heat-transfer and gas-holdup studies in a bubble column: air–water–glass bead system," Chem Eng Commun, 1990.

[50] Measurmrnt of fluid flow by means of pressure differential devices inserted in circular cross-section conduits running. ISO5167.

[51] N. C. Barford, J. W. Richards, and J. B. Kelley, Experimental Measurements: Precision, Error and Truth and Interpretation of Technical Data. Physics Today, Vol. 22(1), pp. 109-111, (2009).

[52] N. P. Cheremisinoff, and P. N. Cheremisinoff, "Cooling towers selection, design and practice," 1981.

[53] R. P. Mandi, R, R. K. Hegde, and S. N. Sinha, "Performance enhancement of cooling towers in thermal power plants through energy conservation," In Power Tech, 2005 IEEE Russia (pp. 1-6). IEEE, 2005.

[54] Nellis, G., and Klein, S. (2008). Heat Transfer, Cambridge University Press.

[55] G. P. Narayan, K. Mistry, M. H. Sharqawy, and J. H. Lienhard, "Energy effectiveness of simultaneous heat and mass exchange devices.Frontiers in Heat and Mass Transfer (FHMT), Vol. 1(2), 2010.

[56] E. Chafik, "A new seawater desalination process using solar energy," Desalination, Vol. 153 (1), pp. 25-37, 2003.

[57] E. Chafik, "A new type of seawater desalination plants using solar energy." Desalination, Vol. 153 (1), pp. 338-348, 2003.

[58] G. P. Narayan, M. G. S. John, S. M. Zubair, & J. H. Lienhard, "Thermal design of the humidification dehumidification desalination system: An experimental investigation. International Journal of Heat and Mass Transfer, Vol. 58(1), pp. 740-748, 2013.

Vitae

Name:	Hafiz Muhammad Abd-ur-Rehman
Nationality:	Pakistan
Date of Birth:	6/2/1990
Email:	abd-ur-rehman_@hotmail.com
Address:	77/C satellite Town Bahawalpur (Punjab) Pakistan
Academic Background:	Mechanical Engineering

Research Publications

1) Abd-ur-Rehman, H.M. & Al-Sulaiman, F.A. (2014). Techno-economic evaluation of different types of solar collectors for water heating application in domestic sector of Saudi Arabia. 5th International Renewable Energy Congress (IREC),1-6.

2) Abd-ur-Rehman, H.M. & Al-Sulaiman, F.A. (2015). Mathematical modelling of bubbler humidifier for humidification dehumidification (HDH) water desalination System. Recent Advances in Mechanics and Mechanical Engineering, 147-156.
   Proceedings of the 6th International Conference on fluid mechanics and heat & mass transfer (FLUIDSHEAT‘15), Kuala Lumpur, Malaysia.

3) Abd-ur-Rehman, H.M., Al-Sulaiman, F.A., Budaiwi, I.M., & Shakir, S. (2015). Energy conservation measures and solar energy integration in hot climate residential buildings. Recent Advances in Renewable Energy Sources, 21-28.
   Proceedings of the 9th International Conference on renewable energy sources (RES ‘15), Kuala Lumpur, Malaysia.

4) Abd-ur-Rehman, H.M. & Al-Sulaiman, F.A. (2015). Experimental analysis of solar driven bubbler humidifier for humidification-dehumidification (HDH) water desalination System," ISES Solar World Congress 2015, Daegu, Korea.

5) Al-Mahmoud, H., Al-Sulaiman, F.A., & Abd-ur-Rehman, H.M.(2015).Techno-economic evaluation of solar water heating applications in hospitals at Saudi Arabia," ISES Solar World Congress 2015, Daegu, Korea.

6) Al-Sulaiman, F.A., Atif, M., & Abd-ur-Rehman, H.M. (2015). Performance analysis of solar tower power plants driven supercritical carbon dioxide recompression cycles for six different locations in Saudi Arabia, ISES Solar World Congress 2015, Daegu, Korea.